University of Nebraska Medical Center
BREAKTHROUGHS FOR LIFE

University of Nebraska Medical Center
DigitalCommons@UNMC

Theses & Dissertations

Graduate Studies

Fall 12-16-2016

Staphylococcus Aureus Biofilms Interfere With Macrophage Antimicrobial Responses Through Differential Gene Regulation, Toxin Production, and Purine Metabolism

Tyler D. Scherr
University of Nebraska Medical Center

Tell us how you used this information in this short survey.

Follow this and additional works at: https://digitalcommons.unmc.edu/etd

 Part of the Immunology and Infectious Disease Commons

Recommended Citation

Scherr, Tyler D., "Staphylococcus Aureus Biofilms Interfere With Macrophage Antimicrobial Responses Through Differential Gene Regulation, Toxin Production, and Purine Metabolism" (2016). *Theses & Dissertations*. 145.
https://digitalcommons.unmc.edu/etd/145

This Dissertation is brought to you for free and open access by the Graduate Studies at DigitalCommons@UNMC. It has been accepted for inclusion in Theses & Dissertations by an authorized administrator of DigitalCommons@UNMC. For more information, please contact digitalcommons@unmc.edu.

STAPHYLOCOCCUS AUREUS BIOFILMS INTERFERE WITH MACROPHAGE ANTIMICROBIAL RESPONSES THROUGH DIFFERENTIAL GENE REGULATION, TOXIN PRODUCTION, AND PURINE METABOLISM

By

Tyler Scherr

A DISSERTATION

Presented to the Faculty of

The Graduate College of the University of Nebraska Medical Center

In partial fulfillment of the requirements for the degree of

Doctor of Philosophy

Department of Pathology and Microbiology

Under the supervision of Professor Tammy Kielian, Ph.D.

University of Nebraska Medical Center

Omaha, NE

September 2016

Table of contents:

Acknowledgements

I would first like to thank my mentor, Dr. Tammy Kielian, for her constant support, guidance, and encouragement. I came to UNMC hoping to have the opportunity to work on translational research; to spend my time researching something that might eventually have a positive impact on people. Everything Tammy does with her lab is always with the patient in mind, and I couldn't have asked for a better mentor. Her scientific curiosity and passion for translational research is infectious and, through all of the ups and downs of scientific research, I've been proud to be a small part of her lab and almost always looked forward to putting in a full-days' work there.

I would also like to thank my supervisory committee, Dr. Kenneth Bayles, Dr. Paul Fey, Dr. Curtis Hartman, Dr. Jessica Snowden, and Dr. Geoffrey Thiele for sharing their time and expertise in providing invaluable guidance in shaping my educational experience and insightful suggestions regarding my scientific projects.

Next, I need to thank all of the members of the Kielian lab past and present that I have had the pleasure working alongside over the past 5 years. Mark Hanke, Cortney Heim, Debbie Vidlak, Amy Aldrich, and Amanda Angle welcomed me into the lab and patiently showed me the ropes and helped me considerably with completing my projects and maintaining my sanity. Richa Hanamsagar, Jane Xiong, Nikolay Karpuk, Maria Burkovetskaya, Rachel Fallet, Jessica Odvody, Megan Bosch, and Venkata Kakulavarapu have all provided valuable feedback on my research and/or contributed directly to the success of my experiments. Finally, Casey Gries, Kelsey Yamada, and Anna Staudacher have more recently been a pleasure to work with and near on the Staph side of the lab, and I owe each of them a debt of gratitude for their assistance as well.

I also owe a big thank you to several members of the Fey, Bayles, Chittezham Thomas, and Snowden labs past and present for their assistance on various projects: Cortney Halsey, Carolyn Schaeffer, Austin Nuxoll, Jill Lindgren, Marat Sadykov, Jennifer Endres, Derek Moormeier, Vijaya Yajjala, Todd Widhelm, Matthew Beaver, Vinai Chittezham Thomas, and Sujata Chaudhari. Several of our collaborators have also been instrumental to my project, including Dr. Jeffrey Bose, Dr. Alex Horswill, Dr. Keer Sun, Dr. Victor Torres, and Dr. David James. I also owe a special thanks to members of the UNMC Proteomics Facility (Dr. Pawel Ciborowski and Jayme Horning) and the UNMC Flow Cytometry Facility (Dr. Charles Kuszynski, Dr. Phil Hexley, Victoria Smith, and Sam Wall) for their patience and assistance with several experiments.

Finally, I would like to thank my family and friends for their unceasing love and support. First and foremost, to my beautiful wife Joelle, without whose constant support none of this would have been nearly as successful. Next, my wild son Jax, who gives me a fresh perspective every day and without whom none of this would be nearly as meaningful. To my parents, who shaped me and without whom none of this would have been possible. To my family, who provided love and support throughout my life and balance the past five years, especially my sister, Jennie, brothers-in-law Ryan and Josh, my parents-in-law Tom and Kerry, and my Perry. And to all of my UNMC friends who have made this journey in part or full with me (including the BRTP class of 2011, Intramural Disc Golfers, 2015 GSA Officers, and UNMC Makers); I could have definitely gotten my Ph.D. without you, but it most definitely would not have been as fun!

Abbreviations:

Agr	Accessory gene regulator
AIP	Autoinducing peptide
ANOVA	Analysis of variance
BHI	Brain-heart infusion
BMDMΦ	Bone marrow-derived macrophage
CA-MRSA	Community-acquired Methicillin-resistant *Staphylococcus aureus*
CFU	Colony forming units
DMEM	Dulbecco's Modified Eagle's Medium
DNA	Deoxyribonucleic acid
ECM	Extracellular matrix
eDNA	extracellular DNA
ELISA	Enzyme-linked immunosorbent assay
Erm	Erythromycin
EtOH	Ethanol
FACS	Fluorescence-activated cell sorting
FBS	Fetal bovine serum
Fc	Fragment, crystallizable
FITC	Fluorescein isothocyanate
GFP	Green fluorescent protein
GM-CSF	Granulocyte-macrophage colony-stimulating factor

HEPES	4-(2-hydroxyethyl)-1-piperazineethanesulfonic acid
Hla	α-hemolysin
HRP	Horseradish peroxidase
IFN	Interferon
Ig	Immunoglobulin
IL	Interleukin
iNOS	Inducible nitric oxide synthase
i.p.	Intraperitoneal
KO	Knockout
K-wire	Kirschner wire
LAC	Los Angeles County
L-glut	L-glutamine
LTA	Lipoteichoic acid
LukAB	Leukocidin AB
МΦ	Macrophage
MACS	Magnetic-activated cell sorting
M-CSF	Macrophage colony-stimulating factor
MDSC	Myeloid-derived suppressor cell
MRSA	Methicillin-resistant *Staphylococcus aureus*
MSCRAMM	Microbial surface components recognizing adhesive matrix molecules
MET	Macrophage extracellular trap

MyD88	Myeloid differentiation primary response gene 88
NADPH	Nicotinamide adenine dinucleotide phosphate
NET	Neutrophil extracellular trap
NOD2	Nucleotide-binding oligomerization domain-containing protein 2
NOS	Nitric oxide synthase
OD	Optical density
PAMP	Pathogen associated molecular pattern
PBP2a	Penicillin-binding protein 2a
PBS	Phosphate-buffered saline
PCR	Polymerase chain reaction
PE	Phycoerythrin
PerCP	Peridinin-chlorophyll-protein complex
PFA	Paraformaldehyde
PGN	Peptidoglycan
PIA	Polysaccharide intercellular adhesion
PJI	Prosthetic joint infection
PMN	Polymorphonuclear cell
PRR	Pattern recognition receptor
PVL	Panton-Valentine Leukocidin
qRT-PCR	Quantitative real time-polyemerase chain reaction
RNA	Ribonucleic acid

ROS	Reactive oxygen species
RPMI	Roswell Park Memorial Institute
S. aureus	*Staphylococcus aureus*
s.c.	Subcutaneous
SCC	Staphylococcal cassette chromosome
S. epidermidis	*Staphylococcus epidermidis*
TCR	T cell receptor
TNF	Tumor necrosis factor
TSA	Tryptic soy agar
TSB	Tryptic soy broth
WT	Wild-type

List of Figures and Tables

University of Nebraska Medical Center

Omaha, NE

September, 2016

STAPHYLOCOCCUS AUREUS BIOFILMS INTERFERE WITH MACROPHAGE ANTIMICROBIAL RESPONSES THROUGH DIFFERENTIAL GENE REGULATION, TOXIN PRODUCTION, AND PURINE METABOLISM

Tyler Scherr, Ph.D.

University of Nebraska Medical Center, 2015

Advisor: Tammy Kielian, Ph.D.

Abstract

Staphylococcus aureus (*S. aureus*) is an opportunistic pathogen that is a leading cause of both nosocomial and community-associated infections. Armed with a myriad of virulence factors and the propensity to form a biofilm on native tissues and implanted medical devices alike, *S. aureus* infections represent a very real public health threat, the treatment of which results in an excessive economic burden. *S. aureus* biofilm infections are notoriously recalcitrant to antibiotic therapy and adept at evading and neutralizing the host immune antimicrobial response. Previous studies from our laboratory have shown that *S. aureus* biofilms are able to cause persistent infections, in part, through the reprogramming of the macrophage (MΦ) immune response. While macrophages are readily able to recognize and respond to *S. aureus* in a planktonic state, their ability to mount a functional antimicrobial attack is thwarted upon encountering *S. aureus* biofilm. We have observed that MΦs in close proximity to *S. aureus* biofilms are less phagocytic and skewed towards an anti-inflammatory profile typified by arginase and IL-10 production. We have demonstrated that the ability of *S. aureus* biofilms to cause chronic infections is due, in part, to TLR2 or TLR9 evasion. However, we have shown that MyD88 signaling does provide some benefit to the host in combating *S. aureus* biofilm infections, which may be attributed to IL-1 receptor signaling. To better understand how *S. aureus* biofilms subvert the MΦ antimicrobial response, the work described in this dissertation assessed *S. aureus* transcriptional activity during co-culture with MΦs, whether *S. aureus* biofilms inhibit MΦ activity through secreted molecules, and performed a high-throughput screen of the Nebraska Transposon Mutant Library to identify key genes involved in dampening the MΦ NF-κB-regulated proinflammatory response. We found that *S. aureus* biofilms attenuate their transcriptional activity following MΦ exposure, augment α-hemolysin (Hla) and leukocidin AB (LukAB) secretion to inhibit MΦ phagocytosis and induce cell death, and rely on a functional purine biosynthetic pathway to prevent MΦ invasion and phagocytosis, in part, through controlling the amount of eDNA available for MΦ recognition at

the surface of the biofilm extracellular matrix (ECM). Collectively, these studies build upon our previous observations by identifying key mechanisms whereby *S. aureus* biofilms are able to thwart the MΦ antimicrobial response.

Chapter 1: Introduction

1) *Staphylococcus aureus* (*S. aureus*) biofilm infection

a) Methicillin-resistant *S. aureus* (MRSA)

Staphylococcus aureus (*S. aureus*) is a gram-positive, opportunistic pathogen that in the past few decades has become a leading cause of both nosocomial and community-associated infections (1). *S. aureus* is the most virulent of the staphylococcus genus, with the ability to cause a wide range of diseases, from relatively minor skin and soft tissue infections (SSTIs) to more severe pneumonia and sepsis potentially leading to toxic shock syndrome (2). *S. aureus* has remained a successful pathogen throughout the antibiotic era due, in part, to its propensity to rapidly acquire antibiotic resistance, and methicillin-resistant *S. aureus* (MRSA) is no exception. Methicillin, a beta-lactamase insensitive beta-lactam that is bacteriocidal by inhibiting peptidoglycan synthesis, began being used in the 1950s in response to the emergence of penicillin-resistant *S. aureus* (PRSA). However, within ten years MRSA isolates began to emerge in hospitals across the US, with one of the first known incidences occurring at Boston City Hospital (3). Through the intervening decades, MRSA continued to slowly spread, but generally only affected immune compromised patients, until the late 1990s when a dramatic surge in MRSA rates began (4). It was around this time that community-associated MRSA (CA-MRSA) began to occur outside of hospitals, inflicting otherwise healthy individuals (5) who, had historically encountered primarily methicillin-sensitive *S. aureus* (MSSA) strains.

CA-MRSA infection is now considered a worldwide epidemic and SSTIs are common, particularly among athletes, children, homeless persons, military personnel, and many other groups (6). While exact numbers vary from study to study, some reports place the percentage of CA-MRSA as responsible for over 50% of all CA-*S. aureus* infections (7). The emergence of MRSA coincides with the ability of *S. aureus* to express a low-affinity penicillin binding protein (PBP) known as PBP2a (3), which is encoded by the *mecA* gene and carried on a mobile genetic element known as Staphylococcal Cassette Chromosome (SCC) mec (8), which also contains

intact or truncated sets of the divergently transcribed regulatory genes, mecR1 and mecI (3). In the presence of beta-lactams, such as methicillin, mecR1 cleaves mecI bound to the operator region of the *mecA* promoter, thereby de-repressing PBP2a production (9). Since methicillin cannot bind PBP2a, cell wall synthesis is able to proceed and *S. aureus* is able to replicate in its presence (3). While both are MRSA, CA-MRSA usually differs from nosocomial MRSA in that it harbors smaller SCCmec variants, Type IV and V, is less resistant to other types of antibiotics, produces more toxins including Panton-Valentine Leukocidin (PVL), and most commonly causes SSTIs (3).

b) *S. aureus* biofilms

Many bacteria can form biofilms, which are generally defined as an adherent community of bacteria encased within a self-produced matrix typically composed of a combination of exopolysaccharides, proteins, and extracellular DNA (eDNA) (10-12). The biofilm composition is often dependent on environmental factors, such as nutrient availability and mechanical stress (11). As biofilms represent a distinct lifestyle, biofilm-associated bacteria exhibit an altered phenotype from planktonic cells with regard to metabolism, gene expression, and protein production , undoubtedly in part due to nutrient, pH, and oxygen gradients present throughout the characteristic tower-like biofilm structures (13). Biofilms represent a communal virulence determinant to circumvent immune-mediated clearance and establish persistent infection (13-16). Most medical device-associated biofilm infections are caused by *S. epidermidis* and *S. aureus*, and both species can also establish biofilms on native host surfaces, such as heart and bone tissue (17-19). The biofilm mode of growth has been recognized as a major mediator of infection, contributing to an estimated 80% of all infections (20).

Biofilm formation is classically considered to occur in a stepwise fashion, consisting of initial attachment, cell aggregation (21, 22) and proliferation, accumulation of an ECM and tower formation, and detachment of cells and biofilm dispersal (10, 23, 24). Initial attachment is

believed to be largely physico-chemical in nature, due to features such as hydrophobicity during the process of passive adsorption (10, 24). *S. aureus* can form biofilms on both native tissue and abiotic surfaces, and while the specific mechanisms for attachment likely differ between the two types of surfaces, it is believed to be mainly governed by the interaction of bacteria with human matrix proteins either present on native tissue or deposited on implanted medical devices shortly after placement (24). Following initial attachment, *S. aureus* cells begin to accumulate and aggregate into multiple layers in a process that is largely mediated by the expression of microbial surface components recognizing adhesive matrix molecules (MSCRAMMs) (10). As the name suggests, these are surface-attached proteins (e.g. fibronectin- and fibrinogen-binding proteins)(25, 26) that help anchor the bacteria to the surface by linking with human matrix proteins (24). Next, cells began to proliferate and form biofilm structures through the production of exopolysaccharides (e.g. polysaccharide intercellular adhesion [PIA]) (27-29), proteins (e.g. *S. aureus* surface proteins C and G [SasC, G]) (30, 31), and eDNA (10, 24, 32). The formation of channels and tower-like structures are thought to facilitate nutrient and waste exchange within the base of the biofilm (13, 23). Finally, upon full maturity biofilm-associated bacteria begin to detach, facilitating biofilm dispersal in a process influenced by quorum-sensing (QS). QS is a phenomenon whereby increased bacterial cell density triggers changes in gene expression and, in *S. aureus*, is governed, in part, by the accessory gene regulator (*agr*) system (24).

c) *S. aureus* prosthetic joint infections (PJIs)

An increasing world population coupled with increased life expectancies has led to a progressive rise in primary and revision arthroplasties (33). By 2030, the demand for primary total hip and knee arthroplasties in the United States alone is estimated to increase by 174% and 673%, respectively, over the number of procedures performed in 2005 (17). Due to its commensal nature, it has been estimated that 20% of healthy adults are *S. aureus* carriers, typically in the nasal cavity, with another 60% experiencing transient carriage (34), placing a vast majority of the

adult population at increased risk of infection (35). Infection is the major complication of orthopedic implants, with incidences reportedly between 1-2% for both knee and hip replacements (36-40), and *S. aureus* is a leading cause of orthopedic implant infections with serious morbidity and mortality outcomes (17, 41) in large part due to its ability to form a biofilm. Biofilm infections are recalcitrant to antibiotics (42, 43), which often necessitates removal of the infected device or native tissue, and are associated with significant morbidity and economic impact (17, 44, 45). Indeed, it has been estimated that approximately $1.8 billion is spent annually in the US for the treatment and clinical management of orthopedic implant-related infections (46, 47).

While the exact mechanisms of prosthetic infection are still unclear, studies have indicated that the presence of a foreign body reduces the minimal inoculum of *S. aureus* required to cause infection by a factor of greater than 10^5 (48, 49). Experimental evidence in animal models, for instance, have shown that an infection can occur with fewer than 100 colony forming units (CFU) of microorganisms, and despite the use of perioperative antimicrobial prophylaxis, when a foreign body is present (50). These animal observations have seemingly held true in human patients as well, with higher relapse of infection following bacteremia in patients with orthopedic implants, 30-40% of which followed *S. aureus* bacteremia (51, 52).

d) Mouse models of *S. aureus* prosthetic joint infection (PJI)

There are currently two published murine models of *S. aureus* PJI, both of which explore static biofilm growth and host-pathogen interactions during a persistent infection in an implant-associated osteomyelitis setting, but which differ slightly in placement of the metal implant and observed host response. In the mouse tibial implant model, C57BL/6 mice have been shown to establish a chronic infection resulting in upregulation of IL-2, IL-12p70, TNF-α, IL-1β, IL-6, and IL-17 (53). In this model, it has been proposed that early activation of the inflammatory response may not only be ineffective at microbial clearance, but may also be detrimental to the host due to

collateral tissue damage caused by neutrophil (PMN) activation and inflammatory mediator influx. In contrast, the early inflammatory response gives way to a chronic anti-inflammatory milieu during the femur implant model, typified by myeloid-derived suppressor cell (MDSC) infiltration in part through IL-12p70-mediated recruitment, a dampening of proinflammatory signaling (e.g. IL-1β and IL-6), an increase in anti-inflammatory signaling (e.g. IL-10) (54-56).

2) *S. aureus* virulence and host immune evasion

a) Accessory gene regulator (*agr*)

S. aureus regulates protein production via a number of two-component systems, including a bacterial density-dependent mechanism of cell-to-cell communication known as QS. QS operates through the secretion and detection of a signal molecule, in this case autoinducing peptide (AIP), which triggers a cascade of cellular responses (57). In *S. aureus*, the QS system is encoded by the *agr* locus, composed of four co-transcribed genes (*agr*A, *agr*C, *agr*D, and *agr*B) encoding a two-component trans-membrane transduction complex, a pro-signaling peptide, and a membrane transporter (58). In *S. aureus*, at least four *agr* allelic genes exist that are characterized by a specific signaling peptide (numbered I to IV) and it has been observed that the *agr* activity within a group inhibits that of the other groups (59). The effector molecule of the *agr* system is a regulatory RNA, RNAIII, whose synthesis is dependent on *agr* activation and driven by the P3 promoter (10). Altogether, the *agr* system acts as a trigger, switching from the expression of surface-associated proteins to secreted proteins and has been shown to regulate numerous virulence factors (e.g. α-toxin, leukocidins, phenol-soluble modulins [PSMs], adhesins, proteases, etc.) and even play a role in the biofilm maturation process (60, 61). For example, the DNA-binding regulatory protein SarA is critical for biofilm formation and virulence factor expression in *S. aureus* and SarA acts, in part, through the accessory gene regulator *agr*, which can thus be thought of as an important regulatory switch between planktonic and biofilm lifestyles (62-65).

b) Microenvironment modulation

Previous work has characterized numerous secreted virulence factors used by staphylococci that target specific host cell populations. *S. aureus*, in particular, utilizes numerous hemolysins (66), leukocidins (67, 68), and proteases to evade the host immune system (69). While staphylococci certainly divert resources from secreted to structural proteins during early biofilm growth, protein secretion is still maintained in biofilms. For example, several reports have demonstrated that various bacterial biofilm-forming species secrete peptides and full-length proteins (i.e. Esp) that interfere with biofilm development of competing organisms, presumably to eliminate competition for a biofilm-friendly niche (70-72). Additionally, studies have demonstrated evidence of host-biofilm cross-talk involving the QS molecules N-Acyl homoserine lactones (AHL), presumably to facilitate biofilm formation and bacterial persistence (73, 74). Therefore, it is likely that staphylococcal biofilms also secrete factors *in vivo*, perhaps under QS system regulation, in an attempt to evade immune recognition and clearance. For example, we have recently shown that *S. aureus* biofilms are uniquely enriched in Hla and LukAB in an *agr*-dependent manner *in vitro* and that the ability of *S. aureus* biofilm-conditioned medium to inhibit MΦ phagocytosis is partially dependent on an intact biofilm (75). However, the identity of such molecules remains to be elucidated but could represent future attractive anti-biofilm agents (76).

Besides virulence factors, staphylococci also secrete molecules for nutrient procurement and cell signaling. For example, siderophores are critical for iron acquisition (77), while several signaling molecules are important for biofilm remodeling and dispersal, such as AIP (65), nuclease (78), and PSMs (79). While the primary roles of these molecules are apparently unrelated to immune interactions, recent evidence suggests the potential for alternative functions. For example, nuclease, which mediates biofilm dispersal (64, 78), can also participate in neutrophil extracellular trap (NET) degradation (80). Recently, nuclease in combination with adenosine synthase has been implicated in the conversion of NETs to leukotoxic deoxyadenosine, highlighting a clever means whereby *S. aureus* turns the immune response against itself (81). In

addition, *S. aureus* PSM expression is induced following PMN phagocytosis, resulting in PMN lysis and bacterial escape (79, 82, 83). This process is regulated by the stringent response characterized by the synthesis of the intracellular signaling alarmone (p)ppGpp (83). Therefore, the stringent response provides yet another means of staphylococcal adaptation in response to select immune pressures, something that has previously been well-established in relation to nutrient availability and metabolism (84-89). Indeed, recent evidence has implicated (p)ppGpp and di-cyclic NTPs as critical signals in the switch from planktonic to biofilm growth (76, 90).

However, secreted factors are not the only means whereby staphylococcal biofilms could regulate the host response in an exogenous manner. While bacteria have a plethora of environmental sensory mechanisms at their disposal, host immune cells are also very sensitive to their surrounding environment (91-93). Because biofilms represent a large biomass, the sum metabolic activity of the bacteria themselves would be expected to have an impact on pH and oxygen levels in the surrounding tissue microenvironment. Indeed, even subtle changes in pH (92, 94) or oxygen (91) can significantly alter the nature of the immune response. Furthermore, novel research with fungal and bacterial biofilms has identified a coordinated system of ROS signaling for biofilm maturation (95). It will be interesting to see what, if any, impact this biofilm ROS gradient has on the host immune response and whether host-generated ROS can also act as a signaling molecule within the biofilm to influence target pathways, such as biofilm formation via QS (76, 95).

3) Innate immune response to *S. aureus* infection

a) Innate immune recognition of *S. aureus*

The innate immune system is well equipped to recognize foreign invaders through germ-line encoded pattern recognition receptors (PRRs) that identify broad, highly conserved microbial patterns known as pathogen-associated molecular patterns (PAMPs) (96). One such class of PRRs is the Toll-like receptors (TLRs), which are responsible for the recognition of several key PAMPs

from both gram-positive and gram-negative bacterial pathogens (97, 98). Of particular importance to *S. aureus* infections are TLR2 and TLR9, which recognize PGN and lipoproteins in the bacterial cell wall and unmethylated CpG motifs characteristic of bacterial DNA, respectively (99-102). TLR2 is expressed on the outer cell surface where it recognizes its ligands that are naturally secreted and/or released from growing bacteria. TLR9, on the other hand, is an intracellular receptor that could engage liberated bacterial DNA following phagocytosis and degradation in the phagosome. In total, 12 TLRs have been identified in mice and 10 in humans, each with their own unique ligand specificity (96, 103). While TLRs recognize different bacterial PAMPs, most utilize a common signaling pathway through myeloid differentiation factor 88 (MyD88) and NF-κB that results in the transcriptional activation of several proinflammatory cytokines and chemokines (104-107) that are critically important for coordinating an effective antimicrobial immune response.

Although TLRs have been demonstrated to be critically important in mediating innate immune recognition and clearance of *S. aureus* during planktonic growth (101, 108-111), several recent studies have shown that *S. aureus* biofilms are able to circumvent TLR2 and TLR9 recognition (15, 56). These findings also agree with the observations that TLR2-deficient patients show no increased risk of developing post-arthroplasty *S. aureus* infections (112). While the mechanism responsible for TLR2/9 evasion by *S. aureus* biofilms are unknown, this could in part be explained by ligand inaccessibility via the protective barrier provided by the complex biofilm ECM (16). However, it is still possible that *S. aureus* biofilms may be recognized by alternative PRRs, such as AIM2, DNA-dependent activator of IFN-regulator factors (DAI), and nucleotide-binding oligomerization domain-containing protein 2 (NOD2) (113-116). Additionally, while TLR2 and TLR9 do not appear to be important for *S. aureus* biofilm recognition and clearance, IL-1β has been demonstrated to be critical for controlling early bacterial burdens in PJI (56). Likewise, studies from our laboratory and others have shown that MyD88 signaling is critical for

controlling bacterial burdens during *S. aureus* biofilm infections (15, 117, 118). Interestingly, both the IL-1 receptor (IL-1R) and TLRs signal through the adaptor MyD88 for the eventual induction of NF-kB-mediated transcription (16).

b) MΦ and neutrophil (PMN) response to planktonic *S. aureus*

The MΦ is a key innate immune responder that resides in nearly all tissues in the body and arises upon maturation from extravasating monocytes from the peripheral circulation (119-121). MΦs are highly plastic in that they can display a spectrum of functional states depending on their environment. For example, *in vitro* experimentation has shown that monocytes treated with granulocyte-macrophage colony-stimulating factor (GM-CSF) and inflammatory stimuli such as PAMPs give rise to microbicidal M1 MΦs, whereas monocytes treated with macrophage colony-stimulating factor (M-CSF) and IL-4 give rise to anti-inflammatory M2 MΦs that function in tissue repair and fibrosis (122-124). *In vivo*, however, the situation is believed to be more complex, with MΦ functionality existing on a dynamic spectrum of polarized states. Previous work from our laboratory and others has shown that upon encountering *S. aureus* in a planktonic state, MΦs become classically activated (M1) and exert their microbicidal effector functions, in part, through the production of reactive oxygen and nitrogen species, in addition to proinflammatory cytokines (125-128). MΦs also clear planktonic bacteria by phagocytosis, which is tightly linked with proinflammatory cytokine and chemokine production to initiate adaptive immune responses (129-131). Collectively, these innate leukocyte responses, coupled with complement activation, usually ensure the successful clearance of planktonic staphylococcal infections in an immune competent host.

The neutrophil (PMN) is typically the most prominent cellular component of the host innate immune response to bacterial infections (132). PMNs are frequently the first responders to microbial invaders and, as such, it has been observed that individuals with PMN defects (e.g. chronic granulomatous disease) are highly susceptible to severe and life-threatening *S. aureus*

infections (133). PMNs originate and mature in the bone marrow, maintain immune surveillance by circulating in the peripheral vasculature, and are rapidly recruited to infected tissues through chemotactic signals produced by host cells (e.g. IL-8, GRO-alpha, and MIP-2) (134-136) and/or shed and secreted bacterial molecules (e.g. lipoteichoic acid or *n*-formyl peptides) (109, 137-141). Upon encountering a foreign invader, PMNs will attempt to phagocytose the microbes, a process which can be stimulated by PRRs but greatly enhanced when the pathogens are opsonized with host serum molecules, including antibodies and cleavage products of the complement cascade (142-146). Upon phagocytosis, PMNs use both oxygen-dependent (e.g. NADPH-dependent oxidase) (147-150) and oxygen–independent (e.g. granules containing microbicidal agents such as cathepsins) (151-154) processes to kill microbes. Recently, PMN and MΦ extracellular traps (NETs and METs, respectively) have been identified as another means of antimicrobial action (80, 155-157). This "beyond the grave" mechanism is typified by an extracellular net of DNA released from dying phagocytes that contains localized islands of lytic enzymes that kill ensnared extracellular bacteria. Collectively, these innate leukocyte responses, coupled with complement activation, usually ensure the successful clearance of planktonic staphylococcal infections in an immune competent host (76).

c) MΦ and PMN response to *S. aureus* biofilms

In contrast to planktonic *S. aureus* infections, a very different scenario has emerged regarding biofilm infections. Recent studies have demonstrated that staphylococcal biofilms actively skew host immunity toward an anti-inflammatory, pro-fibrotic response that favors bacterial persistence (15, 158-160). This is typified by alternatively-activated (M2) MΦs and arginase-1 (Arg1) activity, resulting in urea and ornithine production, which are involved in collagen formation and tissue remodeling (127, 161, 162). Our laboratory has shown that MΦs associated with *S. aureus* biofilms both *in vitro* and *in vivo* have decreased inducible nitric oxide synthase (iNOS) concomitant with increased Arg1 expression, as well as attenuated cytokine and

chemokine production (15, 159, 160). Similar findings have been reported in response to *S. epidermidis* biofilms (158, 163-165) and biofilms from other bacterial species (166-169), suggesting a conserved mechanism exists to thwart host immunity to ensure biofilm persistence (76, 170).

4) Overview of dissertation

Initial experiments from our laboratory demonstrated that *S. aureus* biofilms were able to cause persistent infections, in part, through the reprogramming of the MΦ immune response (15). Specifically, we observed that MΦs in close proximity to *S. aureus* biofilms were less phagocytic and skewed towards an anti-inflammatory M2 profile typified by Arg1 and IL-10 expression (15). We hypothesized that this was due, in part, to the physical barrier presented by the biofilm ECM, and that this matrix could be facilitating immune evasion by occluding otherwise recognizable PAMPs as well as inducing "frustrated phagocytosis". Additionally, we found that *S. aureus* biofilms evade TLR2- and TLR9-mediated recognition in a murine model of biofilm infection (15). However, we did demonstrate that MyD88 signaling does provide some benefit to the host in combating *S. aureus* biofilm infections and that injecting exogenously activated M1 MΦs into an established biofilm infection can promote clearance *in vivo* (159, 160).

During the course of my research, I have further identified multiple mechanisms that contribute to *S. aureus* biofilm evasion of MΦ antimicrobial activity. First, I determined that *S. aureus* biofilm-associated bacteria dampen their transcriptional activity upon encountering MΦs, perhaps allowing the bacteria to limit the possibility of MΦ detection (171). Next, I observed that *S. aureus* biofilm-conditioned medium is able to inhibit MΦ activation and induce MΦ cell death due to heightened Hla and LukAB production (75). Finally, I performed a high-throughput screen of the Nebraska Transposon Mutant Library and discovered the importance of purine biosynthesis towards the ability of *S. aureus* biofilms to prevent MΦ phagocytosis. My research adds to the growing literature describing the ability of *S. aureus* biofilms to circumvent the MΦ antimicrobial

response and highlights some potential targets for novel treatments and prevention of chronic biofilm related infections.

Chapter 2: Materials and Methods

1) Bacterial strains and microbiological techniques

Bacterial strains

S. aureus USA300 LAC is a community-associated methicillin-resistant (CA-MRSA) strain isolated from a Los Angeles county (LAC) jail inmate with a SSTI and was also responsible for the CA-MRSA outbreak of 2002 (172-175). We received the isolate from Dr. Frank DeLeo (National Institute of Allergy and Infectious Diseases Rocky Mountain Laboratories, Hamilton, MT) and cured it of its 27 kb LAC-p03 plasmid encoding erythromycin resistance (176) by screening for spontaneous erythromycin sensitivity as previously described and was designated as USA300 LAC 13C. For the purposes of this thesis, this wild type strain will be referred to as USA300 LAC. The isogenic USA300 LAC *agr* mutant (*Δagr*) was provided by Dr. Alex Horswill (University of Iowa Medical Center, Iowa City, IA) (11). The isogenic LAC Δ*hla* strain was constructed by an insertion mutation using site-directed mutagenesis with the pE194 erythromycin resistance cassette (*ermB*) as previously described (177), with a *hla* complemented strain (177) and a *hla* constitutively active strain (178) included to confirm the specificity of toxin action. The USA300 JE2 Nebraska Transposon Mutant Library (NTML) (179) mutants, Δ*lukA/H*, Δ*lukB/G,* Δ*lukD*, Δ*spl*, and Δ*purB* were moved to the USA300 LAC 13C background by transduction with Φ11 bacteriophage. Allelic replacement mutants of *lukA* and *lukB* and complemented strains were generously provided by Dr. Victor Torres (New York University, New York, NY). *In vitro* complementation of the USA300 Δ*purB* strain was performed by the introduction of a functional *purB* gene on the pCM29 plasmid (180) under induction by the *sarA* promoter, named pTS1. *In vivo* complementation of the USA300 Δ*purB* strain was performed by the introduction of a functional *purB* gene with the native promoter on the pKK22 plasmid generously provided by Dr. Jeffrey Bose (University of Kansas Medical Center, Kansas City, KS). For confocal imaging, all strains were either transformed with pCM11 (erm10) or pCM29 (ca10) to express GFP driven by the *sarA* P1 promoter.

Bacterial storage and preparation

Bacterial strains were stored as glycerol stocks at -80^{0}C, struck out on fresh TSA plates containing antibiotics for selection when necessary, and grown overnight at 37^{0}C prior to experimentation. A new streak plate was prepared for each experiment in an effort to avoid mutation of bacteria by prolonged storage at 4^{0}C. For experimentation, overnight cultures were grown in the desired medium by selecting a single bacterial colony from the streak plate using a sterile loop and incubating at 37^{0}C overnight for 12-16 h with constant shaking at 250 rpm.

***In vitro S. aureus* biofilms**

Sterile 12-well plates (Falcon, Corning, NY) or sterile 2-well glass chamber slides (Nunc, Rochester, NY) were treated with 20% human plasma overnight at 4° C to facilitate bacterial attachment. The following day, plasma coating buffer was removed and each chamber inoculated with USA300 LAC at an OD_{600} of 0.05, whereupon bacteria were incubated at 37° C under static aerobic conditions for a period of up to 6 days to generate mature biofilms. Our prior studies have demonstrated that 6 day-old *S. aureus* biofilms propagated in RPMI-1640 are mature based on the presence of tower structures and thickness (15, 160). Medium was carefully replenished every 24 h, and biofilms were visualized using a Zeiss laser scanning confocal microscope (LSM 510 META; Carl Zeiss, Oberkochen, Germany). Z-stacks were collected from beneath the glass slide extending to above the point where bacteria could no longer be detected. Three-dimensional images of biofilms and measurements to demonstrate biofilm thickness were performed using Zen 2009 and 2012 software (Carl Zeiss).

2) Mouse strains

A breeding colony of C57BL/6 mice was established in Dr. Kielian's laboratory after purchasing animals from the National Cancer Institute (Frederick, MD) or Jackson Laboratories (Bar Harbor

ME). These studies were performed in strict accordance with the recommendations provided in the Guide for the Care and Use of Laboratory Animals of the National Institutes of Health (NIH) and were reviewed by the Institutional Animal Care and Use Committee of the University of Nebraska Medical Center.

BALB/c NF-κB luciferase (NF-κB-luc) reporter mice (Caliper Life Sciences; Hopkinton, MA) were generously provided by Caliper Life Sciences. These mice produce firefly luciferase under the control of the mouse NF-κB promoter, allowing for the measurement of luminescence when cells are provided with the substrate luciferin as an indicator of inflammatory status.

GFP transgenic (Tg) mice (C57BL/6-Tg[CAG-EGFP]) were purchased from The Jackson Laboratory (Bar Harbor, ME). These mice produce GFP under the control of a chicken beta-actin promoter and cytomegalovirus enhancer, which makes all of the tissues, with the exception of erythrocytes and hair, appear green under excitation light.

TLR9 KO mice were obtained from The Jackson Laboratory (Bar Harbor, ME). These mice do not express TLR9 and are therefore deficient in the ability of their immune cells to recognize foreign, unmethylated CpG-DNA.

MyD88 KO mice (originally from Dr. S. Akira, Osaka University, Suita, Osaka, Japan) (26) were purchased from the Centre de La Recherche Scientifique and have been previously backcrossed with C57BL/6 mice for over 10 generations (29, 34). These mice do not express the adaptor protein MyD88 which functions downstream of most TLR signaling pathways, connecting bacterial PAMP recognition to NF-κB activity.

3) Cell culture techniques

Primary mouse bone marrow-derived macrophage (BMDMΦ) culture

Adult BALB/c NF-κB-luc, C57BL/6 WT, CAG-EGFP, TLR9KO, and MyD88 KO mice were euthanized with an overdose of inhaled isoflurane (Isothesia, VetUS, Dublin, OH) using a euthanasia chamber and cervical dislocation as the secondary method of euthanasia. The abdominal surface of each mouse was washed with an excess of 70% EtOH to minimize contamination and a subcutaneous incision was made near the midline of the abdomen opening up the peritoneum. Skin was separated until the hind limbs were exposed and excess muscle was dissected away, allowing for the hind limbs to be removed at the hip joint and placed in 1X PBS on ice. Hind limbs were then submerged in 70% EtOH, excess tissue and muscle was removed with Kimwipes, and clean bones were placed in fresh 1X PBS on ice. The following steps were performed under aseptic conditions in a biological safety cabinet with sterile autoclaved instruments. Both ends of the bones were cut with scissors and bone marrow was flushed with sterile, cold DMEM using a 26-gauge needle into a 50ml conical tube. Once all bones were flushed, cells were pipetted to disrupt aggregates, filtered through a 70µm cell strainer, and centrifuged at 1,200 rpm for 5 min at 4^0C. The supernatant was aspirated and red blood cells lysed by the addition of 900µl sterile water for 5 sec, followed by 100µl 10X PBS to restore osmotic pressure. Finally, cells were washed with medium, centrifuged, and counted using trypan blue (Lonza, Walkersville, Germany) on a hemacytometer. Cells were plated in 175mm^2 tissue culture dishes at a density of 10^7 cells/plate in 15ml of medium. BMDMΦ medium was composed of Dulbecco's modified eagle's medium (DMEM, 4.5g/L glucose supplemented with 4mM L-glutamine) containing heat-inactivated fetal bovine serum (10% v/v FBS, HyClone, Logan, UT; inactivated at 55^0C for 30 min, with mixing at 10 min intervals), 20% conditioned medium from L929 cells (ATCC) as a source of MΦ colony stimulating factor (M-CSF) (181) or 40ng/ml M-CSF (eBioscience Inc., San Diego, CA), 1% v/v HEPES, 1% v/v Glutamine (both HyClone,

South Logan, UT), 0.1% v/v 50 mM Beta-mercaptoethanol (Fischer Scientific, Pittsburgh, PA) and antibiotic/antimycotic solution (penicillin, streptomycin, and ampotericin B, final 1% v/v, Mediatech Inc., Manassas, VA). Medium was changed on cultures at days 2, 4, and 6 after initial plating and cells were harvested on day 7 for experimentation.

Neutrophil isolation from the mouse bone marrow

Adult C57BL/6 mice were euthanized and bone marrow was isolated as previously described above and placed on a three-layer Percoll gradient (Amersham Pharmaca, Biotech, Uppsala, Sweden). After filtration, cells were centrifuged at 400 x *g* for 10 min at 4°C, resuspended in 3 ml of 78% Stock Isotonic Percoll (SIP, 100% SIP [9 parts Percoll to 1 part 10X PBS] in 1X PBS), followed by layering 3 ml of 69% and 52% SIP on top. The three-layer gradient was then centrifuged at 1500 x *g* for 30 min at 15°C with no brake. PMNs were carefully collected from the 69%/78% interface and upper portion of the 78% layer, washed with PBS, centrifuged at 400 x *g* for 10 min at 4°C, resuspended in 1 ml 1X Lysing Buffer (BD Pharm Lyse, BD Biosciences, Franklin Lakes, NJ) and incubated at room temperature for 2 min. Lysis was stopped by addition of HBSS + 10% FBS and cells were centrifuged at 400 x *g* for 10 min at 4°C prior to resuspsension in 2 ml buffer for magnetic-activated cell sorting (MACS, PBS without Ca, Mg, + 2% FBS), vortexed and counted with trypan blue on a hemacytometer. Magnetic labeling was performed using a Miltenyi anti-Ly6G MicroBead Kit (Miltenyi Biotec, San Diego, CA) according to manufacturer's instructions. Magnetic separation was performed using an MS column on a MACS Separator. Columns were prepared by rinsing with 500 µl buffer, whereupon the cell suspension was added to the column. Unlabeled cells were flushed by washing the column 3X with 500 µl buffer prior to flushing buffer through with a plunger to elute the fraction of labeled cells into a collection tube. Cells were counted and at least 600,000 $Ly6G^+$ cells were removed to check purity by flow cytometry, while the remaining cells were immediately used for experimentation.

4) Immune cell co-culture with *S. aureus* biofilms *in vitro*

Co-cultures for microarray studies

BMDMΦs or PMNs (10^7 and 10^6, respectively) were co-cultured with *S. aureus* biofilms for various periods to assess their impact on the biofilm transcriptome, which equated to a MOI of 10:1 (bacteria/MΦ) or 100:1 (bacteria/PMN). PMNs or BMDMΦs were incubated with biofilms in RPMI-1640 supplemented with 10% FBS at 37° C under static aerobic conditions until they were harvested by mechanical dissociation at two different time points (1 and 24 h for BMDMΦs; 1 and 4 h for PMNs) to collect RNA for microarray analysis.

For visualization of BMDMΦ- or PMN-biofilm interactions, leukocytes were labeled with 5 μM CellTracker Orange or CellTracker Blue (both from Molecular Probes, San Diego, CA) depending on the experimental setup. BMDMΦ and PMN cell death was assessed using Propidium Iodide Staining Solution (eBioscience Inc., San Diego, CA). Leukocyte-biofilm interactions were visualized using a Zeiss laser scanning confocal microscope (LSM 510 META or LSM 710), where Z-stacks were collected from beneath the glass slide extending to above the point where labeled BMDMΦs or PMNs could no longer be detected. Three-dimensional images and measurements to demonstrate leukocyte invasion into the biofilm were performed using Zen 2009 software and Zeiss LSM Image Browser (both from Carl Zeiss).

Co-cultures for ELISA studies

To determine the effect of *S. aureus* biofilms on MΦ cytokine secretion profiles, 10^6 BMDMΦs were incubated with mature USA300 LAC biofilms or planktonic bacteria for 6 h at 37°C under static aerobic conditions as previously described above, whereupon supernatants were clarified by centrifugation and filtration (0.2 μm) to quantitate TNF-α, IL-10, IL-1β (OptiEIA; BD Biosciences, Franklin Lakes, NJ), and IL-1RA (DuoSet; R & D Systems, Minneapolis, MN)

production by ELISA. To account for potential interference by *S. aureus* protein A (Spa) in ELISA assays, two separate controls were utilized; first, biofilm-conditioned supernatants without MΦs were tested, which resulted in minimal cytokine signals. Second, conditioned supernatants from USA300 LAC Δ*spa* biofilm-MΦ co-cultures were also examined and produced similar results to what was observed for isogenic wild type biofilms (data not shown).

Co-cultures prior to FACS

To evaluate whether MΦs exposed to intact biofilms were refractory to further activation with well-characterized microbial antigens, BMDMΦs from GFP Tg mice were co-cultured with USA300 LAC static biofilms or an equivalent number of planktonic bacteria for 2 h as described above and subsequently dissociated by trituration. Next, the suspension was incubated with the vital dye 7-aminoactinomycin D (7-AAD; eBioscience, San Diego, CA) and viable BMDMΦs (GFP^+, $7\text{-}AAD^-$) were recovered by fluorescence-activated cell sorting (FACS). A total of 10^5 biofilm- or planktonic-exposed BMDMΦs were subsequently treated with 10 μg/ml peptidoglycan (PGN), 0.1 μM CpG oligodeoxynucleotide (ODN), or 1 μg/ml of the synthetic lipoprotein Pam3CSK4, or left untreated for an additional 24 h, whereupon supernatants were evaluated for TNF-α and IL-10 production by ELISA (OptiEIA; BD Biosciences).

Co-cultures for eDNA/DNase treatments

For visualization of BMDMΦ-biofilm interactions, BMDMΦs were labeled with 5 μM CellTracker blue (Molecular Probes, San Diego, CA) and added to biofilms in fresh medium for 4-6 h. Propidium iodide staining solution (eBioscience Inc., San Diego, CA) was used to assess eDNA as well as MΦ and bacterial cell death. MΦ-biofilm interactions were visualized using a Zeiss laser scanning confocal microscope (LSM 710 META), where z-stacks were collected from beneath the glass slide extending to above the point where labeled MΦs could no longer be detected. Three-dimensional imaging and measurements to demonstrate MΦ invasion and phagocytosis of biofilm-associated bacteria were performed using Zen 2012 software and the

Zeiss LSM Image Browser (both from Carl Zeiss). In some experiments, biofilms were pretreated for 30 min with 100 U/ml DNase (Sigma, St. Louis, MO) or exogenous eDNA isolated from *S. aureus* biofilm was added to the surface prior to co-culture. Biofilm height and live/dead quantitation was performed using COMSTAT (182) via ImageJ.

5) Nebraska Transposon Mutant Library screens

The Nebraska Transposon Mutant Library (NTML) (179) is a collection of sequence-defined mutants where 1,952 non-essential genes in the *S. aureus* USA300 LAC genome have been disrupted by insertion of the mariner-based transposon, *bursa aurealis* (183). We screened the NTML to identify genes expressed during biofilm growth that influenced MΦ phagocytosis, inflammatory activity, and viability as described below. *S. aureus* mutants that displayed changes in MΦ activity but still formed a biofilm were selected for further analysis.

BMDMΦ phagocytosis

The NTML was screened using a microtiter plate assay to identify biofilm-associated genes regulating secreted products that inhibit BMDMΦ phagocytosis. Briefly, starter cultures of NTML mutants were prepared from glycerol stocks and incubated for 16 h in RPMI-1640 supplemented with 10% FBS and 5 μg/ml erm at 37°C while shaking at 250 rpm under aerobic conditions. 96-well microtiter plates were pre-coated with 20% human plasma diluted in sterile carbonate-bicarbonate buffer (Sigma) at 4°C. The following day, plasma coating buffer was removed and starter cultures were inoculated at a 1:200 dilution and incubated at 37°C under static aerobic conditions for 4 days. Medium was carefully replenished every 24 h using an ep*Motion* 5075 LH robotics platform (Eppendorf, Hamburg, Germany) to minimize cross contamination and prevent disruption of the biofilm structure.

BMDMΦ s were seeded at 10^5 cells/well in tissue culture-treated 96-well plates (Becton Dickinson, Franklin Lakes, NJ) and incubated overnight at 37°C, 5% CO_2, whereupon BMDMΦs were treated for 2 h at 37°C with biofilm-conditioned supernatants diluted 1:2 in fresh RPMI-1640/10% FBS, followed by 1 h incubation with 10^6 yellow-green fluorescent microspheres (2.0 µm particle size; Molecular Probes, San Diego, CA) to assess phagocytic activity. After the 1 h incubation period, BMDMΦs were washed extensively with sterile PBS to remove any residual extracellular microspheres and phagocytic activity was assessed as a measure of total fluorescence using a Victor^{3}V 1420 plate reader (Perkin Elmer, Waltham, MA) or TECAN M200 PRO (Tecan Group Ltd., Mannedorf, Germany) running Magellan 7.0 software (Tecan Austria GmbH, Grodig, Austria).

BMDMΦ NF-κB activation

The NTML was also screened to identify mutants that affected MΦ NF-κB activation during biofilm growth. This assay utilized BMDMΦs from NF-κB-luciferase reporter mice (NF-κB-luc BMDMΦs), where NF-κB promoter activity is detected with the substrate D-luciferin and quantitated using a luminometer. Static biofilms were grown in luminescence-compatible 96-well microtiter plates (Perkin Elmer, Waltham, MA) until mature (as described above), whereupon NF-κB-luc BMDMΦs (10^5/well) were co-cultured with *S. aureus* biofilms for 4 h, after which samples were lysed using ddH_2O and 100 µl/well of D-luciferin (15mg/ml; Gold Biotechnology, St. Louis, MO) was added to detect luciferase expression. Luminescence was quantified using a Victor^{3}V 1420 plate reader (Perkin Elmer). Positive and negative controls included NF-κB-luc BMDMΦs treated with 10 µg/ml *S. aureus* PGN and untreated cells, respectively. Biofilms alone produced minimal luminescence signal compared to background (data not shown).

6) BMDMΦ treatments with biofilm-conditioned medium

Preparation of biofilm-conditioned medium

Static biofilms were generated in two-well glass chamber slides (Nunc, Rochester, NY) or 12-well plates (Becton Dickinson, Franklin Lakes, NJ) with *S. aureus* grown in RPMI-1640 medium supplemented with 1% casamino acids (CAA; Becton Dickinson) as previously described (15, 184, 185). Spent medium was replaced daily, whereupon conditioned medium for experiments was collected from 6 day-old USA300 LAC biofilms 24 h following the last medium change and filtered (0.2 μm). For comparisons, planktonic-conditioned medium was prepared by growing an overnight culture of USA300 LAC to early (12 h) and late (18 h) stationary phase. As no significant differences in phagocytosis or viability were observed when MΦs were treated with conditioned medium from either early or late stationary phase cultures (data not shown), early stationary phase was utilized throughout these studies. Conditioned medium was also collected from 6 day-old USA300 LAC biofilms that were mechanically disrupted by trituration, whereupon the suspension was incubated for another 24 h with fresh medium before collection as described above. Where indicated, biofilm-conditioned medium was treated with 10μg/ml proteinase K for 1h at 37^0C to degrade proteins, or treated with either 10 μg/ml polyanethole sodium sulfanate (PAS) or mechanically disrupted and incubated with 50 μg/ml lysostaphin (both from Sigma, St. Louis, MO) 24 h prior to collection. In some experiments, fresh RPMI-1640 medium was spiked with 10 μg of purified *S. aureus* Hla (Sigma) or 25 μg of purified bioactive or inactive LukAB (186) to examine effects on MΦ phagocytosis and viability. For some experiments, biofilm-conditioned medium was incubated with rabbit anti-staphylococcal Hla antiserum or control rabbit serum (both from Sigma) for 30 min prior to MΦ treatment.

BMDMΦ phagocytosis and cell viability assay

BMDMΦs were prepared and labeled with 5 μM CellTracker Blue (CTB; Molecular Probes, San Diego, CA) as previously described (15, 187). CTB-labeled MΦs were added to sterile 2-well glass chamber slides ($5x10^6$ cells/chamber) and allowed to adhere for 2 h. Next, MΦs were

exposed to conditioned medium collected from *S. aureus* biofilms or planktonic cultures for 2 h at 37°C, whereupon red or green fluorescent microspheres (2.0 µm particle size; Molecular Probes) were added at a concentration of $4.5x10^{10}$ microspheres/ml for 1 h to assess phagocytic activity. Fluorescent microspheres were used instead of intact *S. aureus*, since pilot studies revealed that similar results were obtained with both reagents (Supplemental Fig. S2.1). MΦs were treated with undiluted biofilm- or planktonic-conditioned medium, since a stronger phenotype was observed under these conditions (Supplemental Fig. S2.1). MΦ phagocytosis was assessed using a Zeiss 510 META laser scanning confocal microscope (Carl Zeiss, Oberkochen, Germany) and quantitated by the number of phagocytic events observed in at least 8, random fields of view (63x) using ZEN 2009 software (Carl Zeiss). Data is expressed as either "percent phagocytosis", which indicates the percentage of phagocytic MΦs observed and manually counted within a given experiment, or "total phagocytosed beads/63x field", where the total number of phagocytic events within a given experiment was calculated by an ImageJ plugin (ImageJ 1.47v, Wayne Rasband, NIH, USA) based on an experimentally determined average pixel area and RGB color code specific to the co-localization of phagocytosis. Pilot studies confirmed that identical results were obtained with this calculation compared to manual counts (data not shown). While the number of beads phagocytosed per MΦ was variable within any given incubation condition, we did not observe any trends in this parameter between treatment groups and, therefore, this was not quantified. MΦ viability was assessed by propidium iodide staining at the end of the 3 h incubation period with the total number of viable MΦs quantitated in at least 8 random 63x fields of view using ZEN 2009 software. Where reported, "total viable MΦs" were enumerated by an ImageJ plugin based on an experimentally determined average pixel area and RGB color code specific to viable MΦs and are reported per 63x microscopic field.

7) Mouse model of *S. aureus* orthopedic implant biofilm infection

Preparation of inoculum

A single bacterial colony from a fresh streak plate was used to inoculate 25 ml of autoclaved brain-heart infusion (BHI) broth in a baffled 250 ml flask (10:1 flask:volume ratio) with constant shaking at 250 rpm at 37°C for 12-16 h. The overnight culture was then diluted 1:10 in fresh BHI in order to estimate the total number of bacteria present by measuring OD_{600} (BioMate 3S Spectrophotometer, Thermo Scientific, Waltham, MA). At the same time, 1 ml of the overnight culture was centrifuged in a 1.5 ml Eppendorf microcentrifuge tube at 14,000 rpm for 5 min at 4°C to pellet the bacteria. The supernatant was removed the pellet was resuspended in 1 ml sterile 1X PBS and subsequently washed two more times by centrifuging as previously described. After washing, the pellet was diluted in sterile PBS to a final estimated concentration of $5x10^5$ cfu/ml ($1x10^3$ cfu/2µl). The actual inoculum concentration was then determined by serial diluting the washed culture in triplicate to 10^{-8} and plating 100 µl of the 10^{-7} and 10^{-8} dilutions on TSA.

Infection procedure

Age and sex-matched mice (8-10 weeks old) were weighed and anesthetized with ketamine/xylazine (100 mg/kg and 5 mg/kg, respectively) by i.p. injection prior to the surgical site being shaved and disinfected with povidone-iodine. A scalpel was then used to make an incision along the midline of the knee exposing the patella. Next, a medial parapatellar arthrotomy was performed with the scalpel to access the knee joint, allowing for a lateral retraction of the patella to expose the entire distal femur. A 26-gauge needle was then used to bore a hole through the trochlea into the intramedullary canal creating space for the insertion of a precut and autoclaved 0.8-cm orthopedic-grade Kirschner wire (0.6 mm diameter, Nitinol [nickel-titanium]; Custom Wire Technologies, Port Washington, WI) leaving approximately 1 mm exposed as an inoculation site. A total of 10^3 cfu of the USA300 LAC strain was inoculated in 2 µl at the implant tip, and the patella was relocated prior to surgical wound closure with 6-0 metric absorbable sutures and skin closure with 6-0 metric nylon sutures (both from Covidien,

Mansfield, MA). Immediately following surgery and again at 24 h post-surgery, all animals received Buprenex (0.1 mg/kg s.c.; Reckitt Benckiser, Hull, U.K.) for pain management, after which all mice exhibited normal ambulation with no discernible pain.

Recovery of implant and surrounding tissues

Animals were sacrificed by an overdose of inhaled isoflurane followed by cervical dislocation. The flank and left leg were then disinfected with 70% EtOH prior to the skin of the left leg being carefully removed to expose the infected tissue. Excess underlying adipose tissue and muscle was removed prior to collection of the tissue immediately proximal to the infection site, which was then weighed and placed in 500 µl homogenization buffer (1X PBS + protease inhibitor cocktail tablet, Roche, Indianapolis, IN) on ice. The tissue was then dissociated with the blunt end of a plunger from a 30-cc syringe and filtered through a 35 µm filter (BD Falcon, Bedford, MA). Next, a 150µl aliquot was removed for quantitation of bacterial burdens and potential assessment of inflammatory mediator production (e.g. ELISA). The remaining filtrate was further processed for flow cytometry as described below. Following tissue collection, the knee joint and femur were collected, weighed, and placed in 500 µl homogenization buffer prior to being homogenized by a combination of handheld Polytron homogenizer at the highest setting for 30 s and a Bullet Blender (Next Advance, Averill Park, NY) with a combination of 0.9-2.0 mm diameter blend and 3.2 mm diameter stainless steel beads (Next Advance, Averill Park, NY). Implants were removed from the femur and vortexed in 500 µl PBS for 5 min at 2000 rpm. Serial dilutions of effluents from tissue, joint, femur, and implant were plated on TSA and grown overnight at 37°C to determine bacterial colonization. For some experiments, the spleen, heart, and kidneys were collected as described above to determine dissemination.

Flow cytometry

Characterization of immune infiltrates was performed via Fluorescence-activated cell sorting (FACS). Animals were sacrificed with an overdose of inhaled isoflurane and tissues were excised

and processed as previously described above. The tissue filtrate was washed with ice-cold 1X PBS + 2% FBS and centrifuged at 1200 rpm for 5 min at 4°C, after which RBCs were lysed using BD Pharm lyse (BD Biosciences, San Diego, CA) per the manufacturer instructions. After lysis, cells were resuspended in 500 µl 1X PBS followed by Fc Block (2 µl/sample, eBioscience, San Diego, CA) for 20 min at 4°C to minimize nonspecific antibody binding. 100 µl of each sample was pooled and subsequently aliquoted into single color compensation and isotype control tubes to identify gaiting thresholds and assess the degree of nonspecific staining, respectively. The remaining 400 µl was divided between two tubes for subsequent staining with two panels (e.g. innate and T cell) and q.s. to 500 µl with 1X PBS. Cells were then stained for 30 min at 4^0C protected from light with directly-conjugated antibodies for multi-color flow cytometry analysis, prior to being washed with 1X PBS, centrifuged as previously described, and resuspended in 1X PBS + 1% paraformaldehyde. The innate immune panel included: CD45-APC, Ly6G-PE, Ly6C-PerCP-Cy5.5, and F4/80 PE-Cy7. The T cell panel included: CD3ε-APC, CD4-Pacific Blue, CD8a-FITC, Ly6C-PerCP-Cy5.5, and TCR γδ-PE. All fluorochrome-conjugated antibodies were purchased from either BD Biosciences or eBioscience. For the exclusion of dead cells, a Live/Dead Fixable Stain Kit (Life Technologies, Eugene, OR) was also used, following manufacturer's instructions. Analysis was performed using BD FACSDiva software with cells gated on the live $CD45^+$ leukocyte population.

8) Bacterial microarray analysis and qRT-PCR

RNA isolation

At the appropriate intervals after biofilm-leukocyte co-culture, excess medium was removed from biofilm chambers and 2X the remaining volume of RNAprotect (QIAGEN, Hilden, Germany) was added. Biofilms were collected from the bottom of the chamber slide using a cell scraper.

RNA isolated from biofilms alone (i.e. no leukocyte addition) was included as a control for comparisons. The resulting suspension of biofilm cells was transferred to a tube and sonicated for 5 min to facilitate dispersal. After sonication, cells were pelleted by centrifugation for 5 min and RNAprotect was decanted. The resulting pellet was resuspended in 700 µl of RLT Buffer supplemented with β-mercaptoethanol and transferred to a 2 ml FastPrep lysing tube (MP Biomedicals, Santa Ana, CA). Biofilm cells were lysed in a FastPrep high-speed homogenizer (MP Biomedicals) for 20 sec on a speed setting of 6. The resulting lysate was incubated for 5 min on ice and then centrifuged at 14,000 rpm at 4°C for 15 min. RNA was isolated from the clarified supernatant using a RNeasy mini kit (QIAGEN) and contaminating DNA was removed by on-column DNase digestion using the RNase-Free DNase Set (QIAGEN). RNA was isolated from eight samples for each time point and co-culture condition with three independent experimental replicates performed to assess the reproducibility of microarray results. RNA quality and quantity were determined using an Agilent RNA6000 NANO kit and Agilent 2100 Bioanalyzer (Agilent Technologies, Santa Clara, CA).

RNA labeling and DNA microarray analysis

Following the manufacturer's recommendations, 75 ng of total RNA from each sample was amplified using ExpressArt Bacterial mRNA amplification Nano kits (AmpTec GmbH, Germany) and labeled using BioArray HighYield RNA Transcript Labeling kits (Enzo Life Sciences, Inc., Farmingdale, NY). Three micrograms of resulting labeled RNA was hybridized to a *S. aureus* GeneChip® following the manufacturer's recommendations for antisense prokaryotic arrays (Affymetrix, Santa Clara, CA) then washed, stained, and scanned as previously described (22, 188). Commercially available GeneChips® were used in this study, representing > 3300 *S. aureus* ORFs and > 4800 intergenic regions from strains N315, Mu50, NCTC 8325, and COL (Affymetrix). GeneChip® signal intensity values for each biofilm sample at each replicate time point ($n \geq 3$) were normalized to the median signal intensity value for each GeneChip® and

averaged using GENESPRING 7.2 software (Agilent Technologies, Redwood City, CA). Transcripts that demonstrated 1) at least two-fold change in expression; 2) greater than background signal intensity value and determined to be "Present" by Affymetrix algorithms; and 3) significant by Student's *t*-test (*p* value = 0.05) were considered differentially expressed.

Verification of differentially expressed genes by qRT-PCR

A subset of biofilm genes that were differentially regulated after leukocyte co-culture (i.e. *sodA*, *saeS*, *saeR*, *agrB*, *rsbU*, *atl*, *recA*, and *nuc*) was verified by qRT-PCR using Sybr Green. Primers were designed using Primer 3.0 software and melt-curve analysis was performed at the end of each amplification run to verify signal specificity. Results are presented as the relative expression compared to biofilms that were not co-cultured with leukocytes as a reference standard.

9) Bacterial proteomics

Sequential Windowed data-independent Acquisition of the Total High-resolution Mass Spectra (SWATH-MS)

Conditioned medium from *S. aureus* WT and Δ*agr* strains grown under biofilm or planktonic conditions as described above were harvested, treated with a protease inhibitor cocktail (Roche, Basel, Switzerland), and proteins precipitated with 20% TCA. Relative protein concentrations were compared between groups using three independent replicates per sample by Sequential Windowed data-independent Acquisition of the Total High-resolution Mass Spectra (SWATH-MS) as previously described (189). A Z-transformation followed by a Z-test was performed on all positively identified proteins (>98% confidence) between two sample sets at a time (i.e. WT biofilm vs. Δ*agr* biofilm or WT biofilm vs. WT planktonic) to assess significant differences in relative protein abundance as previously described (189). Identified proteins were functionally grouped by UniProt identifier utilizing the DAVID bioinformatics resource 6.7

(http://david.abcc.ncifcrf.gov/) (190). Protein-protein interactions were predicted using STRING 9.05 (http://string-db.com) (191, 192).

Western blots

Conditioned medium from *S. aureus* WT and Δ*agr* biofilm and planktonic growth conditions was sterile-filtered and treated with a protease inhibitor cocktail (Roche) prior to storage at -80^{0}C. Upon thawing, samples were TCA precipitated overnight and suspended in 30 µl of Laemmli buffer, whereupon 5 µl of each sample was loaded onto a gel, transferred to a PVDF membrane, and probed for *S. aureus* LukA and Hla.

Enzyme-linked Immunosorbent Assay (ELISA)

Conditioned medium from WT *S. aureus* biofilm and planktonic cultures was sterile-filtered (0.2µm) and analyzed for Hla concentrations by direct ELISA. Briefly, experimental samples or serial dilutions of purified *S. aureus* Hla (Sigma), to generate a standard curve, were diluted in carbonate-bicarbonate buffer and incubated in 96-well ELISA plates overnight at 4^{0}C. The following day, wells were washed extensively with 1X PBS/0.5% Tween and incubated with a rabbit anti-Hla antibody followed by an anti-rabbit IgG-HRP antibody (both from Sigma) for detection. Plates were developed using a TMB substrate (Becton Dickinson) with the reaction halted using stop solution prior to reading at 450nm. Hla concentrations were normalized to total protein as measured by a Pierce BCA Protein Assay.

10) Bioflim extracellular DNA (eDNA) isolation

Isolation of eDNA from static biofilms grown in 12-well plates was performed as described previously (32). Briefly, day 6-old mature biofilms were chilled to 4^{0}C followed by the addition of 50 mM EDTA prior to removal of supernatant, resusupended and mechanically disrupted in TES Buffer (Tris-HCL; pH 8.0/500mM NaCl). Next, a phenol:chloroform:isoamyl alcohol

(25:24:1) extraction followed by a chloroform/isoamyl alcohol (24:1) extraction was performed prior to storage overnight at -20^{0}C in 100% ice-cold ethanol and 10% 3M NaAcetate. The next day, the eDNA was pelleted and washed prior to a final resuspension in TE buffer. qRT-PCR was performed on 1:10 dilutions of each sample with the LightCycler DNA Master SYBR Green I (Roche) using *gyrA*.

Supplemental Figure S2.1

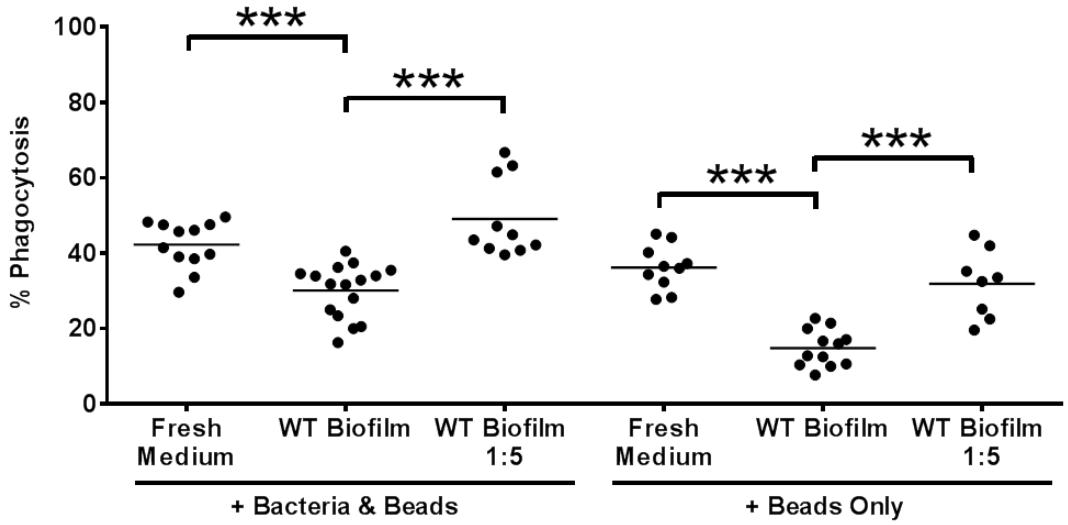

Fluorescent microspheres can be used as a surrogate for live *S. aureus* to assess MΦ phagocytosis. (A) Bone marrow-derived MΦ were incubated for 3 h with fresh medium or conditioned medium collected from WT biofilms and left undiluted or diluted 1:5 with fresh medium, whereupon phagocytosis was assessed by the uptake of planktonic *S. aureus* + fluorescent microspheres (beads) or microspheres alone. Significant differences are denoted with asterisks (***, $p < 0.001$; unpaired two-tailed student's *t*-test). Results are representative of at least two independent experiments.

Chapter 3: Global transcriptome analysis of *Staphylococcus aureus* biofilms in response to innate immune cells

Published in Infection and Immunity 81(12):4363-76, 2013

Abstract

The potent phagocytic and microbicidal activities of PMNs and MΦs are among the first lines of defense against bacterial infections. Yet *Staphylococcus aureus* is often resistant to innate immune defense mechanisms, especially when organized as a biofilm. To investigate how *S. aureus* biofilms respond to MΦs and PMNs, gene expression patterns were profiled using Affymetrix microarrays. The addition of MΦs to *S. aureus* static biofilms led to a global suppression of the biofilm transcriptome with a wide variety of genes downregulated. Notably, genes involved in metabolism, cell wall synthesis/structure, and transcription/translation/replication were among the most highly downregulated, which was most dramatic at 1 h compared to 24 h following MΦ addition to biofilms. Unexpectedly, few genes were enhanced in biofilms after MΦ challenge. Unlike co-culture with MΦs, co-culture of *S. aureus* static biofilms with PMNs did not greatly influence the biofilm transcriptome. Collectively, these experiments demonstrate that S. aureus biofilms differentially modify their gene expression patterns depending on the leukocyte subset encountered.

Introduction

Staphylococcus aureus produces numerous virulence factors that facilitate its ability to invade, colonize, disseminate to distant sites, and impede host defenses to cause disease (84, 193). These characteristics can be amplified during biofilm formation, which represents a complex multicellular community of organisms encased in a matrix composed primarily of polysaccharides, extracellular DNA (eDNA), and proteins (10-12). *S. aureus* biofilm infections are often difficult to treat due to their heterogeneity and altered metabolic and transcriptional activity (194), which likely contributes to the chronic and recurrent nature of biofilm infections (159, 195-197). Our recent studies have demonstrated that *S. aureus* biofilms interfere with traditional microbial recognition and killing mechanisms by the innate immune system (159, 195). The subversion of these responses is another example of the remarkable success of *S. aureus* as a pathogen and it is now clear that biofilm growth represents yet another immune resistance determinant. However, our understanding of the cross-talk between *S. aureus* biofilms and the immune response is limited.

PMNs are important antimicrobial effectors that possess an arsenal of bactericidal compounds, including defensins, cathelicidins, and lysozyme (156, 198). In terms of their microbicidal activity, PMNs are most notable for their ability to produce large amounts of reactive oxygen intermediates catalyzed by NADPH oxidase. In addition, activated PMNs degranulate and release PMN extracellular traps (NETs), a meshwork of DNA and enzymes that facilitates the extracellular killing of *S. aureus* as well as other bacteria (199). However, the short lifespan of PMNs requires their constant recruitment to sites of infection, and their transcriptional capacity for inflammatory mediator production is more limited compared to other professional phagocytes (i.e. MΦs and dendritic cells). MΦs reside in virtually all tissues and also serve as a critical first line of defense against microbial invasion. In addition, MΦs are a major source of proinflammatory mediators that are critical for amplifying leukocyte recruitment and activation

cascades upon bacterial exposure, as well as providing potent phagocytic and antimicrobial effects (200, 201). Like PMNs, MΦs can form MΦ extracellular traps (METs),which are believed to exert similar antimicrobial activity (157). Both MΦs and PMNs are also equipped with an arsenal of pattern recognition receptors that sense invariant motifs expressed across a broad range of microbial species to trigger inflammatory mediator release (202, 203). Consequently, PMNs and MΦs represent key antimicrobial effector populations and their interactions with *S. aureus* biofilms is likely critical for dictating the outcome of infection. Our previous studies have demonstrated that *S. aureus* biofilms impair MΦ phagocytosis and induce cell death (159, 195, 204); however the response of the biofilm itself to these leukocyte populations remains to be defined.

While considerable progress has been made in defining *S. aureus* virulence factors and their regulatory networks, less is known about the organism's ability to cope with the host immune response during biofilm growth (205-207). Genome-wide transcriptional profiling of planktonic *S. aureus* following PMN exposure has previously been reported (208, 209); however the transcriptional changes occurring in *S. aureus* biofilms in response to PMNs or MΦs has not yet been investigated. We predicted that *S. aureus* biofilms modify their transcriptome in response to these leukocyte subsets to subvert immune recognition and killing, thus favoring biofilm persistence. This possibility was assessed by defining alterations in *S. aureus* biofilm gene expression profiles after co-culture with MΦs or PMNs utilizing *S. aureus* Affymetrix GeneChip® arrays. Here we report that *S. aureus* biofilms respond differently to these leukocyte populations, with kinetic distinctions also observed. For example, MΦ addition induced a generalized repression of the biofilm transcriptome within 1 h, whereas at a later interval this inhibition had dissipated, which correlated with the biofilm's ability to induce MΦ cell death. In contrast, the biofilm transcriptome remained relatively stable following PMN addition, regardless of the interval examined. These results indicate that *S. aureus* biofilms discriminate between leukocyte

subsets and alter their transcriptional profile accordingly, presumably in favor of avoiding detection by the host, leading to biofilm persistence.

Results

Differences in neutrophil and macrophage interactions with *S. aureus* biofilms *in vitro*. To evaluate the impact of leukocyte subsets on *S. aureus* biofilm transcriptional profiles, biofilms that were propagated for either 4 or 6 d were selected for analysis based on their differences in structural maturity (195). Specifically, 4 day-old biofilms were considered more immature in terms of average thickness (32 μm) and irregular density (Fig. 3.1A and C), whereas 6 day-old biofilms were classified as more mature based on a relatively uniform average thickness (47 μm) and a more consistent density (Fig. 3.1B and C).

Previous studies from our group have demonstrated that *S. aureus* biofilms are capable of circumventing MΦ phagocytosis and inducing MΦ death (159, 195, 204). Since the goal of this study was to compare the impact of MΦs versus PMNs on the biofilm transcriptome, side-by-side comparisons of how both populations interact with the biofilm were required. *S. aureus* USA300 LAC-GFP static biofilms were grown for 4 or 6 d, whereupon MΦs or PMNs were co-cultured with biofilms for an additional 1, 4, or 24 h. Three-dimensional confocal microscopy images were constructed to demonstrate the proximity of MΦs or PMNs from the biofilm surface and extent of phagocytosis (Fig. 3.2A and 2B, respectively). MΦs incubated with *S. aureus* biofilms for either a 1 or 24 h period contained few internalized bacteria, a phenomenon that was independent of biofilm age as we have previously described (Fig. 3.2A and 3.3) (195). In contrast, intracellular bacteria were readily discernible in PMN biofilm co-cultures at 1, 4, and 24 h (Fig. 3.2B, 3.3, and Supplemental Fig. 3.1). In addition, the majority of PMNs were found in close association with the biofilm surface, whereas most MΦs remained distant from the biofilm (Fig. 3.2).

Figure 3.1

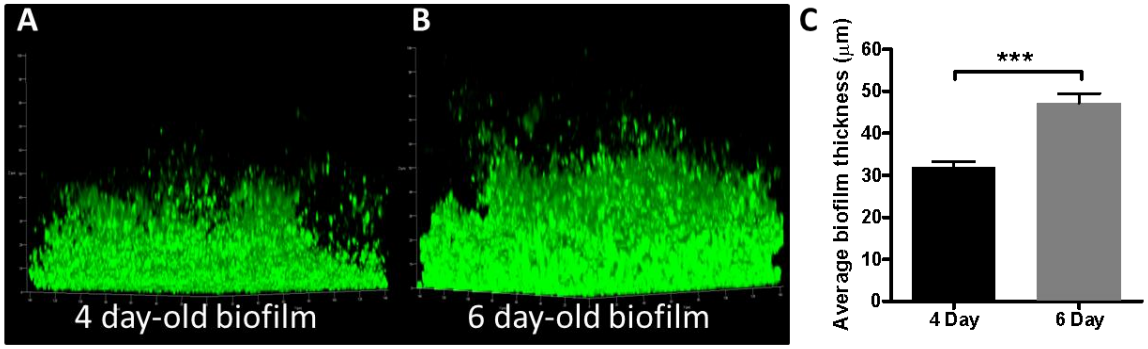

S. aureus* biofilm growth states.** (**A and B**) USA300 LAC-GFP was inoculated into sterile 2-well glass chamber slides and incubated at 37°C under static aerobic conditions for a period of 4 (**A**) or 6 (**B**) days in RPMI 1640 supplemented with 10% FBS with daily medium replacement. Biofilms were visualized using confocal microscopy (magnification, X63; 1-μm slices), and representative three-dimensional images were constructed. (**C**) Quantification of 4- and 6-day-old biofilm thickness. Significant differences are denoted with asterisks (, $P < 0.001$ using an unpaired two-tailed Student *t* test; $n = 30$ biofilms/time point).

Figure 3.2

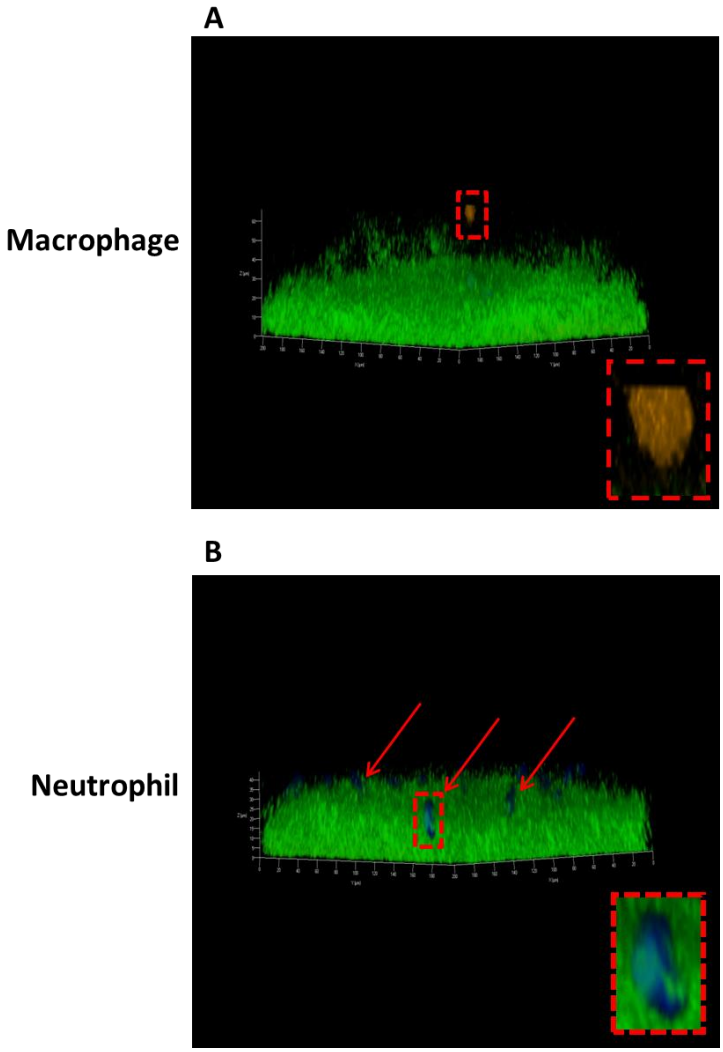

***S. aureus* biofilm-leukocyte co-culture paradigm.** USA300 LAC-GFP static biofilms (green) were grown for 6 days, whereupon BMDMΦs (**A**) (orange) or bone marrow-isolated PMNs (**B**) (blue) were incubated with biofilms for 24 h and 4 h, respectively. Biofilm co-cultures were visualized using confocal microscopy (magnification, X63; 1-μm slices), and representative three-dimensional images were constructed. Insets show a higher magnification to highlight the absence of MΦ phagocytosis (**A**) and the presence of PMN phagocytosis (**B**) of staphylococcal biofilms. Results are representative of two independent experiments examining three individual biofilms each.

Figure 3.3

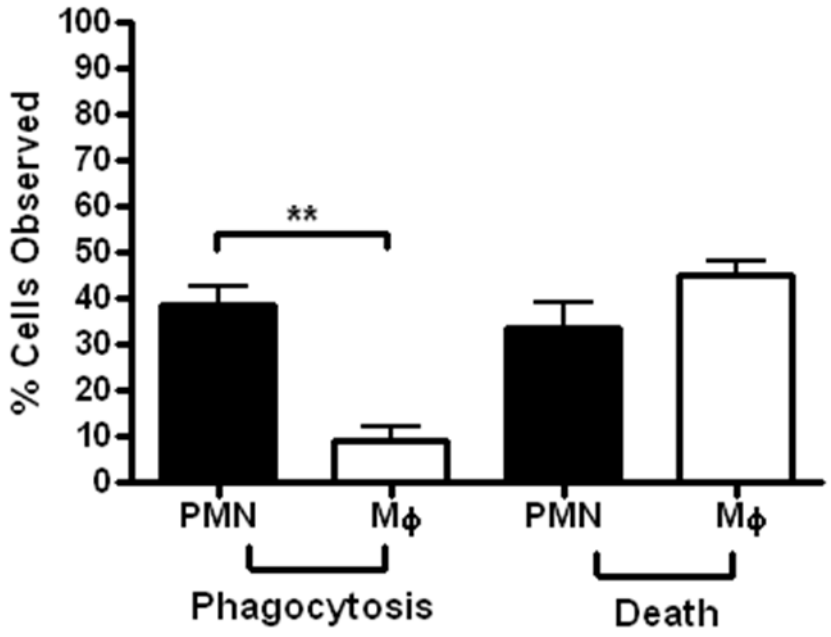

Differential responses of innate immune cells to *S. aureus* biofilms. *S. aureus* USA300 LAC-GFP static biofilms were grown for 6 days and visualized using confocal microscopy (63X magnification, 1 µm slices). A total of 10^7 BMDMΦs or 5 x 10^6 bone marrow-isolated PMNs were incubated with biofilms for 18-24 h, whereupon the percentage of leukocytes exhibiting phagocytosis or death, were enumerated. Significant differences are denoted with asterisks (**, $p < 0.005$ using an unpaired two-tailed Student's *t*-test, n = 3).

Macrophages and neutrophils induce differential gene expression profiles in *S. aureus* biofilms. The disparity between the ability of MΦs and PMNs to phagocytose and invade *S. aureus* biofilms suggested that these cell types may differentially influence biofilm transcriptional activity. To investigate this possibility, Affymetrix *S. aureus* GeneChip® profiles were compared between biofilms incubated in the presence or absence of either MΦs or PMNs. Analysis of the number of differentially expressed genes revealed that MΦs caused the most substantive changes in the biofilm, primarily at an early time point (i.e. 1 h; Fig. 3.4A, 3.5A, 3.5B, and Tables 3.2-3), affecting genes involved in metabolism and transcription/translation/replication for both immature and mature biofilms (Fig. 3.5). Unexpectedly, most biofilm genes were down-regulated in response to acute MΦ exposure, with the exception of several hypothetical genes and a lone gene involved in staphyloxanthin biosynthesis (Supplemental Table 3.1). However, the ability of MΦs to induce global gene repression was transient, as the number of genes altered was dramatically reduced after a 24 h co-culture period (Figs 3.4A, and Tables 3.2, 3.3, and Supplemental Fig. 3.1). This is likely attributable to the fact that a large percentage (≥ 55%) of MΦs are dead approximately 6 h after co-culture with *S. aureus* biofilms and presumably are no longer able to produce factor(s) that influence the biofilm transcriptome (195). A subset of genes identified as differentially expressed by biofilms upon MΦ addition in the microarray analysis were verified by qRT-PCR (Fig. 3.6).

In comparison to MΦs, PMNs were more limited in their ability to affect *S. aureus* biofilm gene transcription (Fig. 3.4B, 3.5C, 3.5D, and Tables 3.4, 3.5, and Supplemental 3.2). Of note, many genes remained unaltered following MΦ or PMN addition to biofilms, suggesting that these genes are important for biofilm maintenance in the face of an immune challenge. Nonetheless, PMNs and MΦs differentially impact the *S. aureus* biofilm transcriptome as revealed by the dichotomy in the observed gene expression patterns.

Figure 3.4

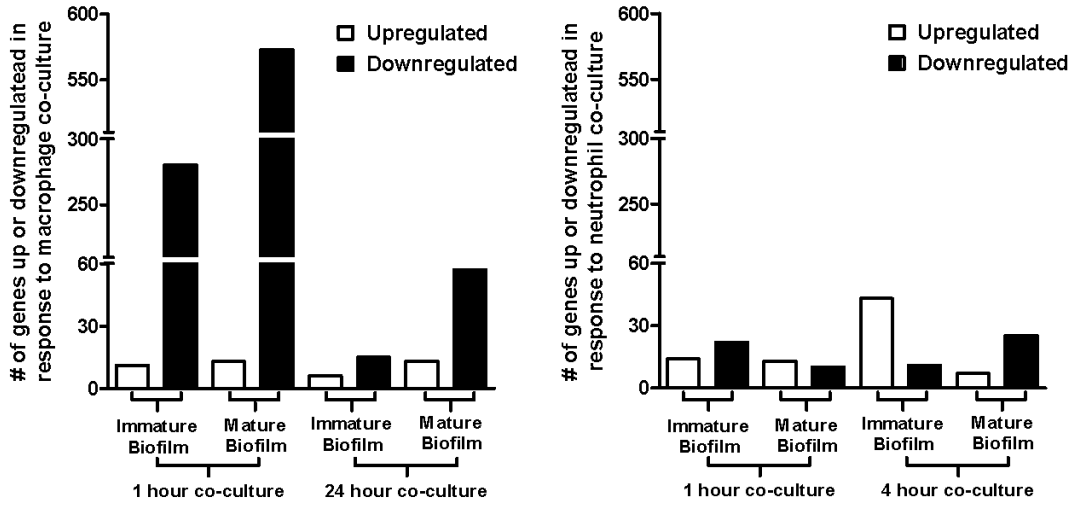

Acute macrophage addition to *S. aureus* biofilms leads to the transcriptional repression of numerous genes. The total number of genes significantly up- or down-regulated in response to MΦ (A) or PMN (B) co-culture in immature (4 day-old) or mature (6 day-old) *S. aureus* biofilms is shown, including those encoding for hypothetical proteins.

Figure 3.5

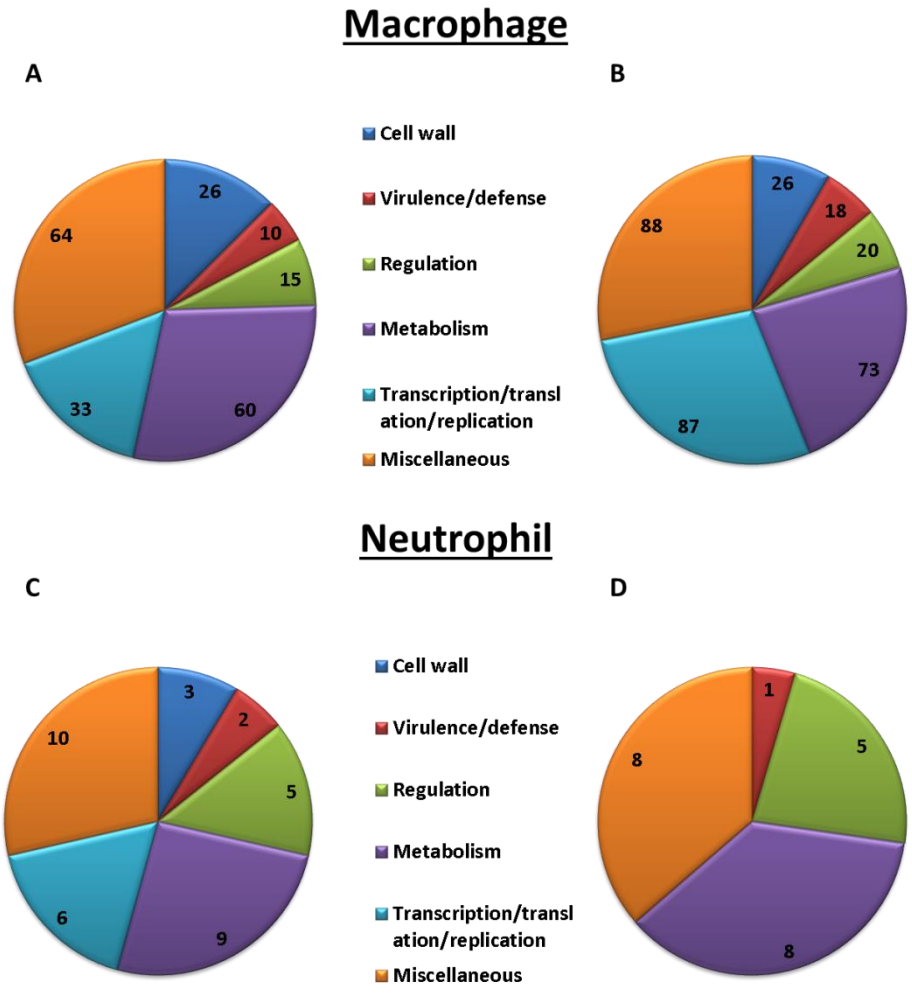

Classification of genes significantly altered by leukocyte addition in *S. aureus* biofilms. *S. aureus* USA300 LAC-GFP static biofilms were grown for 4 or 6 days, whereupon MΦs (A and B) or PMNs (C and D) were incubated with biofilms for 1 h. The numbers of genes with defined functions (grouped into cell wall/membrane, virulence/defense, regulation, metabolism, transcription/translation/replication, and miscellaneous categories) significantly altered after MΦ or PMN challenge are shown. Genes encoding for hypothetical proteins were not included.

Table 3.2. Significantly down-regulated genes between 6 day-old *S. aureus* biofilm versus biofilm-macrophage co-cultures for a 1 h period

Category

Virulence/defense

Fold Change	Common	Locus	Description
-30.01	*nuc*	SA0860	thermonuclease precursor
-13.84	*epiA*	SA1878	lantibiotic epidermin precursor
-12.43		SA2525	ABC transporter, ATP-binding protein
-9.54		SAS0388	exotoxin 3
-6.88	*hlY*	SA1173	alpha-hemolysin precursor
-6.40	*hlb*	BA000017 SA2003	phospholipase C
-5.59	*chp*	SAR2036	chemotaxis-inhibiting protein
-4.99		SA0477	type I restriction-modification system, S subunit, EcoA family, putative
-4.64	*fmhA*	SA2409	fmhA protein
-3.16		SA2430	ABC transporter, ATP-binding/permease protein
-2.91		SA2445	fmtA-like protein
-2.78		SA1098	metallo-beta-lactamase family protein
-2.73	*epiP*	SA1874	epidermin leader peptide processing serine protease
-2.39	*entK*	SA0886	staphylococcal enterotoxin
-2.22	*eprH*	SA1265	endopeptidase resistance gene
-2.04	*set8*	SA0384	exotoxin 8
-2.03	*epiE*	SA1872	epidermin immunity protein F

Cell wall

Fold Change	Common	Locus	Description
-22.02	*isdC*	SA1141	NPQTN cell wall surface anchor protein
-8.42		SA1994	ABC transporter, ATP-binding protein
-8.24	*isdB*	SA1138	LPXTG cell wall surface anchor protein
-7.69		SA1779	transglycosylase domain protein
-7.66	*spsB*	SA0969	signal peptidase IB
-6.44	*isdD*	SA1142	hypothetical protein
-6.39		SA1932	transglycosylase domain protein
-6.23		SA0486	staphylococcus tandem lipoprotein

-5.38	*tagX*	SA0697	teichoic acid biosynthesis protein X
-4.62	*abcA*	SA0700	ABC transporter, ATP-binding/permease protein
-4.40		SA1169	fibrinogen-binding protein precursor-related protein
-3.93	*srtA*	SA2539	sortase
-3.46	*opuBB*	SA0783	osmoprotectant ABC transporter, permease protein
-3.35	*isaB*	SA2660	immunodominant antigen B
-3.34		SA0203	iron compound ABC transporter, iron compound-binding protein, putative
-3.30		SA0611	glycosyl transferase, group 1 family protein
-3.27		SA0242	teichoic acid biosynthesis protein, putative
-3.19	*dltA*	SA0935	D-alanine-activating enzyme/D-alanine-D-alanyl carrier protein ligase
-2.94		SA1806	cell wall surface anchor family protein
-2.93		SA1043	glycosyl transferase, group 1 family protein
-2.48		SA1951	Mur ligase family protein
-2.27		SA2431	ABC transporter, ATP-binding/permease protein
-2.27	*cap1C*	SA2685	capsular polysaccharide biosynthesis protein Cap1C
-2.18	*dltD*	SA0938	DltD protein
-2.13		SA2082	membrane protein, putative
-2.11		SA0119	cell wall surface anchor family protein

Transcription/translation/replication

Fold Change	Common	Locus	Description
-10.99		SA2089	single-stranded DNA-binding protein family
-9.90		SA1900	DNA repair exonuclease family protein
-7.17	*gpxA*	SA1325	glutathione peroxidase
-6.75	*rbf*	SA0725	transcriptional regulator, AraC family
-6.39	*norR*	SA0746	transcriptional regulator, MarR family
-6.28		SA2058	PemK family protein
-6.18	*rpsA*	SA1516	ribosomal protein S1
-6.13		SA2517	transcriptional regulator, MerR family
-5.85	*gmk*	SA1221	guanylate kinase
-5.68		SA1919	transcriptional regulator, Fur family
-5.53		SA1060	transcriptional regulator, MarR family
-5.49		SA0550	S4 domain protein
-5.44		SA2203	ClpA-related protein

-5.42	*recF*	SA0004	recF protein
-5.40		SA1732	replication initiation and membrane attachment protein
-5.29		SA1939	phosphotyrosine protein phosphatase
-5.28		SA0305	ABC transporter, permease protein
-4.87		SA0980	transcriptional regulator, LysR family
-4.77		SA2407	lipoprotein, putative
-4.68		SA1803	pseudouridine synthase, family 1
-4.63		SA0028	IS431mec, transposase
-4.62	*ctsR*	SA0567	transcriptional regulator
-4.51	*licT*	SA1393	transcriptional antiterminator
-4.41		SA1997	transcriptional regulator, GntR family
-4.34	*rpsU*	SA1632	ribosomal protein S21
-4.32		SA2297	monooxygenase family protein
-4.26	*grpE*	SA1638	heat shock protein
-4.22		SA2290	transcriptional regulator, AraC family
-4.13	*glyS*	SA1622	glycyl-tRNA synthetase
-3.97		SA0552	general stress protein 13
-3.88	*tcaR*	SA2353	transcriptional regulator
-3.72		SA2713	rhodanese-like domain protein
-3.63		SA1897	protein export protein PrsA, putative
-3.62		SA1894	HIT family protein
-3.62		SA0526	DNA polymerase III, delta prime subunit, putative
-3.56	*serS*	SA0009	seryl-tRNA synthetase
-3.52	*ftsL*	SA1023	putative cell division protein
-3.44		SA2500	MutT/nudix family protein
-3.43	*rpmG*	SA1369	ribosomal protein L33
-3.38		SA2325	transcriptional regulator, LysR family
-3.36		SA1541	transcriptional regulator, Fur family
-3.33		SA2317	phosphosugar-binding transcriptional regulator
-3.29		SA0535	primase-related protein
-3.24		SA1957	RNA methyltransferase, TrmA family
-3.24	*rnr*	SA0846	exoribonuclease, VacB/RNase II family
-3.23	*rpsP*	SA1254	ribosomal protein S16
-3.23	*czrA*	SA2137	transcriptional regulator CzrA

-3.23	*gidB*	SA2736	glucose-inhibited division protein B
-3.20	*rpmF*	SA1137	ribosomal protein L32
-3.20	*nusB*	SA1569	N utilization substance protein B
-3.12		SA1794	thioredoxin, putative
-3.05		SA1285	N utilization substance protein A, putative
-3.04		SA1205	cell-division initiation protein, putative
-3.00		SA0563	transcriptional regulator, GntR family
-2.99	*dinG*	SA1495	DNA polymerase III, epsilon subunit/ATP-dependent helicase
-2.96		SA0432	spoOJ protein
-2.95		SA1107	transcriptional regulator, Cro/CI family
-2.86		SA0540	endoribonuclease L-PSP, putative
-2.84	*rexB*	SA0970	exonuclease RexB
-2.81		SA1839	transposase, IS200 family
-2.76	*recQ*	SA1523	ATP-dependent DNA helicase RecQ
-2.67	*gltC*	SA0513	transcriptional regulatory protein GltC
-2.61		SA1752	CBS domain protein
-2.61		SA2131	Dps family protein
-2.59		SA0314	conserved hypothetical protein
-2.58	*miaA*	SA1323	tRNA delta(2)-isopentenylpyrophosphate transferase
-2.51	*crcB*	SA1832	crcB protein
-2.51		SA1065	transcriptional regulator, putative
-2.48		SA1954	exonuclease
-2.45	*nrdG*	SA2634	anaerobic ribonucleoside-triphosphate reductase activating protein
-2.45	*dnaK*	SA1637	dnaK protein
-2.45	*pcrA*	SA1966	ATP-dependent DNA helicase
-2.44		SA0024	5-nucleotidase family protein
-2.40	*recG*	SA1241	ATP-dependent DNA helicase RecG
-2.39		SA0551	cell-division protein divIC, putative
-2.35	*asnS*	SA1494	asparaginyl-tRNA synthetase
-2.27	*dnaN*	SA0002	DNA polymerase III, beta subunit
-2.23		SA1771	OsmC/Ohr family protein
-2.21	*htrA*	SA1028	serine protease
-2.20	*hexB*	SA1316	DNA mismatch repair protein
-2.18	*rnhC*	SA1150	ribonuclease HIII

-2.10	*parB*	SA2735	chromosome partioning protein, ParB family
-2.09		SA1153	DNA-dependent DNA polymerase family X
-2.07	*pheT*	SA1149	phenylalanyl-tRNA synthetase, beta subunit
-2.06		SA1250	chromosome segregation SMC protein, putative
-2.05	*map*	SA1946	methionine aminopeptidase, type I
-2.01	*mscL*	SA1182	large-conductance mechanosensitive channel

Regulation

Fold Change	Common	Locus	Description
-8.53	*agrD*	SA2024	accessory gene regulator protein D
-7.97		SA2359	sensor histidine kinase
-6.53	*rsbW*	SA2055	anti-sigma B factor
-5.85		SA1354	sensor histidine kinase, putative
-5.73	*sarZ*	SA2384	staphylococcal accessory protein Z
-5.61	*rsbV*	SA2056	anti-anti-sigma factor RsbV
-5.41	*icaR*	SA2688	intercellular adhesion regulator
-5.13	*sarS*	SA0096	staphylococcal accessory regulator S
-4.95	*vraR*	SA1942	DNA-binding response regulator
-4.91	*rsbU*	SA2057	sigma factor B regulator protein
-4.82	*graS*	SA0717	sensor histidine kinase
-4.50	*arlS*	SA1450	sensor histidine kinase
-4.07	*vraS*	SA1943	sensor histidine kinase
-3.82	*sarY*	SA2289	staphylococcal accessory regulator Y
-3.64	*sarA*	SA0672	staphylococcal accessory regulator A
-3.49		SA1906	sensor histidine kinase, putative
-3.37	*agrB*	SA2023	accessory gene regulator protein B
-2.61		SA1355	DNA-binding response regulator, LuxR family
-2.53	*arlR*	SA1451	DNA-binding response regulator
-2.39	*agrC*	SA2025	accessory gene regulator protein C

Metabolism

Fold Change	Common	Locus	Description
-7.97		SA2167	iron compound ABC transporter, iron compound-binding protein
-7.58	*isdE*	SA1143	iron compound ABC transporter, iron compound-binding protein, putative
-7.32		SA1111	spermidine/putrescine ABC transporter, spermidine/putrescine-binding pro

-7.31	*epiD*	SA1875	epidermin biosynthesis protein
-6.46		SA1920	D-isomer specific 2-hydroxyacid dehydrogenase family protein
-5.66		SA1592	rhodanese-like domain protein
-5.28		SA2363	L-lactate permease
-5.20	*glmM*	SA2151	phosphoglucosamine mutase
-5.19		SA0024	5-nucleotidase family protein
-5.13	*nrdF*	SA0793	ribonucleoside-diphosphate reductase 2, beta subunit
-5.11	*cls1*	SA1351	cardiolipin synthetase
-5.08	*phoU*	SA1420	phosphate transport system protein
-5.06		SA0031	glycerophosphoryl diester phosphodiesterase, putative
-4.97		SA1787	chorismate mutase/phospho-2-dehydro-3-deoxyheptonate aldolase
-4.79	*purB*	SA1969	adenylosuccinate lyase
-4.73	*isdF*	SA1144	iron compound ABC transporter, permease protein, putative
-4.62		SA2459	carboxylesterase
-4.54	*budA*	SA2617	alpha-acetolactate decarboxylase
-4.25		SA1753	universal stress protein family
-4.19	*coaBC*	SA1223	phosphopantothenoylcysteine decarboxylase/phosphopantothenate--cystein
-4.10		SA2138	cation efflux family protein
-4.08	*xpt*	SA0458	xanthine phosphoribosyltransferase
-4.06	*proC*	SA1546	pyrroline-5-carboxylate reductase
-4.00	*xseA*	SA1568	exodeoxyribonuclease VII, large subunit
-3.92	*lacG*	SA2180	6-phospho-beta-galactosidase
-3.71		SA0876	arsenate reductase, putative
-3.62	*sodA*	SA1610	superoxide dismutase
-3.58	*zwf*	SA1549	glucose-6-phosphate 1-dehydrogenase
-3.58		SA1588	proline dipeptidase
-3.56	*betA*	SA2627	choline dehydrogenase
-3.53		SA2375	transporter, CorA family
-3.47		SA1804	polysaccharide biosynthesis protein
-3.32		SA0666	iron compound ABC transporter, permease protein
-3.30	*gcvH*	SA0877	glycine cleavage system H protein
-3.13	*cdsA*	SA1280	phosphatidate cytidylyltransferase
-3.09		SA0024	5-nucleotidase family protein
-3.03	*asd*	SA1429	aspartate-semialdehyde dehydrogenase

-3.02		SA1818	3,4-dihydroxy-2-butanone-4-phosphate synthase/GTP cyclohydrolase II
-3.01		SA0155	cation efflux family protein
-2.98		SA2475	peptide ABC transporter, permease protein, putative
-2.97		SA0712	lipase/esterase
-2.97		SA0687	Na+/H+ antiporter, putative
-2.88		SA2278	acyl-CoA dehydrogenase-related protein
-2.84	*rpe*	SA1235	ribulose-phosphate 3-epimerase
-2.78		SA0024	5-nucleotidase family protein
-2.76		SA1545	oxidoreductase, short-chain dehydrogenase/reductase family
-2.73		SA1553	glyoxalase family protein
-2.65	*nagB*	SA0616	glucosamine-6-phosphate isomerase
-2.63		SA0024	5-nucleotidase family protein
-2.61	*corA*	SA2342	magnesium and cobalt transport protein CorA, putative
-2.57		SA0409	conserved hypothetical protein
-2.57	*bglA*	SA0251	6-phospho-beta-glucosidase
-2.57		SA1825	N-acetylmuramoyl-L-alanine amidase, family 4
-2.57		SA0200	phosphoglycerate transporter family protein
-2.54	*tyrA*	SA1401	prephenate dehydrogenase
-2.52	*ribD*	SA1820	riboflavin biosynthesis protein
-2.46	*aroK*	SA1596	shikimate kinase
-2.42	*arcC*	SA1182	carbamate kinase
-2.41	*lysA*	SA1435	diaminopimelate decarboxylase
-2.40	*thrB*	SA1364	homoserine kinase
-2.38	*cidC*	SA2553	pyruvate oxidase
-2.31		SA1814	lysophospholipase, putative
-2.31		SA2303	inositol monophosphatase family protein
-2.28	*yajC*	SA1693	preprotein translocase, YajC subunit
-2.27		SA0655	oxidoreductase, aldo/keto reductase family
-2.23		SA1109	spermidine/putrescine ABC transporter, permease protein
-2.15	*nrdD*	SA2635	anaerobic ribonucleoside-triphosphate reductase
-2.13	*menE*	SA1844	O-succinylbenzoic acid--CoA ligase, putative
-2.13		SA0308	carbohydrate kinase, PfkB family
-2.11		SA2195	M23/M37 peptidase domain protein
-2.08		SA0921	CBS domain protein

-2.07	*epiC*	SA1876	epidermin biosynthesis protein
-2.01		SA1309	pyruvate ferredoxin oxidoreductase, beta subunit

Miscellaneous

Fold Change	Common	Locus	Description
-15.57		SA2526	membrane protein, putative, authentic point mutation
-11.95	*isdG*	SA1146	conserved hypothetical protein
-9.42	*asp23*	SA2173	alkaline shock protein 23
-9.15		SA0893	pathogenicity island protein
-8.72		SA0658	HD domain protein
-7.42		SA1439	acylphosphatase
-7.16		SA0821	HD domain protein
-6.87		SA0606	hydrolase, haloacid dehalogenase-like family
-6.33		SA2378	transcriptional regulator, AraC family
-6.30		SA0668	hydrolase, alpha/beta hydrolase fold family
-6.15		SA1573	integrase/recombinase, core domain family, authentic frameshift
-5.80		SA0602	hydrolase, haloacid dehalogenase-like family
-5.75		SA1365	hydrolase, haloacid dehalogenase-like family
-5.51		SA0318	prophage L54a, integrase
-5.42		SA2666	N-acetylmuramoyl-L-alanine amidase domain protein
-5.20		SA2245	acetyltransferase, GNAT family
-4.77		SA2328	abortive infection protein family
-4.69		SA2159	drug transporter, putative
-4.65		SA0764	glycosyl transferase, group 2 family protein
-4.52		SA0892	pathogenicity island protein, authentic frameshift
-4.49		SA1806	probable ATP-dependent helicase
-4.49		SA0812	degV family protein
-4.46		SA2036	ABC transporter, ATP-binding protein
-4.46	*dmpI*	SA1339	4-oxalocrotonate tautomerase
-4.31		SA1759	universal stress protein family
-4.26		SA2140	lytic regulatory protein, authentic frameshift
-4.24		SA1855	transposase, putative, degenerate
-4.23		SA0716	DNA-binding response regulator
-4.17		SA2142	SAP domain protein

-4.15	*scpA*	SA1538	segregation and condensation protein A
-4.02		SA1529	metallo-beta-lactamase superfamily protein
-4.02		SA0181	conserved domain protein
-3.89		SA1941	ribonuclease BN, putative
-3.89		SA2499	helicase, putative
-3.77		SA0630	amino acid permease
-3.76		SA2533	glyoxalase family protein
-3.76		SA0736	acetyltransferase, GNAT family
-3.63	*cbf1*	SA1898	cmp-binding-factor 1
-3.57		SA0747	cobalamin synthesis protein/P47K family protein
-3.44		SA1677	aminotransferase, class V
-3.41		SA0607	azoreductase
-3.38		SA1933	ThiJ/PfpI family protein
-3.34		SA1515	GTP-binding protein, Era/TrmE family
-3.33		SA1287	30S ribosomal protein L7 Ae
-3.30		SA1179	exotoxin 4, putative
-3.30	*trxA*	SA1155	thioredoxin
-3.24		SA0803	lipoprotein, putative
-3.19		SA1047	conserved domain protein
-3.19		SA1180	exotoxin 3, putative
-3.17		SA0874	nitroreductase family protein
-3.09		SA1207	glyoxalase family protein
-3.03		SA1855	transposase, putative, degenerate
-3.00	*bcr*	SA2437	bicyclomycin resistance protein
-2.97		SA0891	transcriptional regulator, putative
-2.95		SA2354	membrane protein, putative
-2.93	*orfX*	SA0023	conserved hypothetical protein
-2.89		SAV1941	putative membrane protein
-2.87		SA0978	membrane protein, putative
-2.86		SA1412	hydrolase-related protein
-2.79		SA0553	MesJ/Ycf62 family protein
-2.79		SA1240	DAK2 domain protein
-2.67		SA1189	acetyltransferase (GNAT) family protein
-2.66	*tcaA*	SA2352	tcaA protein

-2.53		SA1708	type III leader peptidase family protein
-2.52		SA0875	thioredoxin, putative
-2.49		SA2339	DNA-3-methyladenine glycosylase
-2.49		SA2499	helicase, putative
-2.47		SA0262	Choloylglycine hydrolase family protein
-2.46		SA2522	DedA family protein
-2.41		SA1644	putative competence protein ComEC/Rec2
-2.40		SA0855	acetyltransferase, GNAT family
-2.39		SA1437	cold shock protein, CSD family
-2.38		SA2018	abortive infection protein family
-2.35		SAV1976	similar to phi PVL ORF 52 homolog
-2.34		SA1615	ATP-dependent RNA helicase, DEAD/DEAH box family
-2.30		SA1751	DHH subfamily 1 protein
-2.28		SA2014	phage terminase family protein
-2.28	*int*	SA1810	integrase
-2.27		SA0595	peptidase, M20/M25/M40 family
-2.26		SA0201	DNA-binding response regulator, AraC family
-2.25		SA0250	PTS system, IIA component
-2.24		SA0744	ABC transporter, ATP-binding protein, MsbA family
-2.23	*relA*	SA1010	GTP pyrophosphokinase
-2.19		SA1589	lipoprotein, putative
-2.18		SAV1976	similar to phi PVL ORF 52 homolog
-2.15	*fmtC*	SA1396	fmtC protein
-2.02		SA2490	similar to N-hydroxyarylamine O-acetyltransferase
-2.02		SA1063	serine/threonine-protein kinase

Table 3.3. Differentially expressed genes between 6 day-old *S. aureus* biofilm versus biofilm-macrophage co-cultures for a 24 h period

Category

Upregulated

Metabolism

Fold change	Common	Locus	Description
11.68		SA0215	propionate CoA-transferase, putative
9.94		SA0214	long-chain-fatty-acid--CoA ligase, putative
5.14		SA0213	acyl-CoA dehydrogenase family protein
4.68		SA0211	acetyl-CoA acetyltransferase
2.88	*gltS*	SA2340	sodium:glutamate symporter

Virulence/defense

Fold change	Common	Locus	Description
4.23	*spa*	SA0095	immunoglobulin G binding protein A precursor

Cell wall

Fold change	Common	Locus	Description
2.55	pbp1	SA1194	penicillin-binding protein 1
2.46	dat	SA1800	D-alanine aminotransferase
2.37	sdrD	SA0520	Ser-Asp rich fibrinogen-binding, bone sialoprotein-binding protein

Transcription/translation/replication

Fold change	Common	Locus	Description
2.06	*glnR*	SA1328	glutamine synthetase repressor

Miscellaneous

Fold change	Common	Locus	Description
2.73		SA1433	peptidase, M20/M25/M40 family

Category

Downregulated

Metabolism

Fold Change	Common	Locus	Description

-3.85		SA1912	glucosamine-6-phosphate isomerase, putative
-3.04		SA2579	phytoene dehydrogenase
-2.42		SA0921	CBS domain protein
-2.30		SA2369	pyridine nucleotide-disulfide oxidoreductase
-2.27		SA2708	ABC transporter, ATP-binding protein

Transcription/translation/replication

Fold Change	Common	Locus	Description
-3.41	*fabG*	SA2482	3-oxoacyl-(acyl carrier protein) reductase, authentic point mutation
-3.23	*rpsA*	SA1516	ribosomal protein S1
-2.59	*hutG*	SA2327	formiminoglutamase
-2.56		SA1753	universal stress protein family
-2.08	*rpmB*	SA1238	ribosomal protein L28

Cell wall

Fold Change	Common	Locus	Description
-3.26	*isdC*	SA1141	NPQTN cell wall surface anchor protein
-2.93		SA0764	glycosyl transferase, group 2 family protein
-2.20	*cap5E*	SA0140	capsular polysaccharide biosynthesis protein

Virulence/defense

Fold Change	Common	Locus	Description
-2.91		SA1529	metallo-beta-lactamase superfamily protein
-2.76	*nuc*	SA0860	thermonuclease precursor
-2.67	*epiE*	SA1872	epidermin immunity protein F
-2.42		SA1797	metallo-beta-lactamase family protein
-2.37		SA2167	iron compound ABC transporter, iron compound-binding protein

Regulation

Fold Change	Common	Locus	Description
-2.26	*arlR*	SA1451	DNA-binding response regulator

Miscellaneous

Fold Change	Common	Locus	Description
-3.21	*asp23*	SA2173	alkaline shock protein 23
-3.20	*dmpI*	SA1339	4-oxalocrotonate tautomerase

-3.05	SA1038	membrane protein
-2.82	SA2007	peptidase, M20/M25/M40 family, authentic frameshift
-2.68	SA0671	hydrolase, alpha/beta hydrolase fold family
-2.54	SA1576	traG protein, putative
-2.40	SA2434	membrane protein, putative
-2.12	SA1941	ribonuclease BN, putative

Figure 3.6

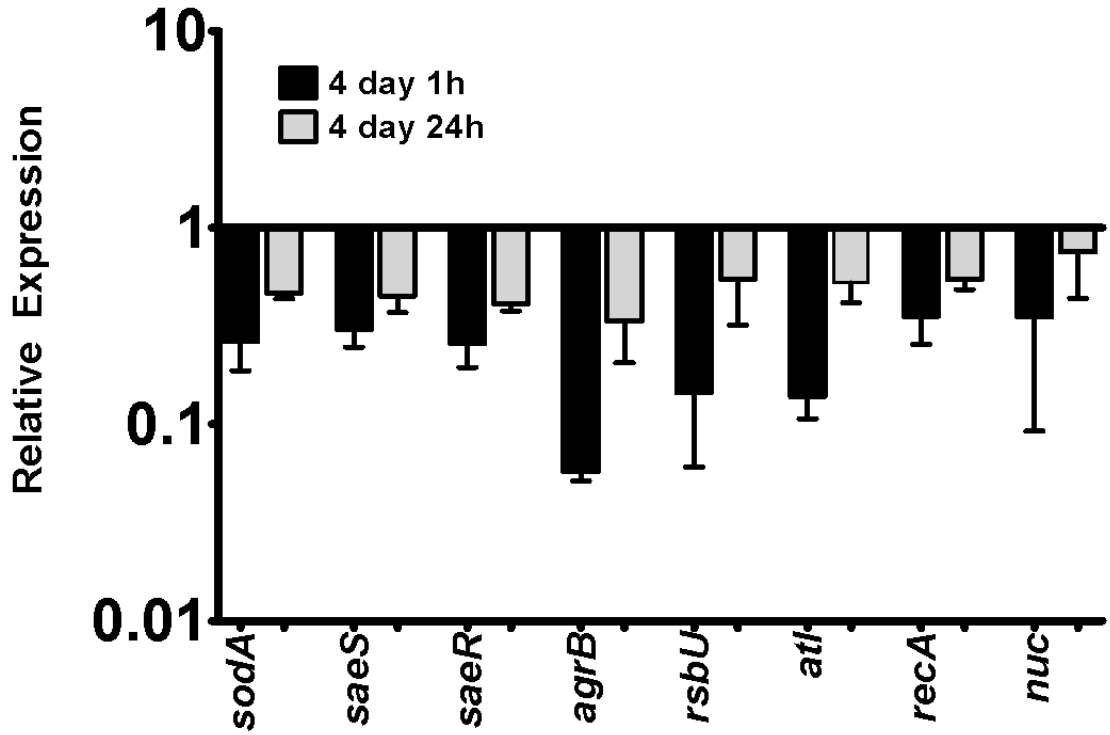

qRT-PCR validation of down-regulated genes in *S. aureus* biofilms identified by microarray analysis. A subset of genes identified by microarray analysis was confirmed by qRT-PCR following either a 1 or 24 h co-culture period of MΦs with 4 day-old USA300 LAC static biofilms. Results are presented as the relative gene expression after MΦ-biofilm co-culture compared to biofilms that were not incubated with MΦs as a reference standard.

Table 3.4. Differentially expressed genes between 6 day-old *S. aureus* biofilm versus biofilm-neutrophil co-cultures for a 1 h period

Category

Upregulated

Metabolism

Fold Change	Common	Locus	Description
3.1		SACOL0200	phosphoglycerate transporter family protein
2.4	*pyrE*	SACOL1217	orotate phosphoribosyltransferase
2.2	*feoB*	SACOL2564	ferrous iron transport protein B
2.2		SACOL2322	peptidase, M20/M25/M40 family
2.0	*carB*	SACOL1215	carbamoyl-phosphate synthase, large subunit
2.0		SACOL0217	ABC transporter, substrate-binding protein

Virulence/defense

Fold Change	Common	Locus	Description
2.0		SACOL2449	drug transporter, putative

Regulation

Fold Change	Common	Locus	Description
2.1	*lytS*	SACOL0245	sensor histidine kinase LytS
2.0		SACOL2585	regulatory protein, putative

Miscellaneous

Fold Change	Common	Locus	Description
2.7			intergenic upstream of ORF sa_c4971s4276
2.5			intergenic upstream of ORF sa_c7173s10144
2.4			intergenic upstream of ORF sa_c8901s7819

Category

Downregulated

Metabolism

Fold Change	Common	Locus	Description
-3.7		SACOL2131	Dps family protein
-2.5		SACOL1952	ferritins family protein

Regulation

Fold Change	Common	Locus	Description
-2.7	*groES*	SACOL2017	chaperonin, 10 kDa
-2.4	*grpE*	SACOL1638	heat shock protein
-2.3	*groEL*	SACOL2016	chaperonin, 60 kDa

Miscellaneous

Fold Change	Common	Locus	Description
-2.6			intergenic upstream of ORF sa_c2703s2276
-2.6			intergenic upstream of ORF sa_c7269s10166
-2.2			reverse complement of intergenic upstream of ORF sa_c2703s2276
-2.1			reverse complement of intergenic upstream of ORF sa_c8455s7417
-2.1			intergenic upstream of ORF sa_c8544s7501

Table 3.5. Differentially expressed genes between 6 day-old *S. aureus* biofilm versus biofilm-neutrophil co-cultures for a 4 h period

Category

Upregulated

Metabolism

Fold Change	Common	Locus	Description
3.4	*purK*	SACOL1074	phosphoribosylaminoimidazole carboxylase, ATPase subunit
2.3		SACOL0240	4-diphosphocytidyl-2C-methyl-D-erythritol synthase, putative
2.1	*gltB*	SACOL0514	glutamate synthase, large subunit

Cell wall

Fold Change	Common	Locus	Description
2.5		SACOL0191	M23/M37 peptidase domain protein

Miscellaneous

Fold Change	Common	Locus	Description
2.5			reverse complement of intergenic upstream of ORF sa_c10613s11068
2.2		SAS058	conserved hypothetical protein (all strains, N315)
2.1			intergenic downstream of ORF sa_c121s9459

Increased *agr* transcription by *S. aureus* biofilms promotes resistance to neutrophil challenge. *agrA* and *agrB* were both significantly enhanced in 4 day-old *S. aureus* biofilms following a 1 h exposure to PMNs (Supplemental Table 3.2). To evaluate the importance of increased *agr* transcriptional activity in the face of PMN challenge, we compared the extent of biofilm phagocytosis and death of PMNs after co-culture with USA300 LAC or its isogenic *agr* mutant (*Δagr*). While *Δagr* displayed significantly thicker biofilms as previously reported by others (Fig. 3.7A) (64, 210), PMNs co-incubated with *Δagr* demonstrated significantly less cell death and slightly enhanced phagocytosis of biofilm-associated bacteria, although the latter did not reach statistical significance (Fig. 3.7B). These results suggest that while the physical nature of the biofilm can limit the extent of phagocytosis, secreted factors also appear to play a role in evasion of PMN effector functions, at least *in vitro*; a hypothesis further corroborated by the types of genes known to be regulated by the *agr* operon (211, 212) as well as data previously reported by others (180). This functional study further substantiates our microarray data by illustrating how the enhanced expression of specific genes may facilitate biofilm evasion of innate immune mechanisms.

Figure 3.7

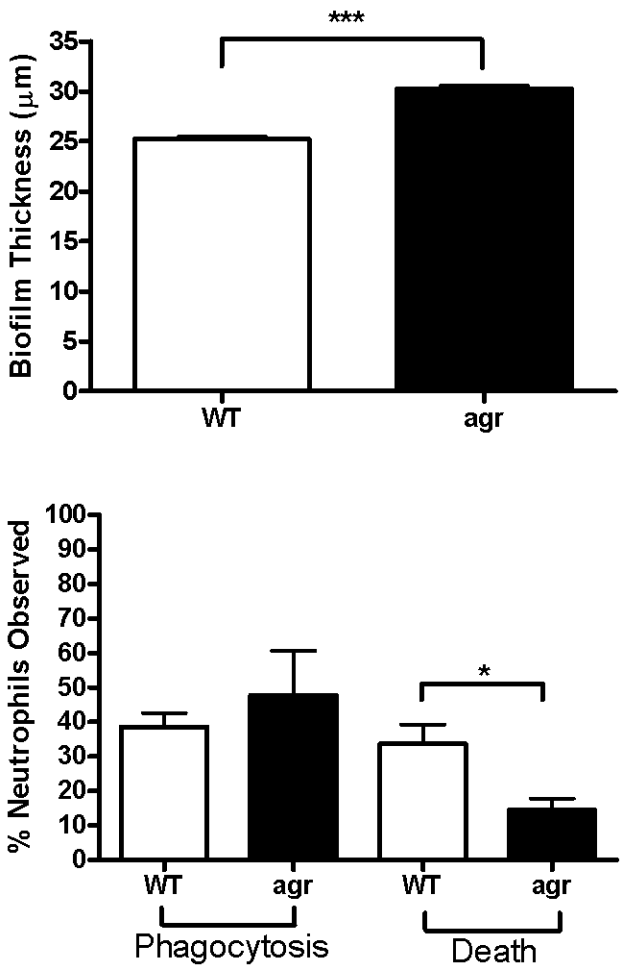

***agr* promotes *S. aureus* biofilm resistance to neutrophil challenge.** *S. aureus* USA300 LAC-GFP wild type (WT) and isogenic *Δagr* static biofilms were grown for 6 days and visualized using confocal microscopy (63X magnification, 1 μm slices). (A) Quantification of 4 and 6 day-old biofilm thickness. (B) PMNs (5×10^6) were incubated with biofilms for 20 h, whereupon the percent of phagocytic and dead PMNs was enumerated. Significant differences are denoted with asterisks, [(A) ***, $p < 0.0001$ using an unpaired two-tailed Student's *t*-test, n = 60; (B) *, $p < 0.05$ using an unpaired two-tailed Student's *t*-test, n = 3].

Differential responses of macrophages and neutrophils to *S. aureus* biofilms are cell autonomous. To determine whether the differences between MΦs and PMNs to phagocytose biofilm-associated bacteria could be influenced by one another, both leukocyte populations were co-cultured with WT USA300 LAC biofilms. The extent of MΦ and PMN invasion into the biofilm was similar whether cells were added together (Fig. 3.8A) or separately (Fig. 3.8C). Similarly, MΦs were incapable of phagocytosing biofilm-associated *S. aureus* whether co-cultured with PMNs (Fig. 3.8B) or alone (Fig. 3.8D), whereas PMNs were equally phagocytic under both conditions (Fig. 3.8B, D). This data demonstrates that the phagocytic ability of PMNs over MΦs in regard to *S. aureus* biofilm is cell autonomous and is not influenced by the other population *in vitro*.

Figure 3.8

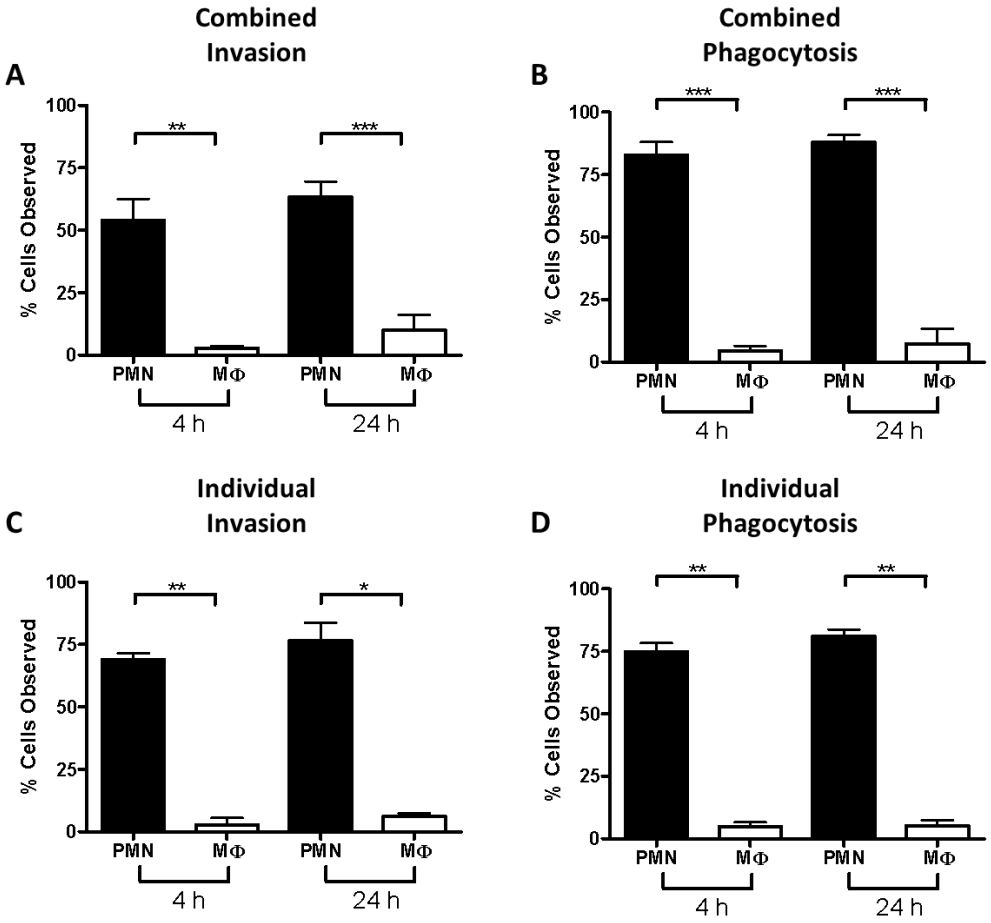

Differential responses of macrophages and neutrophils to *S. aureus* biofilms are cell autonomous. *S. aureus* USA300 LAC-GFP static biofilms were grown for 6 days and visualized using confocal microscopy (63X magnification, 1 µm slices). Quantification of invasion or phagocytosis of MΦs and PMNs (5 x 10^6 each) cultured either together (A and B) or separately (C and D) with 6 day-old biofilms at 4 and 24 h. Significant differences are denoted with asterisks [(A and B) **, $p < 0.01$ using an unpaired two-tailed Student's *t*-test, n = 4; ***, $p < 0.0001$ using an unpaired two-tailed Student's *t*-test, n = 4; (C and D) *, $p < 0.05$ using an unpaired two-tailed Student's *t*-test, n = 2; **, $p < 0.01$ using an unpaired two-tailed Student's *t*-test, n =2].

Supplemental Figure S3.1

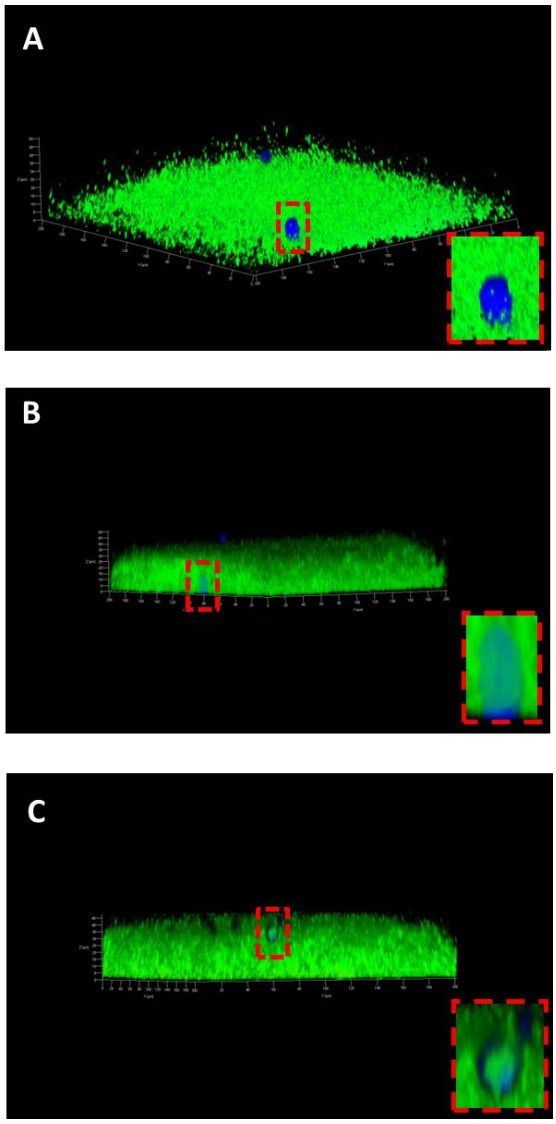

Neutrophils phagocytose *S. aureus* biofilms throughout the co-culture period. USA300 LAC-GFP static biofilms were grown for 6 days, whereupon bone marrow-isolated PMNs were incubated with biofilms for 1, 4, or 24 h (A-C, respectively). Biofilm co-cultures were visualized using confocal microscopy (63X magnification, 1 µm slices) and representative three-dimensional images were constructed. Insets are provided at higher magnification to highlight the presence of intracellular bacteria. Results are representative of at least two independent experiments.

Supplemental Table S3.1. Significantly increased genes between 6 day-old S. aureus biofilm versus biofilm-macrophage co-cultures for a 1 h period

Category

Virulence/Defense

Fold Change	Common	Locus	Description
4.5		SA2291	staphyloxanthin biosynthesis protein

Miscellaneous

Fold Change	Common	Locus	Description
2.2	ssr161		Hypothetical
2.2	ssr162		Hypothetical
2.2	ssr169		Hypothetical
2.2	ssr166		Hypothetical
2.2	ssr167		Hypothetical
2.1	ssr168		Hypothetical
2.1	ssr159		Hypothetical
2.1	ssr160		Hypothetical

Supplemental Table S3.2. Significantly increased genes between 4 day-old *S. aureus* biofilm versus biofilm-neutrophil co-cultures for a 1 h period

Category

Regulation

Fold change	Common	Locus	Description
5.6	*agrB*	SA2381	accessory gene regulator protein B
4.7	*agrA*	SACOL2026	accessory gene regulator protein A

Virulence/defense

Fold change	Common	Locus	Description
3.6		SACOL1187	antibacterial protein

Miscellaneous

Fold change	Common	Locus	Description
3.6		SA1773	hypothetical protein

3.0		SACOL2565	conserved hypothetical protein
2.0		SACOL2557	conserved domain protein
2.0		SACOL2503	hypothetical protein

Transcription/translation/replication

Fold change	Common	Locus	Description
2.4	*glnR*	SACOL1328	glutamine synthetase repressor

Cell Wall

Fold change	Common	Locus	Description
2.4	*atl*	SACOL1062	bifunctional autolysin
2.1		SACOL0507	LysM domain protein
2.0	*isaA*	SACOL2584	Immunodominant antigen A

Metabolism

Fold change	Common	Locus	Description
2.2	*abcA*	SACOL0700	ABC transporter, ATP-binding/permease protein
2.1		SACOL1114	Mn^{2+}/Fe^{2+} transporter, NRAMP family

Discussion

One facet of *S. aureus* pathogenesis is the organism's ability to maintain cellular homeostasis while enduring immune-mediated stresses (174). *S. aureus* has been shown to interfere with virtually every level of the host immune response, including increased resistance to antimicrobial peptides, impairment of phagocyte recruitment, escape from NETs, resistance to intracellular killing, and interference with complement function as well as antibody-mediated opsonization (213). The objective of this study was to examine how relevant innate immune cell populations, such as PMNs and MΦs, alter the *S. aureus* biofilm transcriptome. To our knowledge, there have been no studies to date examining biofilm gene expression profiles after incubation with innate immune cell populations with any species of bacterial biofilm. Based on our preliminary data and the fact that PMNs are generally shorter-lived than MΦs, we chose early (i.e. 1 and 4 h) and late (i.e. 1 and 24 h) time points for biofilm co-cultures, respectively. Surprisingly, in subsequent experiments, we found that a significant number of PMNs remained viable at 24 h after biofilm addition; therefore, PMN co-incubation periods were extended in subsequent confocal experiments.

In the current study, the greatest transcriptional impact on *S. aureus* biofilms was achieved during an early (i.e. 1 h) co-culture period with MΦs. This effect was independent of phagocytosis, since we observed few internalized bacteria within MΦs incubated with *S. aureus* biofilms (195, 204). Although numerous genes were repressed following biofilm exposure to MΦs after 1 h of co-culture, surprisingly many genes remained unaltered. These unaffected genes are likely important for biofilm maintenance, and may represent an essential core transcriptome needed to maintain biofilm survival and/or evade host antimicrobial effector mechanisms in the face of an immune challenge. In contrast, few genes were altered in *S. aureus* biofilms following a 24 h exposure to MΦs, which may be explained by changes in MΦ viability following extended biofilm co-culture periods. Specifically, our previous work demonstrated that most MΦs remain

viable during a 1 h co-culture period with biofilms; however, by 6 h MΦ viability is significantly reduced as measured by the live/dead stain 7-aminoactinomycin D (7-ADD)(195). Together, these findings suggest that *S. aureus* biofilms rapidly transition into a transcriptionally dormant mode after MΦ challenge, which is reversed once the pressure of viable MΦs has dissipated. We cannot exclude the possibility that minor changes in biofilm gene expression could have occurred following leukocyte addition that were not detected due to limitations in microarray sensitivity. In addition, although extreme care was taken to ensure rapid processing of biofilms prior to RNA isolation, it remains possible that some transcriptional changes may have occurred during this interval due to the short half-life of many bacterial mRNAs (214). However, since we compared the transcriptional profiles of biofilms alone concurrent with leukocyte co-culture conditions, any changes in mRNA turnover would be expected to decay at the same rate.

Despite the extensive microbicidal mechanisms employed by PMNs, these cells did not significantly alter the *S. aureus* biofilm transcriptome. This was unexpected, since we predicted that PMN challenge would enhance bacterial virulence factor expression to interfere with recognition/killing mechanisms. While recent studies have demonstrated the ability of *S. aureus* to survive intracellularly within PMNs and, to a lesser extent, MΦs, one would expect this adaptation to necessitate large scale transcriptional changes (215). One possibility to explain the discrepancy between MΦs and PMNs in regulating biofilm transcriptional responses is that PMNs were added to biofilms at a 10-fold reduced density than MΦs. However, our confocal analysis indicated that PMNs invade the biofilm in greater numbers, remain viable for a longer period than MΦs, and exhibit phagocytosis. Nonetheless, the latter appears to be futile, since PMN phagocytosis of *S. aureus* biofilms does not significantly decrease bacterial numbers *in vitro* (204). Additionally, PMNs have not proven to play a key microbicidal role in a *S. aureus* catheter-associated biofilm model *in vivo*, showing minimal impact on bacterial burdens (197, 204).

While MΦs and PMNs perform many overlapping functions in terms of bactericidal activity, subtle specialization of labor could potentially account for the *S. aureus* biofilm transcriptional differences reported in this study. For example, while PMNs are considered potent phagocytic effectors against numerous extracellular bacteria, activated MΦs are recognized as a signaling hub during bacterial infections through their secretion of numerous immune stimulatory and bactericidal factors (200, 201, 216-218). Therefore, it is possible that *S. aureus* biofilms are more responsive to this secreted milieu than physical disruption via phagocytosis, although this remains speculative.

In addition to producing molecules to circumvent the host immune system, *S. aureus* biofilms must adapt to nutrient-limiting conditions encountered during growth. Interestingly, MΦ addition to *S. aureus* biofilms repressed numerous metabolism-associated genes, further suggesting that biofilms transition into a dormant mode to evade immune killing pathways. Correspondingly, MΦ exposure also lead to the repression of genes implicated in transcription, translation, and replication as well as cell wall synthesis, which would be expected to conserve energy during a decreased metabolic state. The repression of cell wall synthesis may also be a mechanism to evade innate immune recognition.

The *agr* and *sarA* regulatory systems are among the many controlling the production of staphylococcal virulence and defense factors. The *agr* locus encodes a QS system involved in RNAIII production, which switches the synthesis of surface and adhesive molecules to toxin and exoprotein expression (84). SarA is a DNA-binding regulator protein that influences the expression of multiple genes, including those contributing to virulence and biofilm formation (188, 219). In this study, *sarA* transcription was reduced in *S. aureus* biofilms following MΦ exposure, which agrees with the generalized decrease in numerous genes regulated by SarA. In contrast, *agr* transcription was significantly increased in *S. aureus* biofilms after PMN addition. The enhanced expression of *agr* in this setting allowed us to examine its contribution to PMN

reactivity using an isogenic *agr* mutant. The percentage of PMNs exhibiting phagocytic activity was increased in Δ*agr* biofilms, despite the significant increase in biofilm thickness. This phenotype may be explained, in part, by alterations in phenol-soluble modulin (PSM) expression. PSMs are surfactant peptides that have recently been implicated in bacterial biofilm formation across a number of species, including *S. aureus* (79). PSM expression is intricately linked to bacterial density and is *agr* regulated (79). Based on this evidence, it is reasonable to predict that although Δ*agr* biofilms are thicker than WT, they are likely less structurally complex and unable to effectively circumvent PMN invasion. In addition, Δ*agr* biofilms elicited less PMN death, likely due to the reduced expression of lytic toxins, such as Hla and PSMs, which have been shown to play key roles in *S. aureus* pathogenesis (82, 220). There were no significant effects on MΦ phagocytosis or viability in response to Δ*agr* biofilms (data not shown), implying that enhanced *agr* transcription is selective for thwarting aspects of PMN function. This finding further substantiates a potential selective role for impaired PSM action on PMNs, since its cytotoxic effects primarily target this cell type(221, 222). Finally, as PSM expression is induced by the stringent response resulting from the harsh conditions within the phagolysosome (83), impaired PSM activity provides a potential explanation for the increased intracellular burden of Δ*agr* biofilms by PMNs. The impressive ability of *S. aureus* biofilms to adapt to PMN challenge correlates with the modest transcriptome changes reported in this study.

In conclusion, the changes in *S. aureus* biofilm transcriptional profiles after leukocyte exposure reported here provides a comprehensive view of the molecules that may impact *S. aureus* immune evasion and survival during biofilm growth. Further investigations into the role of differentially regulated genes will provide a better understanding of the ability of *S. aureus* to adapt to environmental challenges and may provide novel strategies and therapeutic targets for staphylococcal biofilm infections.

Chapter 4: *Staphylococcus aureus* biofilms induce macrophage dysfunction through leukocidin AB and α-toxin

Published in mBio 6(4), 2015

Abstract

The MΦ response to planktonic *S. aureus* involves the induction of proinflammatory, microbicidal activity. However, *S. aureus* biofilms can interfere with these responses, in part, by polarizing MΦs toward an anti-inflammatory, pro-fibrotic phenotype. Here we demonstrate that conditioned medium from mature *S. aureus* biofilms inhibited MΦ phagocytosis and induced cytotoxicity, suggesting the involvement of a secreted factor(s). Iterative testing identified the active factor(s) to be proteinaceous and partially *agr*-dependent. Quantitative mass spectrometry identified Hla and LukAB as critical molecules secreted by *S. aureus* biofilms that inhibit murine MΦ phagocytosis and promote cytotoxicity. A role for Hla and LukAB was confirmed using *hla* and *lukAB* mutants and synergy between both toxins was demonstrated with a *lukAB/hla* double mutant and verified by complementation. Independent confirmation of the effects of Hla and LukAB on MΦ dysfunction was demonstrated using an isogenic strain where Hla was constitutively expressed, a Hla antibody to block toxin activity, and purified LukAB peptide. The importance of Hla and LukAB during *S. aureus* biofilm formation *in vivo* was assessed using a murine orthopedic implant biofilm infection model, where the *lukAB/hla* strain displayed significantly decreased bacterial burdens and increased MΦ infiltrates compared with each single mutant. Collectively, these findings reveal a critical synergistic role for Hla and LukAB in promoting MΦ dysfunction and facilitating *S. aureus* biofilm development *in vivo.*

Introduction

Highly opportunistic pathogens possess attributes that facilitate persistent infections, in part, by shielding themselves from immune-mediated attack (223-225). *S. aureus* is one such example, and in addition to its well-known arsenal of virulence determinants, biofilm formation represents another means to circumvent immune-mediated clearance in the host (15, 16). Biofilms are heterogeneous bacterial communities encased in a complex matrix composed of extracellular DNA (eDNA), proteins, and polysaccharides (11, 32, 226, 227). *S. aureus* has a propensity to form biofilms on medical devices, such as prostheses and indwelling catheters, and the organism remains a major cause of health care- and community-associated infections (194, 228, 229).

Many *S. aureus* virulence factors target innate immune pathways that are elicited during acute planktonic infection, such as phagocytosis and proinflammatory transcription factor activation (15, 160, 213, 230). Phagocytosis leads to the killing of extracellular pathogens as well as proinflammatory cytokine and chemokine production, which collectively orchestrate local and systemic inflammatory responses and initiate adaptive immunity (129-131). Recent studies have demonstrated that biofilms formed by various bacterial species interfere with classical host anti-bacterial effector mechanisms (170, 231-235). With regard to *S. aureus*, work from our laboratory and others has shown that biofilms polarize MΦs towards an anti-inflammatory phenotype by dampening proinflammatory responses and limiting MΦ invasion *in vivo* (15, 159, 160, 236, 237). This response is considered detrimental to biofilm clearance, since polarized MΦs possess poor microbicidal activity and instead promote fibrosis (15). Similar findings of MΦ dysfunction have been reported in response to *S. epidermidis* biofilms (158, 164, 165), suggesting the existence of a conserved effort to thwart efficient biofilm recognition and clearance by the host. However, the molecules responsible for the ability of *S. aureus* biofilms to attenuate MΦ proinflammatory responses remain ill-defined.

The objective of this study was to identify *S. aureus* biofilm-derived products that induce MΦ dysfunction and facilitate biofilm persistence. Quantitative mass spectrometry identified Hla and the bicomponent leukotoxin, LukAB, also known as LukGH, as potential candidates responsible for inhibiting MΦ phagocytosis and promoting cytotoxicity, which was confirmed using *hla* and *lukAB* mutants. A synergistic effect was demonstrated with a *lukAB/hla* double mutant that also revealed decreased biofilm formation *in vivo* using a murine model of orthopedic implant biofilm infection. The reduction in MΦ phagocytosis, concomitant with enhanced cell death, likely facilitates the ability of *S. aureus* to avoid destructive host responses when organized as a biofilm.

Results

S. aureus biofilms secrete a proteinaceous factor(s) that inhibits macrophage phagocytosis. Our previous studies demonstrated that MΦs are unable to phagocytose *S. aureus* biofilms (15, 160); however, the mechanism responsible for this phenomenon remained to be identified. While it is known that the physical size of a biofilm is one factor that impedes phagocytosis (15), we investigated the possibility that a secreted factor(s) was also involved. In order to assess the effect of biofilm-conditioned medium on MΦ phagocytosis, we utilized fluorescent microspheres instead of live bacteria, since live *S. aureus* actively secretes factors during planktonic growth that would have been impossible to differentiate from biofilm-derived molecules. Using this approach, we were able to readily distinguish differences in phagocytosis and viability of murine MΦs exposed to fresh medium (Fig. 4.1A), *S. aureus* biofilm-conditioned medium (Fig. 4.1B), and *S. aureus* planktonic-conditioned medium (Fig. 4.1C) using confocal microscopy. Of note, similar effects of *S. aureus* biofilm-conditioned medium on MΦ phagocytosis were obtained with fluorescent microspheres and intact *S. aureus* in pilot studies (Supplemental Fig. S2.1), supporting the validity of this approach. MΦ phagocytic activity was significantly reduced after treatment with conditioned medium from intact biofilms of the Methicillin-resistant *S. aureus* (MRSA) clinical isolate USA300 LAC (172-175) (Fig. 4.1B and D), revealing a role for an extracellular factor(s). To determine whether this effect relied on an intact biofilm structure, fresh medium was added to mature biofilms that were disrupted by trituration, whereupon conditioned medium was harvested 24 h later. Treatment of MΦs with supernatants collected from disrupted biofilms had less impact on phagocytosis (Fig. 4.1D), suggesting that the putative extracellular factor(s) is enriched in intact biofilms, perhaps via a QS system that is disturbed upon destruction of the biofilm architecture. Similarly, conditioned medium from planktonic organisms was less effective at blocking MΦ phagocytosis (Fig. 4.1C and D), even when cultures were grown to a high cell density (i.e. late stationary phase; data not shown), demonstrating the enrichment of this

secreted factor(s) in intact biofilms. Importantly, these differences did not result from alterations in bacterial density or secreted protein levels, since titers and extracellular protein concentrations of intact biofilms, disrupted biofilms, and planktonic cultures were similar (Supplemental Fig. S4.1 and data not shown).

Whereas little information is currently available regarding the *S. aureus* biofilm secretome, the importance of autolysis to biofilm formation has been well-established (20, 32, 78, 238-240). To determine whether the putative biofilm extracellular factor(s) was actively secreted or a byproduct of cell lysis, mature biofilms were treated for 24 h with polyanethole sodium sulfanate (PAS) to inhibit lysis (241) or disrupted by trituration and treated with lysostaphin to artificially induce lysis. Only biofilm-conditioned medium from PAS-treated supernatants maintained inhibitory activity (Fig. 4.1F), suggesting that *S. aureus* biofilms actively secrete molecule(s) that impede MΦ phagocytosis. To elucidate the chemical nature of secreted inhibitory factor(s), conditioned medium from intact biofilms was treated with proteinase K prior to MΦ addition. Proteinase K completely ablated the inhibitory effect of *S. aureus* biofilm-conditioned medium on MΦ phagocytosis, implicating the action of a protein(s) in this phenomenon (Fig. 4.1H).

In addition to impaired phagocytosis, our prior report demonstrated that *S. aureus* biofilms also induced MΦ cytotoxicity (15). The latter could result from frustrated phagocytosis based on the inability of MΦs to physically engulf the bulky biofilm structure combined with the action of secreted toxins, such as Hla or leukocidins with known cytotoxic activity (131, 213, 242). Exposure of murine MΦs to conditioned medium from intact *S. aureus* biofilms induced significant cell death, whereas minimal cytotoxicity was observed following treatment with medium from either disrupted biofilms or planktonic *S. aureus* (Fig. 4.1A-C, and E). Similar to the approach employed for phagocytosis, biofilms were treated with lysostaphin or PAS, where only lysostaphin prevented the cytotoxic effects of biofilm-conditioned medium (Fig. 1G), again

revealing the action of an actively secreted protein based on its proteinase K-sensitive nature (Fig. 4.1I).

Figure 4.1

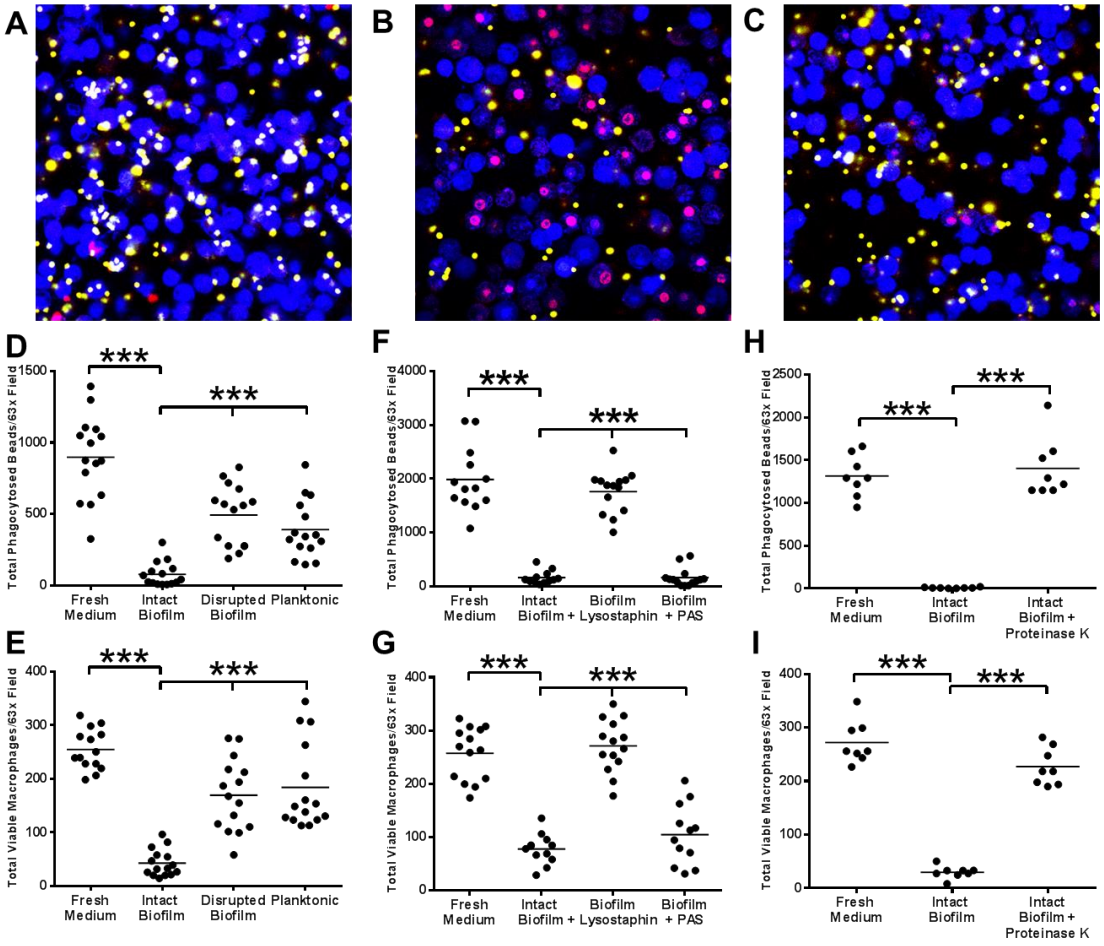

***S. aureus* biofilms secrete a proteinaceous factor(s) that inhibits macrophage phagocytosis.** (A-C) Representative 2D confocal images (63x) of BMDMΦ phagocytosis of fluorescent microspheres (yellow-white) and cell death with propidium iodide stain (red-purple) after exposure to (A) fresh medium, (B) *S. aureus* biofilm-conditioned medium, or (C) *S. aureus* planktonic-conditioned medium. (D and E) BMDMΦs were exposed to fresh medium or conditioned medium collected from an intact biofilm, a mature biofilm that was mechanically disrupted, or a similar number of planktonic *S. aureus*. After a 3 h treatment period, (D) MΦ phagocytosis of fluorescent microspheres and (E) cell viability was quantitated by confocal microscopy. (F and G) Conditioned medium from biofilms treated with either PAS (10 μg/ml) or

lysostaphin (50 μg/ml) were added to MΦs to assess the relative importance of active biofilm secretion versus passive release of products via autolysis, respectively, on MΦ (F) phagocytosis and (G) cell death. (H and I) Biofilm-conditioned supernatants were treated with proteinase K (10 μg/ml) prior to MΦ exposure to assess the chemical nature of the inhibitory molecule(s). Significant differences are denoted with asterisks (***, $p < 0.001$; one-way ANOVA followed by Bonferroni's multiple comparison test). Results are representative of at least two independent experiments.

***S. aureus* biofilm-induced macrophage dysfunction is partially *agr*-dependent.** Our findings that disrupted biofilms were not as effective at blocking MΦ phagocytosis or inducing cytotoxicity suggested that QS systems enriched during biofilm formation may regulate the putative inhibitory molecule(s). The expression of numerous virulence factors in *S. aureus*, including secreted proteases, leukocidins, and Hla, is either directly or indirectly influenced by two-component regulatory systems, such as the *agr* QS system (243). *Agr* modulates virulence factor expression and is an important regulatory switch between planktonic and biofilm lifestyles in *S. aureus* (64, 212, 244-246). Conditioned medium from a Δ*agr* biofilm induced minimal MΦ cell death (Fig. 4.2B), whereas the phagocytic block was significantly attenuated but only partially influenced by *agr* (Fig. 4.2). Since the MΦ inhibitory phenotypes upon exposure to *S. aureus* biofilms were partially *agr*-dependent, the Δ*agr* strain was utilized for subsequent proteomics comparisons with WT biofilms in an attempt to identify secreted proteins enriched during biofilm growth that were capable of inducing MΦ dysfunction.

Figure 4.2

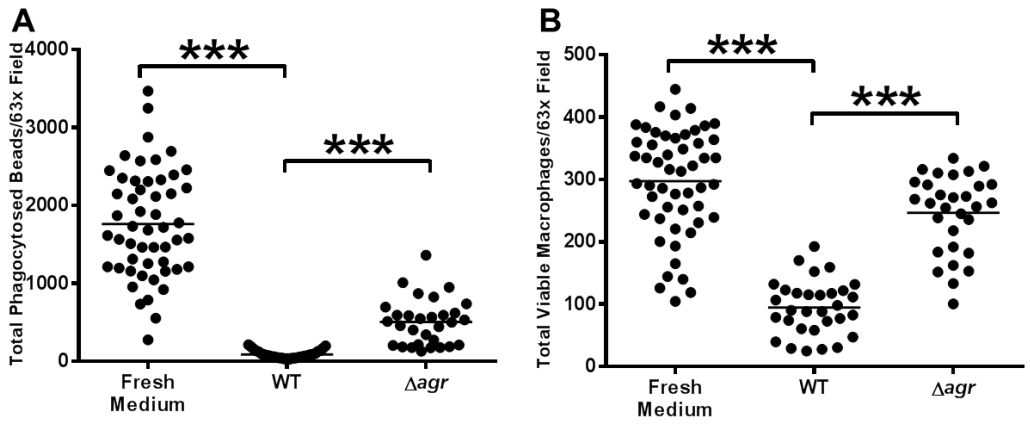

S. aureus* biofilm-induced macrophage dysfunction is partially *agr*-dependent.** BMDMΦs were exposed to fresh or conditioned medium from *S. aureus* WT or isogenic Δ*agr* biofilms for 2 h, whereupon (A) phagocytosis of fluorescent microspheres and (B) total viable MΦs were quantitated by confocal microscopy. Significant differences are denoted with asterisks (, $p < 0.001$; unpaired two-tailed student's *t*-test). Results are representative of at least three independent experiments.

Sequential Windowed data-independent Acquisition of the Total High-resolution Mass Spectra (SWATH-MS) as a tool to identify *S. aureus* biofilm factors that induce macrophage dysfunction. We next employed a proteomics approach to identify candidate molecules that might be responsible for biofilm-mediated MΦ dysfunction. Our proteomics strategy utilized the Δ*agr* strain as a comparator with WT biofilm, since the MΦ inhibitory phenotypes were partially *agr*-dependent (Fig. 4.2). A second comparison was made between biofilm and planktonic conditions because the MΦ inhibitory factors were enriched during biofilm growth (Fig. 4.1). To identify differentially expressed proteins between WT vs. Δ*agr* biofilm- and planktonic-conditioned medium, TCA-precipitated proteins were analyzed by quantitative SWATH-MS (189). As expected, conditioned medium from WT and Δ*agr* biofilms displayed vastly different proteomic profiles, with 68 of 153 (44%) proteins significantly enriched in WT biofilms, 23% of which were either secreted proteases or known virulence factors, such as Hla (Fig. 4.3A and B; Table S4.1). In contrast, cell wall and structural proteins were more abundant in Δ*agr* biofilm-conditioned medium compared to WT (Fig. 4.3A and B). Similarly, proteomic comparisons between WT biofilm- vs. WT planktonic-conditioned medium differed significantly, with 108 of 301 (36%) proteins enriched in WT biofilm, including several secreted virulence factors such as toxins and proteases (Table S4.2). A functional proteomics network constructed with overlapping hits from both comparisons (WT biofilm vs. Δ*agr* biofilm and WT biofilm vs. WT planktonic) identified 17 proteins, including two serine proteases and two leukocidin components, as candidates to account for the inhibitory effects of biofilm-conditioned medium on MΦ function (Fig. 4.3C). Additionally, Hla was significantly enriched in WT compared to Δ*agr* biofilms (Table S4.1), which represented another toxin of interest for its potential role in regulating MΦ dysfunction. Importantly, both Hla and LukAB were significantly enriched in biofilm- compared to planktonic-conditioned medium (Fig. 4.4), suggesting that these two proteins may be responsible for biofilm-induced MΦ dysfunction. LukAB is a bi-component leukotoxin also involved in *S. aureus*-mediated killing of host phagocytes (67, 247, 248).

Therefore, Hla and LukAB were the focus of subsequent mechanistic studies as they likely play a significant role in MΦ dysfunction and death in this setting.

Figure 4.3

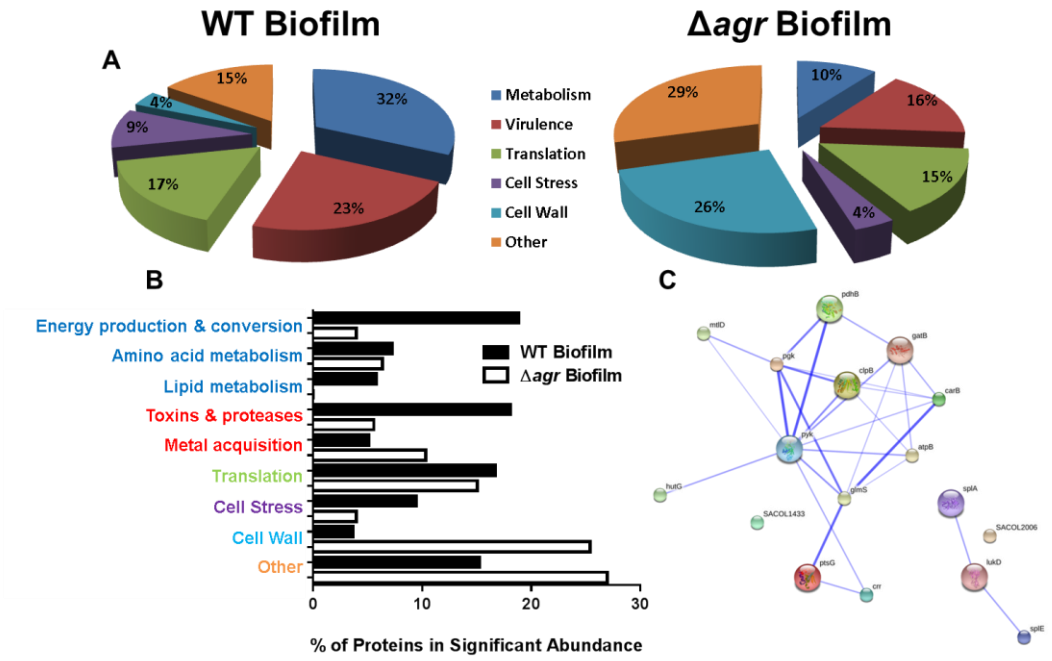

SWATH-MS identifies potential biofilm factors responsible for macrophage dysfunction. Conditioned supernatants from either *S. aureus* WT or Δ*agr* strains grown under planktonic or biofilm conditions were harvested and TCA precipitated for protein isolation in triplicate. Relative protein concentrations were compared between sample sets by Sequential Windowed data independent Acquisition of the Total High-resolution Mass Spectra (SWATH-MS). (A) 68 of 153 (44%) identified proteins were significantly enriched in WT vs. Δ*agr* biofilm, with the largest percentage associated with metabolism and virulence. 85 of 153 (56%) identified proteins were significantly enriched in Δ*agr* biofilm vs. WT biofilm, with the largest percentage of proteins falling into the functional category of cell wall proteins. (B) Direct comparison of significantly expressed proteins in WT vs. Δ*agr* biofilm by functional category, with more refined groups of metabolism and virulence shown. (C) Functional protein association network of SWATH-MS identified proteins significantly enriched in WT biofilm-conditioned supernatant vs. planktonic and Δ*agr* biofilm-conditioned supernatants. For all comparisons, statistical significance was assessed using a Z-test ($p < 0.05$).

Figure 4.4

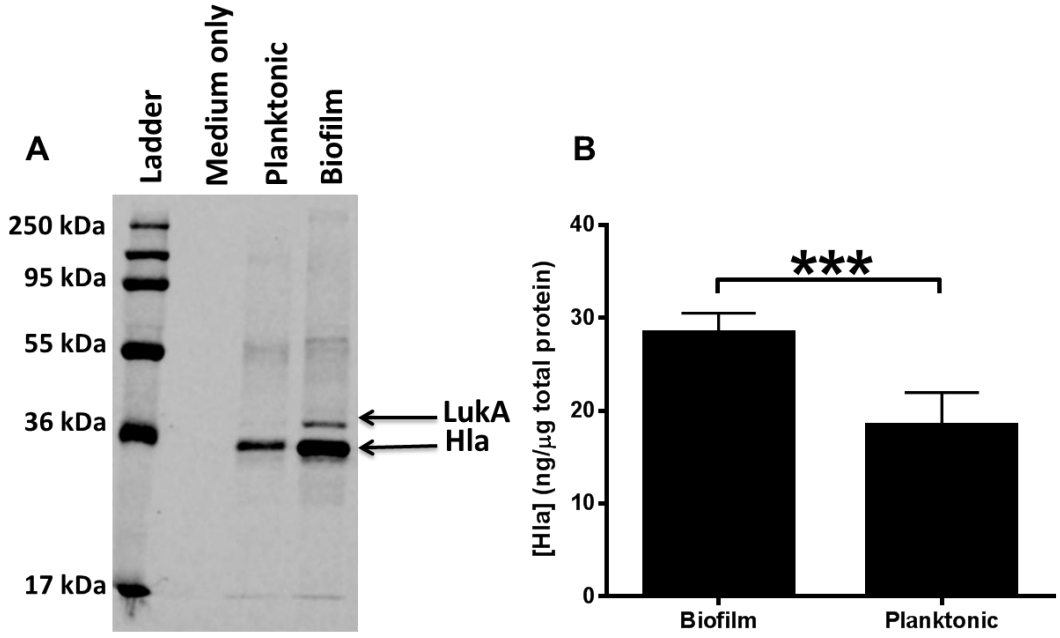

LukA and Hla secretion is enhanced in *S. aureus* biofilms. (A) LukA and Hla levels in *S. aureus* biofilm- vs. planktonic- conditioned medium were assessed by Western blots. (B) Quantitation of Hla levels in conditioned medium from WT *S. aureus* biofilms versus planktonic bacteria. Significant differences are denoted with asterisks (***, $p < 0.001$; unpaired two-tailed student's *t*-test). Results are representative of at least two independent experiments.

LukAB and Hla play significant roles in biofilm-induced macrophage dysfunction. Biofilm-conditioned medium from both Δ*lukA* and Δ*lukB* strains elicited minimal MΦ death compared to WT biofilm (Fig. 4.5B). Likewise, the phagocytic block induced by the Δ*lukA* and Δ*lukB* strains was less pronounced than WT biofilm-conditioned medium, although phagocytosis did not return to baseline levels (Fig. 4.5A). Both Δ*lukA* and Δ*lukB* phenotypes could be complemented, providing direct evidence for LukAB in modulating MΦ survival and phagocytosis (Fig. 4.5A and B). In contrast, while serine proteases were also noted to be elevated by SWATH-MS, biofilm-conditioned medium from serine protease mutants (Δ*spl* or Δ*aur/spl/sspAB/scpA*) as well as another leukocidin mutant (Δ*lukD*) behaved similarly to WT biofilms (data not shown).

Since LukAB did not account for the entire MΦ dysfunction phenotype and SWATH-MS identified increased Hla levels in WT biofilm-conditioned medium (Table S4.1), we next examined the contribution of Hla to MΦ dysfunction. Further justification for investigating Hla stemmed from the vast literature on Hla regulation by the *agr* QS system (242, 249-251), the finding that conditioned medium from Δ*agr* biofilms was less effective at inducing MΦ dysfunction (Fig. 4.2), and that Hla secretion was significantly increased during biofilm growth (Fig. 4.4). Hla inserts into host cell membranes and oligomerizes to form pores, leading to cell death (242, 252). Indeed, MΦ survival was significantly improved following exposure to Δ*hla* biofilm-conditioned medium compared to WT biofilm, which was complementable (Fig. 4.5D). The effects of Δ*hla* on MΦ phagocytosis were less pronounced, but still reached statistical significance (Fig. 4.5C). Furthermore, blockade of Hla activity in WT biofilm-conditioned medium using a Hla neutralizing antibody phenocopied the findings with Δ*hla* (Fig. 4.5C and D). Specificity of the Hla antibody was demonstrated by its ability to inhibit the effects of purified Hla on MΦ survival and viability (Supplemental Fig. S4.3). Additional evidence to support Hla action was provided by the ability of biofilm-conditioned medium from a *S. aureus* strain that

constitutively expresses *hla* (*hla*^{on}) to induce significant MΦ death and inhibit phagocytosis (Fig. 4.5C and D).

Both Hla and LukAB expression were markedly increased in conditioned medium from WT biofilms compared to planktonic bacteria (Fig. 4.4). Therefore, to assess whether LukAB and Hla act cooperatively to effect MΦ activity, Δ*lukA* and Δ*lukB* biofilm-conditioned media were treated with a Hla neutralizing antibody (Fig. 4.6). Interestingly, negating Hla action in Δ*lukA* and Δ*lukB* biofilm-conditioned medium significantly improved MΦ phagocytosis compared to supernatants where Hla was active (Fig. 4.6A). Similar findings were obtained with a Δ*lukAB/*Δ*hla* mutant (Fig. 4.6A). Hla blockade in Δ*lukA* and Δ*lukB* biofilm-conditioned medium had no additional effect on MΦ survival, which was not unexpected since viability had nearly been restored with each of the single mutants to levels observed with fresh medium (Fig. 4.6B). When MΦs were treated with Δ*lukAB* biofilm-conditioned medium (that still produces Hla) in combination with purified LukAB or a point mutant that lacks lytic activity (LukAB^{E323A}) (186), only bioactive LukAB returned both phagocytic inhibition and cytotoxicity to levels observed with WT biofilm-conditioned medium (Fig. S4.3). Collectively, these results demonstrate that LukAB acts in concert with Hla to induce MΦ dysfunction.

Figure 4.5

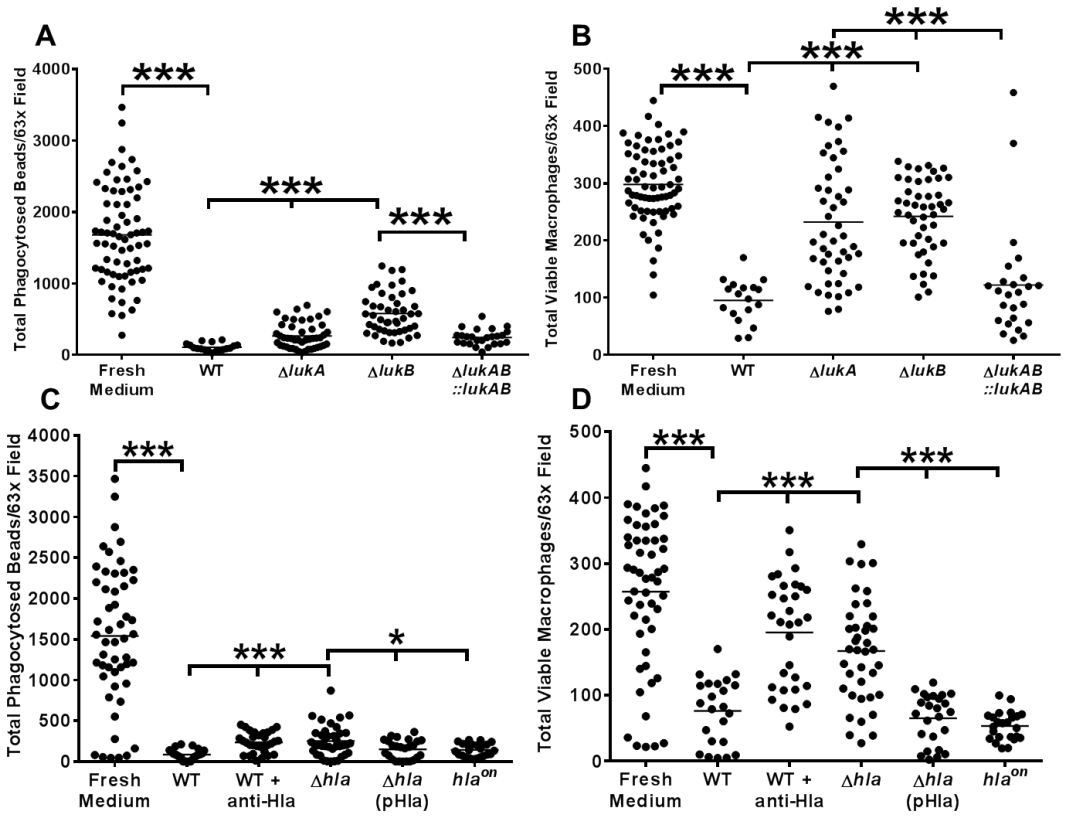

LukAB and Hla play significant roles in biofilm-induced macrophage dysfunction. (A and B) BMDMΦs were exposed to fresh or conditioned medium from *S. aureus* WT, Δ*lukA*, Δ*lukB*, or chromosomally complemented Δ*lukAB* (Δ*lukAB::lukAB*) biofilms. After a 3 h treatment period, (A) phagocytosis of fluorescent microspheres and (B) viable MΦs were quantitated by confocal microscopy. (C and D) BMDMΦs were exposed to fresh or conditioned medium from *S. aureus* WT biofilm ± Hla antibody (α-Hla), Δ*hla*, plasmid complemented Δ*hla* [Δ*hla*(pHla)], and constitutively expressed *hla* (*hla*^{on}) biofilms. After a 3 h treatment period, (C) phagocytosis of fluorescent microspheres and (D) viable MΦs were quantitated by confocal microscopy. Significant differences are denoted with asterisks (*, $p < 0.05$; ***, $p < 0.001$; unpaired two-tailed student's *t*-test). Results are representative of at least three independent experiments.

Figure 4.6

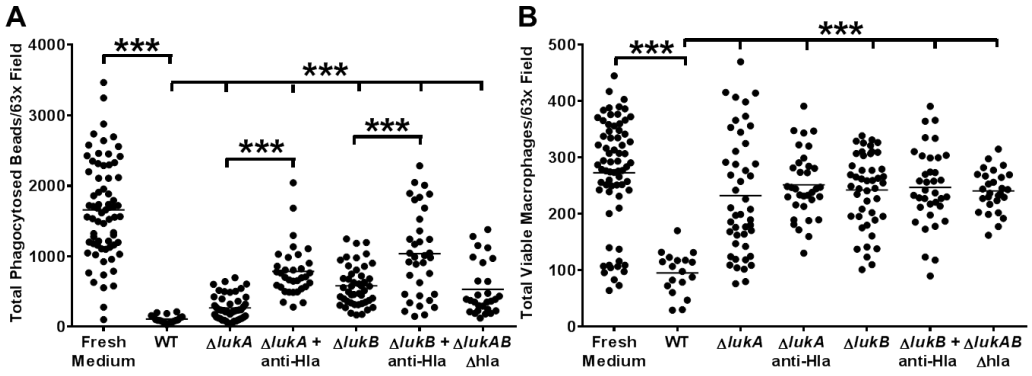

S. aureus* Hla and LukAB act in concert to promote macrophage dysfunction.** BMDMΦs were exposed to fresh or conditioned medium from *S. aureus* WT or isogenic Δ*lukA*, Δ*lukB* and Δ*lukAB/hla* biofilms ± Hla antibody (α-Hla). After a 3 h treatment period, (A) phagocytosis of fluorescent microspheres and (B) viable MΦs were quantitated by confocal microscopy. Significant differences are denoted with asterisks (, $p < 0.001$; unpaired two-tailed student's *t*-test). Results are representative of at least three independent experiments.

LukAB and Hla are important for S. aureus biofilm formation in vivo. Previous work from our laboratory has demonstrated that augmenting MΦ proinflammatory activity is critical for biofilm clearance *in vivo* (160). Therefore, to determine whether the functional role identified for LukAB and Hla in mediating MΦ dysfunction *in vitro* would impact biofilm formation *in vivo*, we utilized a murine model of *S. aureus* orthopedic implant biofilm infection (54, 55, 253). Similar to our *in vitro* studies revealing cooperation between LukAB and Hla, the Δ*lukAB/*Δ*hla* double mutant displayed the greatest reduction in bacterial burdens in the knee joint, surrounding soft tissue, and femur at days 3 and 7 post-infection compared to *ΔlukAB or Δhla* strains (Fig. 4.7A-C). Furthermore, MΦ infiltrates were significantly increased in mice infected with Δ*lukAB/*Δ*hla* (Fig. 4.7D), although they represent a minor population in this model of orthopedic implant biofilm infection, which is dominated by myeloid-derived suppressor cells (MDSCs) (54, 55). Taken together, these results identify LukAB and Hla as important virulence factors for modulating bacterial persistence and MΦ infiltrates during *S. aureus* biofilm formation *in vivo*.

Figure 4.7

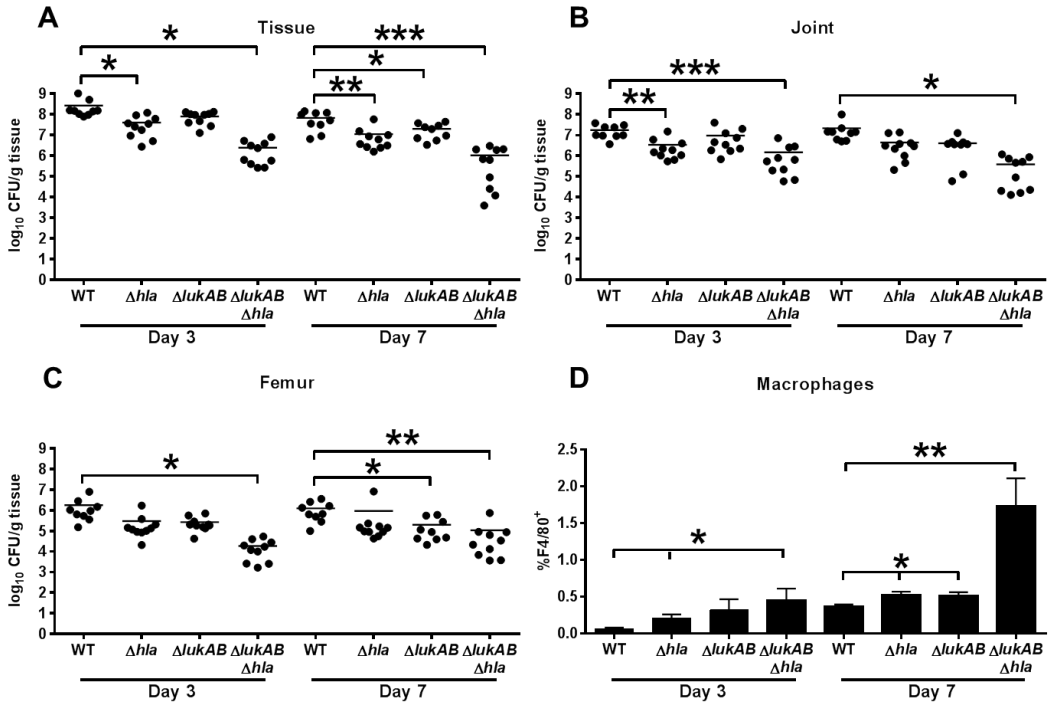

LukAB and Hla are important for *S. aureus* biofilm formation *in vivo*. Bacterial burdens associated with the (A) soft tissue surrounding the knee, (B) knee joint, and (C) femur of mice infected with WT *S. aureus* and isogenic Δ*hla*, Δ*lukAB* and Δ*lukAB/hla* strains at days 3 and 7 post-infection (n = 10 mice per strain for each time point). Results are expressed as the number of CFU per gram of tissue to correct for differences in tissue sampling size. (B) Quantitation of $F4/80^+$ MΦs infiltrating the soft tissue of mice infected with WT *S. aureus* and isogenic Δ*hla*, Δ*lukAB* and Δ*lukAB/hla* strains. Significant differences are denoted with asterisks (*, $p < 0.05$; **, $p < 0.01$; ***, $p < 0.001$; unpaired two-tailed Student's *t*-test). Results are combined from two independent experiments.

Figure 4.8

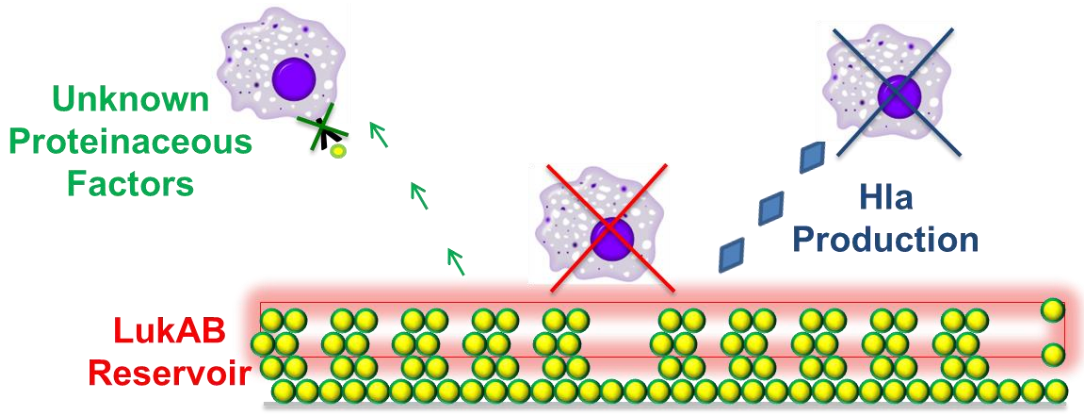

Proposed model for *S. aureus* biofilm-induced macrophage dysfunction. *S. aureus* biofilms produce an abundance of LukAB, which can associate with the cell surface as a toxin reservoir or be actively secreted into the extracellular milieu. Biofilms also secrete Hla that acts synergistically with LukAB to elicit MΦ dysfunction. Other secreted proteins, such as lipoproteins, lantibiotics, or siderophores may also impact MΦ phagocytosis.

Supplemental Figure S4.1

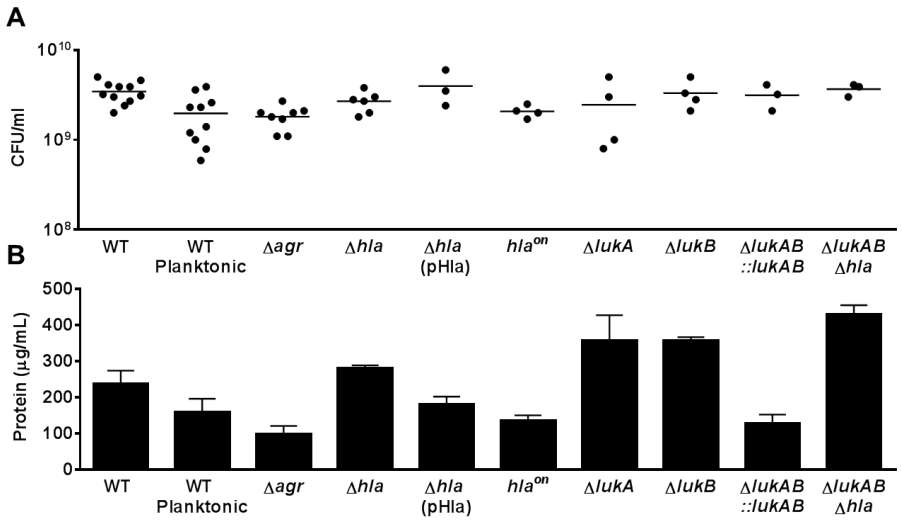

Bacterial counts and extracellular protein concentrations of *S. aureus* WT planktonic, biofilm, and isogenic mutant biofilms are similar. (A) All *S. aureus* strains used in these studies grew to comparable extents after 6 days of culture in RPMI-1640 supplemented with 1% CAA as indicated by the number of viable bacteria determined by quantitative culture with results expressed as colony forming units (CFU) per ml. (B) Quantitation of secreted proteins for each strain. Data are representative of at least two independent experiments. Strains are abbreviated as follows: Δ*agr* = accessory gene regulator mutant; Δ*hla* = α-hemolysin mutant; Δ*hla* (pHla) = plasmid complemented α-hemolysin mutant; hla^{on} = WT strain constitutively expressing α-toxin; Δ*lukA* = leukocidin AB component single mutant; Δ*lukB* = leukocidin AB component single mutant; ; Δ*lukAB::lukAB* = chromosomally complemented leukocidin AB double mutant; Δ*lukAB*/Δ*hla* = leukocidin AB and α-hemolysin double mutant.

Supplemental Figure S4.2

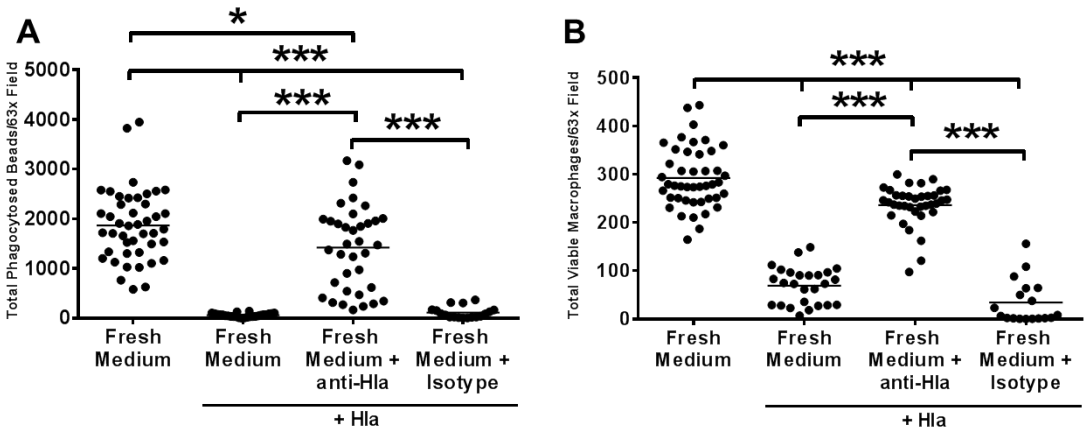

Validation of *S. aureus* Hla action on macrophage dysfunction. BMDMΦs were incubated for 2 h with fresh medium alone or fresh medium with purified *S. aureus* Hla + an isotype control or Hla antibody (α-Hla). After a 2 h treatment period, (A) MΦ phagocytosis of fluorescent microspheres and (B) total viable MΦs were quantitated by confocal microscopy. Significant differences are denoted with asterisks (*, $p < 0.05$; ***, $p < 0.001$; unpaired two-tailed student's t-test). Results are representative of at least two independent experiments.

Supplemental Figure S4.3

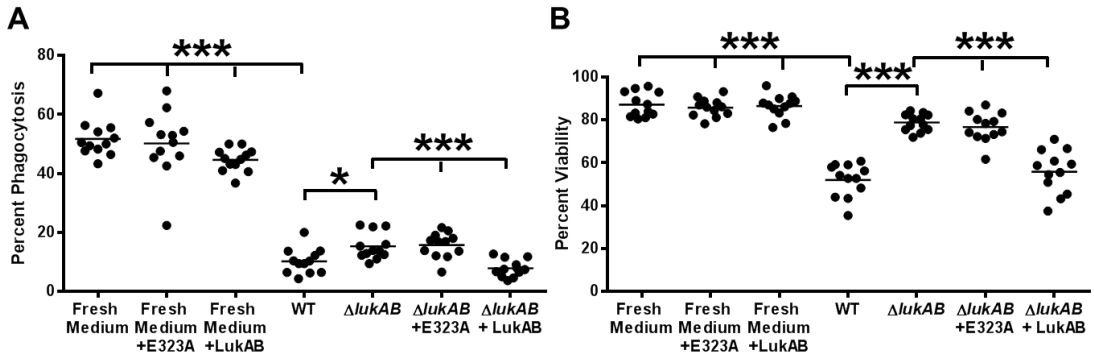

Purified LukAB augments macrophage cytotoxicity. BMDMΦs were exposed to fresh or biofilm-conditioned medium from *S. aureus* WT or isogenic Δ*lukAB* ± purified LukAB or inactive LukAB^{E323A}. After a 3 h treatment period, the (A) percentage of MΦs phagocytosing fluorescent microspheres and (B) percentage of viable MΦs were quantitated by confocal microscopy. Significant differences are denoted with asterisks (***, $p < 0.001$; unpaired two-tailed Student's *t*-test). Results are representative of at least two independent experiments.

Supplemental Figure S4.4

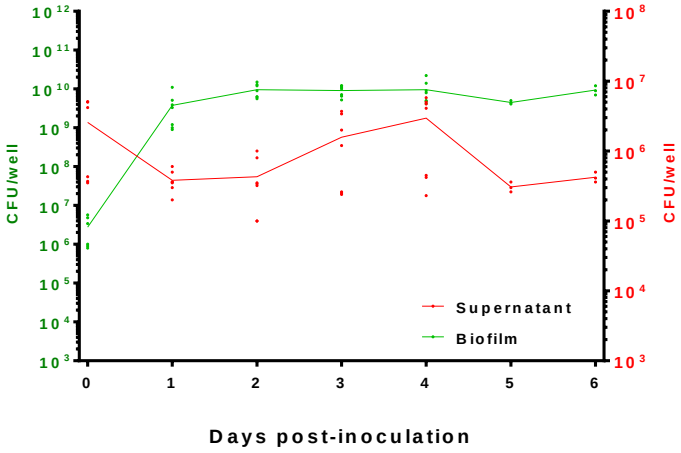

Characterization of *S. aureus* biofilm growth in 1% casamino acids. Total numbers of dispersed (supernatant) vs. biofilm-associated bacteria in RPMI-1640 supplemented with 1% casamino acids were assessed by serial dilution (CFU/well) throughout the 6 day biofilm maturation process.

Table S4.1 Proteins identified to be in greater abundance in WT *S. aureus* biofilm-conditioned medium compared to Δ*agr* biofilm-conditioned medium

Magnitude	Category	Protein	Identity
14.32	Translation	RL5	Ribosomal protein
4.73	Translation	Syn	Asparagine-tRNA ligase
4.09	Translation	RL13	Ribosomal protein
3.32	Translation	RL332	Ribosomal protein
2.90	Translation	EF-TU	Elongation factor
2.72	Translation	RL27	Ribosomal protein
2.56	Translation	GatB	Aspartyl/glutamyl-tRNA amidotransferase subunit B
2.42	Translation	RS7	Ribosomal protein
2.1	Translation	RL16	Ribosomal protein
2.01	Translation	RL10	Ribosomal protein
25.93	Metabolism	CysK	Cysteine synthase
6.92	Metabolism	CarB	Carbamoyl phosphate synthetase subunit B
4.37	Metabolism	OtcC	Ornithine carbamoyltransferase
3.91	Metabolism	KpyK	Pyruvate kinase
3.63	Metabolism	Pur8	Adenylosuccinate lyase
3.07	Metabolism	HutG	Formimidoylglutamase
2.87	Metabolism	Pgk	Phosphoglycerate kinase
2.50	Metabolism	GlmS	Glutamine--fructose-6-phosphate aminotransferase
2.42	Metabolism	OdpB	Pyruvate dehydrogenase E1 component subunit beta
2.29	Metabolism	Ldh1	L-lactate dehydrogenase 1
42.01	**Protease**	SplB	Serine-like protease[a]
33.61	**Protease**	SplD	Serine-like protease
24.78	Protease	SspA	Serine protease
24.78	Protease	SspB	Cysteine protease
14.23	Protease	SspP	Cysteine protease
9.02	Protease	SplA	Serine-like protease
6.48	Protease	SplC	Serine-like protease
2.17	Protease	SplE	Serine-like protease
11.97	Virulence	LukDV/HlgB	Leukocidin component
10.59	Virulence	HlgA	Gamma-hemolysin component A
9.71	Virulence	Hld	Delta-hemolysin
6.38	Virulence	Hla	Alpha-hemolysin
5.09	Virulence	PsmA4	Phenol-soluble modulin alpha 4 peptide
3.90	Virulence	LukB/H	Leukocidin component
3.81	Virulence	LukA/G	Leukocidin component
3.09	Virulence	ClfA	Clumping factor A
9.98	Cell Stress	Asp23	Alkaline shock protein
6.49	Cell Stress Cell	Ch60	60 kDa chaperonin
5.92	Stress Cell	ClpL	ATP-dependent Clp protease ATP-binding subunit
5.08	Stress Cell	OhrL	Organic hydroperoxide resistance protein-like
2.29	Stress	HchA	Molecular chaperone Hsp31 and glyoxalase 3
23.69	Other	Pnp	Polyribonucleotide nucleotidyltransferase
23.39	Other	Lip1	Lipase
6.92	Other	Pbp	Beta-lactam-inducible penicillin-binding protein
6.09	Other	PpaC	Probable manganese-dependent inorganic pyrophosphatase

5.13	Other	Lip2	Lipase
4.33	Other	Ggi3	Antibacterial protein 3 homolog
4.25	Other	AtpB	ATP synthase subunit beta
3.98	Other	AtpA	ATP synthase subunit alpha
3.84	Other	ButA	Diacetyl reductase
3.72	Other	Ispd2	2-C-methyl-D-erythritol 4-phosphate cytidylyltransferase 2
3.69	Other	Y2518	Uncharacterized hydrolase
3.49	Other	Y2365	Uncharacterized lipoprotein
3.44	Other	Ptg3C	PTS system glucose-specific EIICBA component
3.30	Other	GcsT	Aminomethyltransferase
3.17	Other	FtsZ	Cell division
2.94	Other	PdxS	Pyridoxal biosynthesis lyase
2.83	Other	CatA	Catalase
2.63	Other	Y840	Uncharacterized protein
2.46	Other	DldH	Dihydrolipoyl dehydrogenase
2.45	Other	ClpB	Chaperone protein
2.44	Other	PtgA	Glucose-specific phosphotransferase enzyme IIA component
2.36	Other	MtlD	Mannitol-1-phosphate 5-dehydrogenase
2.21	Other	Y370	Uncharacterized protein
2.20	Other	Y941	NADH dehydrogenase-like protein
2.16	Other	UP355	Uncharacterized protein
2.14	Other	Dbh	DNA-binding protein
2.10	Other	Y1797	Uncharacterized protein

[a]Proteins in red were selected for follow-up confirmation with mutant strains

Table S4.2 Proteins identified to be in greater abundance in WT *S. aureus* biofilm-conditioned medium compared to WT planktonic-conditioned medium

Magnitude	Category	Protein	Identity
36.16	Metabolism	GlmS	Glutamine--fructose-6-phosphate aminotransferase
19.56	Metabolism	GlnA	Glutamine synthetase
19.27	Metabolism	PyrB	Aspartate carbamoyltransferase
15.11	Metabolism	Dha1	Alanine dehydrogenase 1
13.88	Metabolism	Alf1	Fructose-bisphosphate aldolase class 1
10.66	Metabolism	Odo1	2-oxoglutarate dehydrogenase E1 component
10.54	Metabolism	Kad	Adenylate kinase
10.16	Metabolism	DaaA	D-alanine aminotransferase
9.01	Metabolism	TpiS	Triosephosphate isomerase
8.12	Metabolism	Pur1	Amidophosphoribosyltransferase
7.95	Metabolism	Odp2	Dihydrolipoyllysine-residue acetyltransferase
7.59	Metabolism	P5cr	Pyrroline-5-carboxylate reductase
7.54	Metabolism	PyrG	CTP synthase
7.47	Metabolism	HutG	Formimidoylglutamase
6.98	Metabolism	LdhD	D-lactate dehydrogenase
6.74	Metabolism	AckA	Acetate kinase
6.71	Metabolism	SdrD	Serine-aspartate repeat-containing protein D
6.48	Metabolism	Acp	Acyl carrier protein
5.97	Metabolism	RocA	1-pyrroline-5-carboxylate dehydrogenase

4.97	Metabolism	TdcB	L-threonine dehydratase catabolic protein
4.86	Metabolism	Pdp	Pyrimidine-nucleoside phosphorylase
4.83	Metabolism	Hps	3-hexulose-6-phosphate synthase
4.56	Metabolism	K6pf	6-phosphofructokinase
4.00	Metabolism	Mqo2	Probable malate:quinone oxidoreductase 2
3.94	Metabolism	Pgk	Phosphoglycerate kinase
3.62	Metabolism	CarB	Carbomoyl phosphate synthetase subunit B
3.56	Metabolism	KpyK	Pyruvate kinase
2.89	Metabolism	OtcC	Ornithine carbamoyltransferase, catabolic subunit
2.88	Metabolism	PyrC	Dihydroorotase
2.83	Metabolism	F16pC	Fructose-1,6-bisphosphatase class 3
2.66	Metabolism	PurM	Phosphoribosylformylglycinamidine cyclo-ligase
2.10	Metabolism	OdpB	Pyruvate dehydrogenase E1 component subunit beta
15.61	Translation	RL29	Ribosomal protein
8.07	Translation	RL3	Ribosomal protein
7.28	Translation	RL25	Ribosomal protein
7.20	Translation	RL14	Ribosomal protein
6.06	Translation	RL24	Ribosomal protein
4.96	Translation	RL7	Ribosomal protein
4.84	Translation	GatB	Aspartyl/glutamyl-tRNA amidotransferase subunit B
4.62	Translation	RS2	Ribosomal protein
4.43	Translation	RL16	Ribosomal protein
4.30	Translation	RS15	Ribosomal protein
3.74	Translation	RL5	Ribosomal protein
3.62	Translation	RL11	Ribosomal protein
2.81	Translation	RS7	Ribosomal protein
13.97	Virulence	FnbA	Fibronectin-binding protein A
9.19	Virulence	GyrA	DNA gyrase subunit A
8.05	Virulence	LukDV/HlgB	Leukocidin component[a]
7.05	Virulence	LukB/H	Leukocidin component
6.59	Virulence	BlaR	Regulatory protein
4.03	Virulence	HlgC	Gamma-hemolysin component C
2.80	Virulence	Emp	Extracellular matrix protein-binding protein
2.48	Virulence	Plc	1-phosphatidylinositol phosphodiesterase
66.31	Redox	MtlD	Mannitol-1-phosphate 5-dehydrogenase
13.95	Redox	Dhe2	NAD-specific glutamate dehydrogenase
7.61	Redox	Y2305	Putative 2-hydroxyacid dehydrogenase
6.05	Redox	AhpF	Alkyl hydroperoxide reductase subunit F
5.14	Redox	Y542	Putative heme-dependent peroxidase
4.46	Redox	Adh	Alcohol dehydrogenase
4.19	Redox	Azo1	FMN-dependent NADPH-azoreductase
7.29	Cell Stress	SodM	Superoxide dismutase
5.11	Cell Stress	RecA	Recombinase A
3.35	Cell Stress	CspA	Cold shock protein
2.75	Cell Stress	GrpE	Putative stress response protein
2.73	Cell Stress	ClpB	Chaperone protein
2.06	Cell Stress	ClpC	ATP-dependent Clp protease ATP-binding subunit
10.98	Structural	Atl	Bifunctional autolysin
2.90	Structural	IsdC	Iron-regulated surface determinant protein C
2.73	Structural	Omp7	77 kDa membrane protein
2.57	Structural	Rot	Repressor of toxin, transcriptional regulator

2.35	Structural	IsdH	Iron-regulated surface determinant protein H
2.00	Structural	SarA	Transcriptional regulator
8.33	Protease	SplF	Serine-like protease
5.74	Protease	SplA	Serine-like protease
5.46	Protease	SplE	Serine-like protease
3.91	Protease	Aur	Zinc metalloproteinase aureolysin
3.70	Protease	PepVL	Putative dipeptidase subunit
87.39	Other	RsbW	Serine-protein kinase
18.16	Other	SrrA	Transcriptional regulatory protein
15.64	Other	Dpo3B	DNA polymerase III subunit beta
14.54	Other	PanB	3-methyl-2-oxobutanoate hydroxymethyltransferase
14.02	Other	AtrF2	Putative acetyltransferase
13.22	Other	RpoE	Probable DNA-directed RNA polymerase subunit delta
11.32	Other	Hem3	Porphobilinogen deaminase
11.29	Other	RpoC	DNA-directed RNA polymerase subunit beta'
8.30	Other	AtpB	ATP synthase subunit beta
7.27	Other	GpsB	Cell cycle protein
6.91	Other	IlvE	Probable branched-chain-amino-acid aminotransferase
6.71	Other	HdoX2	Heme oxygenase (staphylobilin-producing) 2
5.82	Other	Y680	Probable transcriptional regulatory protein\
5.75	Other	CodY	GTP-sensing transcriptional pleiotropic repressor
5.50	Other	SceD	Probable transglycosylase
5.46	Other	Np30	30 kDa neutral phosphatase
4.60	Other	ThlA	Probable acetyl-CoA acyltransferase
4.49	Other	Y1696	UPF0297 protein
4.33	Other	RpoA	DNA-directed RNA polymerase subunit alpha
4.27	Other	Rnj1	Ribonuclease J 1
3.94	Other	PdxT	Glutamine amidotransferase subunit
3.93	Other	FtsL	Cell division protein
3.68	Other	Oat2	Ornithine aminotransferase 2
3.56	Other	Gsa2	Glutamate-1-semialdehyde 2,1-aminomutase 2
3.29	Other	Y2518	Uncharacterized hydrolase
3.23	Other	PtgA	Glucose-specific phosphotransferase enzyme IIA component
3.07	Other	Ptg3C	PTS system glucose-specific EIICBA component
3.06	Other	Y752	Uncharacterized protein
2.75	Other	Y968	Uncharacterized protein
2.40	Other	FabF	3-oxoacyl-[acyl-carrier-protein] synthase 2
2.37	Other	Ldh2	L-lactate dehydrogenase 2

[a]Proteins in red were selected for follow-up confirmation with mutant strains

Discussion

S. aureus subverts the host immune response by numerous mechanisms, including increased resistance to cationic antimicrobial peptides, impairment of phagocyte recruitment, interference with antibody-mediated opsonization and complement activation, and resistance to intracellular killing (213). In addition, biofilm formation further protects *S. aureus* from the host innate immune response, representing a communal virulence determinant (15, 56, 159). We have previously demonstrated that biofilm formation shields *S. aureus* from Toll-like receptor (TLR) detection and interferes with MΦ activation *in vivo* (15, 160). Here we explored the genetic basis of how biofilm growth prevents MΦ phagocytosis. Our earlier study showed that MΦs were capable of phagocytosing bacteria from mechanically disrupted, but not intact biofilms, suggesting that the size of the biofilm and/or density of its matrix represents a physical obstacle, a phenomenon referred to as "frustrated phagocytosis" (15, 254, 255). Here we extend these findings to demonstrate that *S. aureus* biofilms also secrete proteinaceous factors that actively inhibit MΦ phagocytosis and induce cell death. Interestingly, this proteinaceous component was mainly evident in intact biofilms, as conditioned medium from mechanically disrupted biofilms or planktonic cultures grown to early or late stationary phase failed to prevent phagocytosis to the same extent, although bacterial numbers and secreted protein concentrations were similar (Fig. 1D, Supplemental Fig. S4.1, and data not shown). The preferential ability of intact *S. aureus* biofilms to inhibit MΦ phagocytosis suggested the involvement of QS mechanisms that are enriched during biofilm growth and dissipate once the biofilm structure has been disrupted. This was confirmed by the finding that biofilm-mediated MΦ dysfunction, in particular cell death, was less pronounced following exposure to conditioned medium from a Δ*agr* biofilm. These observations, combined with the fact that conditioned medium from PAS-treated biofilms maintained inhibitory activity, whereas lysostaphin-treated biofilms did not, strongly implicated

the importance of active protein secretion by the biofilm (based on proteinase K sensitivity) to inhibit MΦ phagocytosis and induce cell death.

The identification of candidate proteins responsible for inducing MΦ death and inhibiting phagocytosis was facilitated with a relatively new quantitative mass spectrometry technique, namely SWATH-MS (189). After generating a protein library from our combined sample sets (i.e. WT biofilm, Δ*agr* biofilm, WT planktonic, and Δ*agr* planktonic), comparisons were performed to identify the most abundant proteins unique to WT biofilm-conditioned medium. While this list included some proteins undoubtedly released as a result of cell lysis (i.e. metabolic enzymes and ribosomal subunits), we focused on known secreted toxins and proteases that were also detected. Of this list, LukB, as well as its partner component LukA, were shown to have a significant impact on MΦ phagocytosis and viability. LukAB is unique among leukocidins for its ability to either remain cell wall-associated or released into the extracellular milieu (67, 247, 248). A recent study has shown that human leukocytes are exquisitely sensitive to the cytolytic actions of LukAB due to its specificity for CD11b (256) mediated by the binding of a specific glutamic acid residue (323A) (186). While murine leukocytes are less sensitive to LukAB (256, 257), this toxin was still implicated in *S. aureus* pathogenesis in a murine renal abscess model (67), which was confirmed in the current study using a murine *S. aureus* orthopedic implant biofilm model. Therefore, although human cells display a greater sensitivity to LukAB, it is clear from our report and work by others that this bi-component leukotoxin is also active towards murine leukocytes.

In addition to LukAB, Hla also significantly contributed to biofilm-associated murine MΦ death and phagocytosis. The toxic effects of Hla are well-known and, while a recent publication has demonstrated the cytoprotective effects of *S. aureus* Hla within phagosomes (258), it is important to note that this scenario is not applicable in our studies given that our phagocytosis assay utilized microspheres and not viable bacteria. This strategy was employed to avoid

confounds from toxins secreted by live planktonic *S. aureus* if they were used to measure MΦ phagocytosis, which could not be discriminated from biofilm-secreted molecules. Interestingly, the already potent cytolytic effects of *S. aureus* Hla were enhanced with the addition of purified bioactive LukAB. Furthermore, treatment of Δ*lukA* and Δ*lukB* biofilm-conditioned medium with a Hla neutralizing antibody significantly dampened the MΦ phagocytic block. These results suggest a synergistic effect, whereby the presence of LukAB enhances or accelerates Hla-mediated MΦ dysfunction, perhaps via enhanced binding, localization to the cell membrane, or regulating intracellular signaling pathways.

Previous studies have demonstrated the importance of LukAB or Hla for *S. aureus* pathogenesis in murine models of renal abscess (67), pneumonia (259, 260), skin infection (261, 262), bacteremia (263, 264), peritonitis (177, 262, 265), and other localized infection models (242). However, it should be noted that a Δ*lukAB* single mutant displayed no attenuation of virulence in murine models of skin infection and bacteremia (257). In support of our *in vitro* findings, our study is the first to report that LukAB and Hla cooperate to regulate *S. aureus* virulence in a murine orthopedic implant biofilm infection model. While Δ*lukAB* or Δ*hla* single mutants displayed decreased bacterial burdens in some tissues, Δ*lukAB*/Δ*hla* showed the largest reduction in bacterial numbers when compared to mice infected with the isogenic WT strain. In further support of this synergistic effect, Δ*lukAB*/Δ*hla* infected mice displayed the greatest increase in MΦ infiltrates. While this *in vivo* data reveals an important synergistic role for LukAB and Hla during *S. aureus* biofilm infection, it remains unclear whether these toxins are directly altering MΦ survival (i.e. via cell lysis) or indirectly tailoring the immune response (i.e. eliciting tissue damage resulting in altered cytokine signaling to promote MΦ phagocytosis and proinflammatory activity). However, evidence against the former possibility was revealed by the finding that biofilm-conditioned medium elicited similar cytotoxic effects towards proinflammatory (classically activated) and pro-fibrotic (alternatively activated) MΦs (data not

shown). We also investigated whether biofilm-conditioned medium augmented MΦ CD11b expression, which binds LukAB, but found no evidence to support this possibility. Another potential mechanism to link the synergistic effects of Hla and LukAB is the zinc-dependent metalloproteinase ADAM10, since Hla is known to recognize ADAM10 on the host cell surface (266). Once bound, Hla augments ADAM10 activity (267), which could result in increased LukAB dissociation from the bacterial cell surface and, in turn, enhanced Hla activity. However, it should be noted that this interaction may provide an explanation for our *in vivo* findings, but fails to inform the apparent synergistic effect in our *in vitro* assay, since MΦs were treated with biofilm-conditioned medium clarified of bacteria. The mechanism whereby LukAB and Hla influence biofilm formation *in vivo* is an area of active investigation in our laboratory.

While the effect of *S. aureus* biofilm-conditioned medium on MΦ viability was largely LukAB/Hla-dependent, it appears that part of the phagocytic block was not. SWATH-MS identified other potential candidate proteins that could act in concert with Hla/LukAB to maximally impair MΦ phagocytosis, including pyrimidine biosynthetic enzymes, phosphotransferase proteins, pyruvate kinase, and histidine metabolic enzymes. Along these lines, it is important to recognize that biofilms represent a diverse bacterial population influenced by a myriad of complex gradients (e.g. nutrient, oxygen, pH,), metabolic activity, and virulence potential (13, 84, 268, 269). For example, while our studies utilized conditioned medium collected from static biofilms, a subpopulation of planktonic or "dispersed" cells is also present at the air-liquid interface. While this cell population was 2-3 log lower than the biofilm (Supplemental Fig. S4.4), it is probably naïve to disregard their impact; particularly in light of recent studies demonstrating the secretory potential of biofilm-dispersed cells (270). Based on this evidence, we posit that *S. aureus* biofilms prevent MΦ phagocytosis, in part, by inducing cell death through LukAB and Hla production (Fig. 4.8). However, since the phagocytic block was still evident even when MΦ viability was restored to 100% following LukAB/Hla inactivation,

this suggests the action of additional proteins that act together with Hla/LukAB to maximally inhibit MΦ phagocytic activity (Fig. 4.8).

Collectively, this study demonstrates that *S. aureus* biofilms have evolved mechanisms to establish persistent infections, in part, by actively preventing MΦ phagocytosis and eliciting cell death that is mediated by the synergistic actions of LukAB and Hla. These findings not only identify a novel interaction for these secreted proteins, but also highlight the layers of redundancy within the *S. aureus* virulence repertoire.

Chapter 5: *purB* affects eDNA release during *Staphylococcus aureus* biofilm development to evade macrophage recognition

Manuscript in preparation

Abstract

The typical MΦ response to planktonic *S. aureus* involves the induction of proinflammatory, microbicidal activity. However, *S. aureus* biofilms can interfere with anti-bacterial mechanisms, in part, by polarizing MΦs toward an anti-inflammatory, pro-fibrotic phenotype. Here we showed that MΦs exposed to *S. aureus* biofilms failed to induce the proinflammatory transcription factor NF-κB, which translated into minimal inflammatory cytokine production. We took advantage of this phenotype to screen the *S. aureus* Nebraska Transposon Mutant Library to identify mutants that were no longer able to suppress MΦ NF-κB activity. Among the top hits was *purB*, which encodes the enzyme adenylosuccinate lyase and catalyzes two reactions in the purine metabolic pathway. In addition to no longer inhibiting MΦ NF-κB activity, *purB* mutant biofilms were more susceptible to MΦ invasion and phagocytosis in a MyD88-dependent manner. This was attributed, in part, to increased eDNA in the *purB* mutant biofilm matrix that triggered MΦ invasion and phagocytosis of biofilm-associated bacteria via Toll-like receptor 9 (TLR9). *In vivo*, the *purB* mutant displayed significantly decreased bacterial burdens in a mouse orthopedic implant biofilm infection model concomitant with significantly increased MΦ infiltrates that was dependent on TLR9 recognition during acute infection. Collectively, these findings point towards a critical role for *purB* in facilitating biofilm evasion of MΦ microbicidal effector functions.

Introduction

S. aureus is an opportunistic pathogen recognized for its ability to cause both nosocomial and community-associated infections (223). While *S. aureus* isolates encode a myriad of virulence factors, including toxins, proteases, and nutrient acquisition systems that facilitate colonization of numerous locations throughout the host, biofilm formation is another key virulence determinant (15, 16). Biofilms are a heterogeneous population of bacteria surrounded by a self-produced matrix composed of proteins, exopolysaccharides, and eDNA (32, 226, 227). While the biofilm matrix likely provides some physical barrier from the host immune response, heterogeneity within the bacterial population induced by signals such as nutrient and oxygen gradients, likely provides another layer of protection via differential gene expression and protein production throughout the biofilm proper (76). Indeed, our prior work demonstrated that *S. aureus* biofilms alter their transcriptional profiles upon encountering MΦs (Chapter 3) and biofilms are enriched in toxins that attenuate MΦ phagocytosis and induce cell death (Chapter 4) (75, 171).

S. aureus has a number of mechanisms for sensing and responding to environmental stimuli, including several characterized two-component regulatory systems. For example, the *agr* QS system regulates the production of surface-associated versus secreted proteins according to population density (84). In addition, the link between *S. aureus* metabolism and virulence is an active area of investigation (86-89). While many connections are still unclear, previous studies have demonstrated differential gene expression between *S. aureus* in the planktonic versus biofilm lifestyles, including differences in metabolic gene expression (22). Interestingly, the influence of bacterial metabolites on the host immune response is only beginning to be explored and represents an area of investigation in our laboratory.

The innate immune system is well-equipped to recognize pathogens through a variety of cell surface and PRRs. One example is the TLR family, which recognizes PAMPs such as

lipoproteins and PGN in the bacterial cell wall (via TLR2) and unmethylated CpG motifs in bacterial DNA (via TLR9). Once engaged by their microbial ligand, most TLRs (with the exception of TLR3) initiate a proinflammatory signaling cascade through the adapter molecule MyD88, culminating in NF-kB activation and the induction of a robust proinflammatory, antimicrobial immune response. While PMNs are among the first innate immune responders to planktonic bacterial infections such as those caused by *S. aureus*, there has been an increasing appreciation for the role of resident tissue MΦs in this response. Although PMNs are highly phagocytic and possess an arsenal of granules rich in antimicrobial peptides and enzymes (156), MΦs are also professional phagocytes capable of producing high levels of reactive oxygen species (ROS) and serve a critical role in leukocyte recruitment and activation through chemokine/cytokine production as well as inducing adaptive immunity by antigen presentation (125-127, 130).

Our previous work has established that *S. aureus* biofilms, in contrast to planktonic organisms, prevent MΦ invasion and phagocytosis of biofilm-associated bacteria and drive MΦs towards an anti-inflammatory state (15, 160). Recent studies have revealed a synergistic role for the toxins Hla and LukAB in inhibiting MΦ phagocytosis and inducing cell death (75); however, other factors are also involved. The purpose of this work was to identify key genes involved in inhibiting MΦ proinflammatory activity by taking advantage of the NTML to screen for *S. aureus* mutants that were still capable of biofilm formation but lost the ability to skew MΦs towards an anti-inflammatory state, hence transforming them into proinflammatory, phagocytic cells. Our results identified numerous hits in the purine regulatory pathway. In depth analysis of a *purB* mutant (Δ*purB*) revealed increased eDNA release at the outer surface of the biofilm that triggered, in part, TLR9-mediated MΦ activation. In addition, Δ*purB* was less virulent in a mouse orthopedic implant biofilm model that was TLR9-dependent during the early stage of infection.

Collectively, these findings suggest that *S. aureus* carefully regulate eDNA levels and accessibility during biofilm formation to prevent MΦ recognition and proinflammatory activity.

Results

Genes expressed during *S. aureus* biofilm growth that influence macrophage NF-κB activation. Our previous work has shown that MΦs are unable to invade and phagocytose *S. aureus* biofilm-associated bacteria and biofilm exposure drives MΦs towards an anti-inflammatory phenotype (15, 160). Although our recent report demonstrated a synergistic role for Hla and LukAB produced during *S. aureus* biofilm growth in preventing MΦ phagocytosis (Chapter 4) (75), this study revealed that other proteins are also involved. To identify additional molecules important for *S. aureus* biofilms to evade MΦ recognition, we utilized MΦs from NF-κB-luciferase reporter mice to screen the NTML (158, 271, 272). NF-κB is a key transcription factor that drives the expression of numerous cytokines/chemokines and is a widely used readout of MΦ proinflammatory activity (125, 131, 230). To validate this screening approach, NF-κB activation was minimal in MΦs exposed to intact *S. aureus* biofilms, whereas significant NF-κB induction was observed in response to planktonic bacteria and *S. aureus*-derived PGN (Fig 5.1A). The ability of biofilms to attenuate MΦ NF-κB activation is in agreement with significantly impaired cytokine production (Fig 5.1B). Furthermore, after biofilm exposure, MΦs remain refractory to subsequent stimulation by PAMPs, showing a reduction in both proinflammatory and anti-inflammatory cytokines, similar to MΦs exposed to planktonic *S. aureus* (Fig 5.1C, D).

The NTML screen identified 22 mutants where MΦ NF-κB activity was significantly increased compared to WT biofilms (Fig 5.1E, Table 5.1). *S. aureus* mutants were also evaluated for their ability to form biofilms (Fig 5.1F), since impaired biofilm formation could lead to false positive hits by the ability of planktonic bacteria to increase NF-κB activity (Fig 5.1A). Of note, the numbers of mutants identified by our NF-κB screen were of relatively low abundance, representing only 1.1% of the library, revealing the stringency of the assay, which was corroborated by the identification of multiple hits within the purine pathway (i.e. *purA*, *purB*, *purF*, *purM*, and *purS*) and other operons (Table 5.1 and data not shown). Of particular interest

were *purB* and *purA*, since they represented the most robust inducers of MΦ NF-κB activity. *purB* was selected for further analysis, since its phenotype was slightly larger, it participates in two steps of the purine metabolic pathway (whereas *purA* catalyzes a single reaction; Supplemental Fig. S5.1), and *purB* expression has been previously shown to be increased during biofilm growth although functional assessments were not performed (22).

Figure 5.1

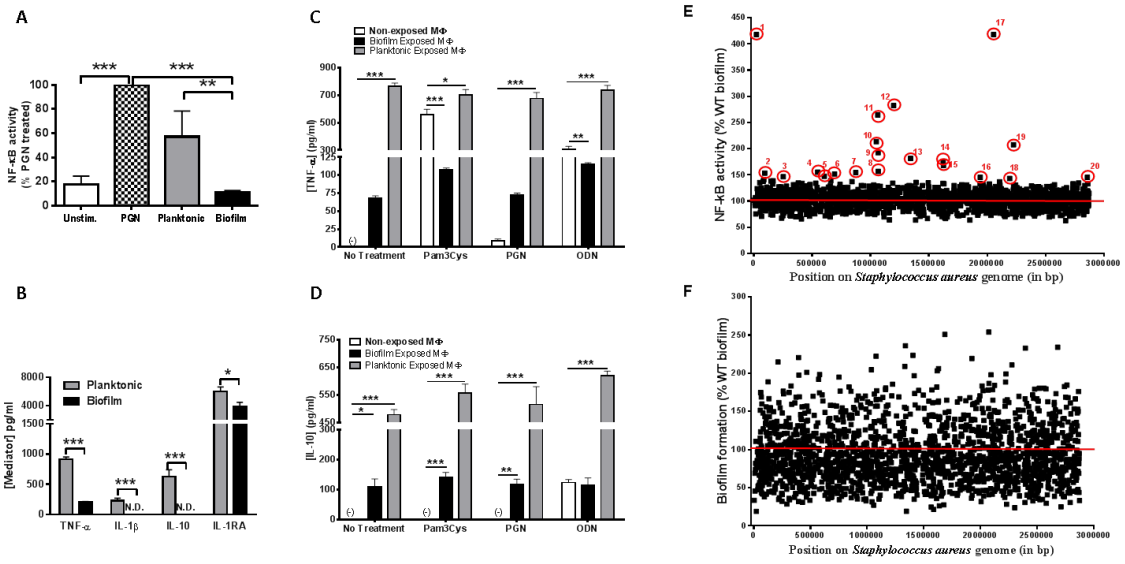

Genes expressed during *S. aureus* biofilm growth that influence macrophage NF-κB activation. (A) BMDMΦs from NF-κB-luciferase reporter mice were incubated with fresh medium (Unstim.), PGN (10 µg/ml), or *S. aureus* planktonic or biofilm cultures for 4 h, whereupon luciferase activity (counts per second) was measured as a function of NF-κB activation and was normalized against PGN stimulated values (set to 100%). (B) MΦs were co-cultured with biofilms or planktonic bacteria for 6 h, whereupon supernatants were collected to quantitate TNF-α, IL-1β, IL-10, and IL-1RA by ELISA (N.D. = not detected). (C) MΦs were incubated alone (non-exposed MΦ) or co-cultured with biofilms or planktonic bacteria for 2 h, whereupon MΦs were separated from bacteria by FACS and treated with medium alone (no treatment), the synthetic lipoprotein Pam3Cys (1 µg/ml), peptidoglycan (PGN; 10 µg/ml), or CpG oligodeoxynucleotides (ODN; 0.1 µM) for an additional 24 h. At 24 h, supernatants were collected for TNF-α and (D) IL-10 quantitation by ELISA [(-) = not detected]. (E) BMDMΦs from NF-κB-luciferase reporter mice were incubated with WT or NTML biofilms for 4 h, whereupon luciferase activity (counts per second) was measured as a function of NF-κB activation. Luciferase activity elicited by each mutant was normalized against WT biofilm

stimulated MΦs, which was set to 100% (solid red line). Red circles represent mutants where NF-κB activity was increased (numbers refer to genes listed in Table 1). (F) Crystal violet staining was utilized as a quantitative assessment of biofilm formation, with each mutant normalized against WT biofilm, which was set to 100% (solid red line). Significant differences are denoted by asterisks (*, $p < 0.05$; **, $p < 0.01$; ***, $p < 0.001$; unpaired two-tailed student's t-test). Results are representative of at least three independent experiments.

Table 5.1. Genes expressed by *S. aureus* biofilms that influence macrophage NF-κB activation *in vitro*

% WT	Locus	Gene	Identity	Function	Location on Fig. 5.1E
418.05	SAUSA300_1889	purB	adenylosuccinate lyase	Purine metabolism	17
417.83	SAUSA300_0017	purA	adenylosuccinate synthetase	Purine metabolism	1
282.23	SAUSA300_1095	carA	carbamoyl phosphate synthase small subunit	Pyrimidine metabolism	12
264.28	SAUSA300_0969	purS	phosphoribosylformylglycinamidine synthase	Purine metabolism	11
213.39	SAUSA300_0957		Hypothetical protein	hypothetical	10
207.64	SAUSA300_2060	atpA	F0F1 ATP synthase subunit alpha	metabolism	19
192.36	SAUSA300_0972	purF	amidophosphoribosyltransferase	Purine metabolism	9
181.38	SAUSA300_1225		aspartate kinase	Amino acid metabolism	14
175.67	SAUSA300_1467	ipdA	dihydrolipoamide dehydrogenase	Amino acid metabolism	15
157.96	SAUSA300_1105	priA	primosomal protein N	DNA replication	13
156.74	SAUSA300_0973	purM	phosphoribosylaminoimidazole synthetase	Purine metabolism	8
155.16	SAUSA300_0489		putative cell division protein FtsH	Protease	4
154.37	SAUSA300_0787	aroD	biosynthesis of aromatic amino acids	Amino acid metabolism	7
153.29	SAUSA300_0086		Hypothetical protein	Hypothetical	2
151.66	SAUSA300_0618		ABC transporter substrate-binding protein	Metal transport	6
147.22	SAUSA300_0538		NAD-dependent epimerase/dehydratase family protein	Carbohydrate transport	5
146.53	SAUSA300_0213		oxidoreductase; Gfo/Idh/MocA family	Oxidoreductase	3
145.23	SAUSA300_1754	splE	Serine-like protease	Protease	16
145.22	SAUSA300_2631		Putative N-acetyltransferase	Metabolites	20
142.94	SAUSA300_2030		Hypothetical protein	Hypothetical	18

***purB* is important for preventing macrophage invasion and phagocytosis of mature *S. aureus* biofilms.** To determine whether the ability of the *purB* mutant to augment MΦ NF-κB activity translated into increased invasion and phagocytosis of biofilm-associated bacteria, MΦs were co-cultured with WT, Δ*purB*, and Δ*purB* complemented USA300 LAC biofilms. Indeed, MΦ invasion into mature Δ*purB* biofilms was significantly increased compared to WT (Fig. 5.2A) concomitant with enhanced phagocytosis (Fig. 5.2B). To confirm that these changes were not the result of increased planktonic growth of Δ*purB*, biofilm formation was assessed. Δ*purB* was capable of biofilm formation and although biofilm height was significantly reduced (Fig. 5.2C), quantitation revealed a minor reduction in bacterial counts (i.e. < 2-fold; Fig. 5.2D). The increases in MΦ invasion and phagocytosis of Δ*purB* biofilms was complementable (Fig. 5.2A, B), underscoring the importance of *purB* in inhibiting MΦ activity.

Figure 5.2

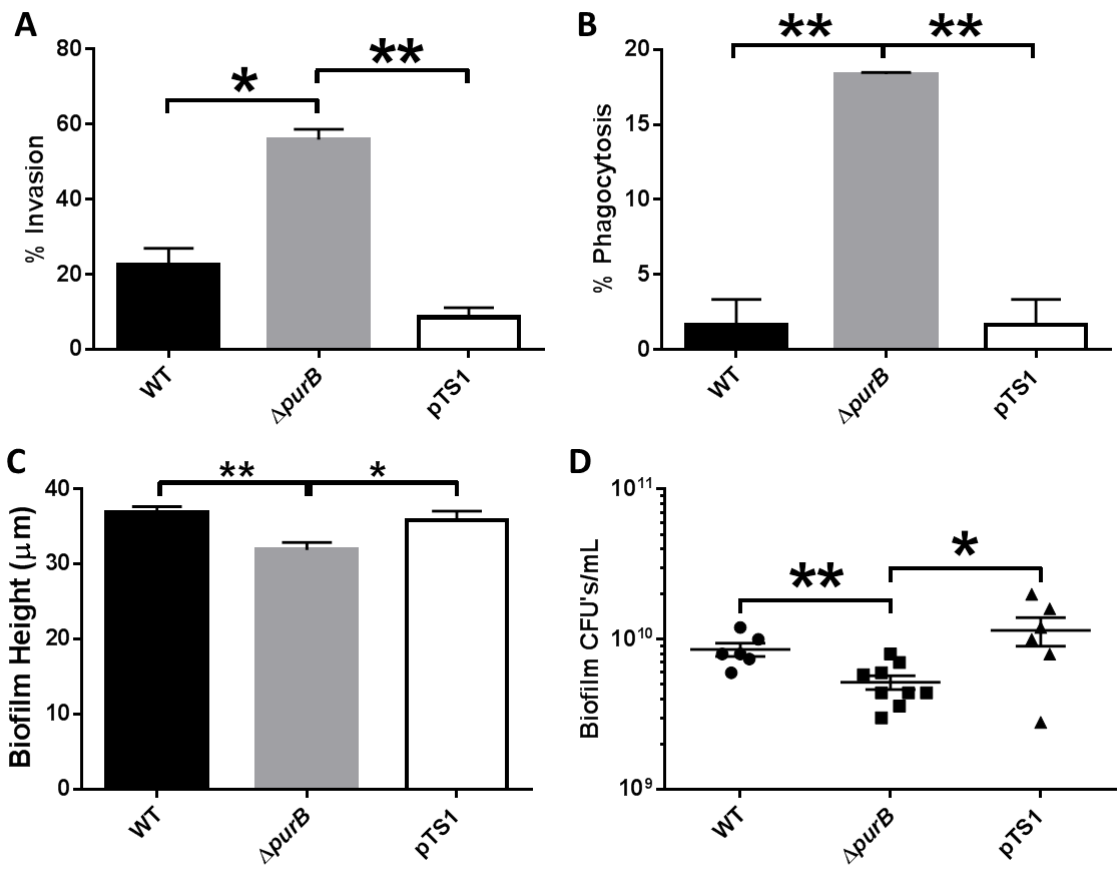

***purB* is important for preventing macrophage invasion and phagocytosis of mature *S. aureus* biofilms.** BMDMΦs were co-cultured with mature WT, Δ*purB*, or Δ*purB* + pTS1 GFP biofilms for 4-6 h, after which the percentage of MΦs (A) invading or (B) phagocytosing the biofilms was enumerated using confocal microscopy. (C) Mature GFP biofilms alone were observed by confocal microscopy to measure average biofilm height, (D) after which mature biofilms were mechanically disrupted, serially diluted in PBS, and plated to quantitate viable bacteria. Significant differences are denoted by asterisks (*, $p < 0.05$; **, $p < 0.01$; one-way ANOVA, followed by Bonferroni's multiple-comparison test). Results are representative of at least three independent experiments.

***eDNA* is increased in *S. aureus* Δ*purB* biofilms.** Since the ability of MΦs to invade and phagocytose biofilms is likely dictated, in part, by the accessibility of immune stimulatory motifs at the outer biofilm surface, we next focused on the biofilm ECM. As eDNA is required for *S. aureus* biofilm development (32) and bacterial DNA is a known TLR9 ligand (101, 102), USA300 LAC GFP biofilms were stained with PI to visualize eDNA (Fig. 5.3A). The ratio of PI (eDNA/dead bacteria) to GFP (live) signal was quantitated in z-stacks acquired by confocal microscopy, which revealed a significant increase in eDNA/dead bacteria in Δ*purB* throughout biofilm maturation (Fig. 5.3B). As PI is not specific for eDNA, but also stains dead cells present in the biofilm, eDNA was isolated from mature biofilms and the housekeeping gene *gyrA* was quantitated by qRT-PCR. Results confirmed that Δ*purB* biofilms contained significantly increased eDNA (Fig. 5.3C) and all Δ*purB* phenotypes could be complemented (Fig. 5.3). Another interesting finding was that more PI staining was observed at the outer surface of Δ*purB* biofilms, presumably making it more accessible to MΦ recognition, compared to the WT and complemented strains where eDNA was mainly buried at the base of the biofilm (Fig. 5.3A). To determine whether the failure of MΦs to invade and phagocytose WT biofilms resulted, in part, from inaccessibility to immune stimulatory eDNA, purified biofilm-derived eDNA was added to the surface of mature WT biofilms, which phenotypically transformed the MΦ response to what was observed with Δ*purB*, namely increased biofilm invasion and phagocytosis (Fig. 5.3D).

Figure 5.3

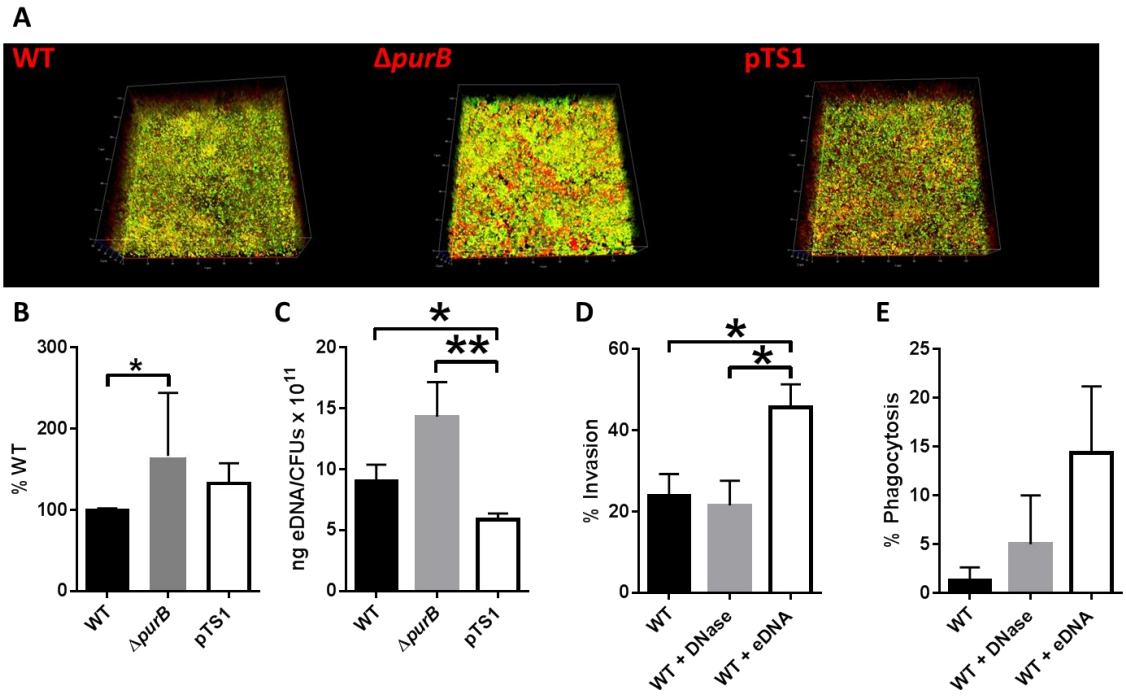

eDNA is increased in *S. aureus* Δ*purB* biofilms. (A) Propidium iodide was added to mature (6 day-old) WT, Δ*purB*, or Δ*purB* + pTS1 GFP biofilms, visualized by confocal microscopy (X63, 1-µm slices), and representative three-dimensional images were constructed. (B) GFP and PI signals were quantitated by COMSTAT analysis to determine a PI/GFP signal ratio. (C) eDNA was collected from mature biofilms and quantitated by performing qRT-PCR with *gyrA*. (D) BMDMΦs were co-cultured for 4-6 h with mature WT GFP biofilms alone, biofilms pretreated for 30 min with 100 U/ml DNase1, and biofilms with additional eDNA added to the surface after which the percentage of MΦs (D) invading or (E) phagocytosing biofilms was enumerated using confocal microscopy. Significant differences are denoted by asterisks (*, $p < 0.05$; **, $p < 0.01$; one-way ANOVA, followed by Bonferroni's multiple-comparison test). Results are representative of at least three independent experiments.

S. aureus **Δ*purB* biofilm eDNA can be detected by MΦs and trigger activation.** MΦs are equipped with a variety of PRRs. Among these are TLRs, including TLR9, which senses bacterial DNA and signals via the adapter molecule MyD88 to trigger NF-κB activation and proinflammatory properties (101, 102). Since Δ*purB* augmented MΦ NF-κB activation, biofilm invasion, and phagocytosis, we next investigated whether this was TLR9-dependent based on increased eDNA in the Δ*purB* biofilm matrix and its accessibility at the surface. Again, WT MΦs displayed significantly increased invasion (Fig. 5.4A) and phagocytosis (Fig. 5.4B) of Δ*purB* biofilms; however, this was diminished upon co-culture of Δ*purB* biofilms with TLR9 KO MΦs, and completely abrogated in the presence of MyD88 KO MΦs (Fig. 5.4A, B). Collectively, these results suggest that *purB* is important for regulating eDNA levels and localization in biofilms, which is partially responsible for the ability of WT biofilms to evade MΦ detection by preventing TLR9-dependent proinflammatory activity. However, additional MyD88-dependent signaling receptors are also involved, the identity of which remains to be determined.

Figure 5.4

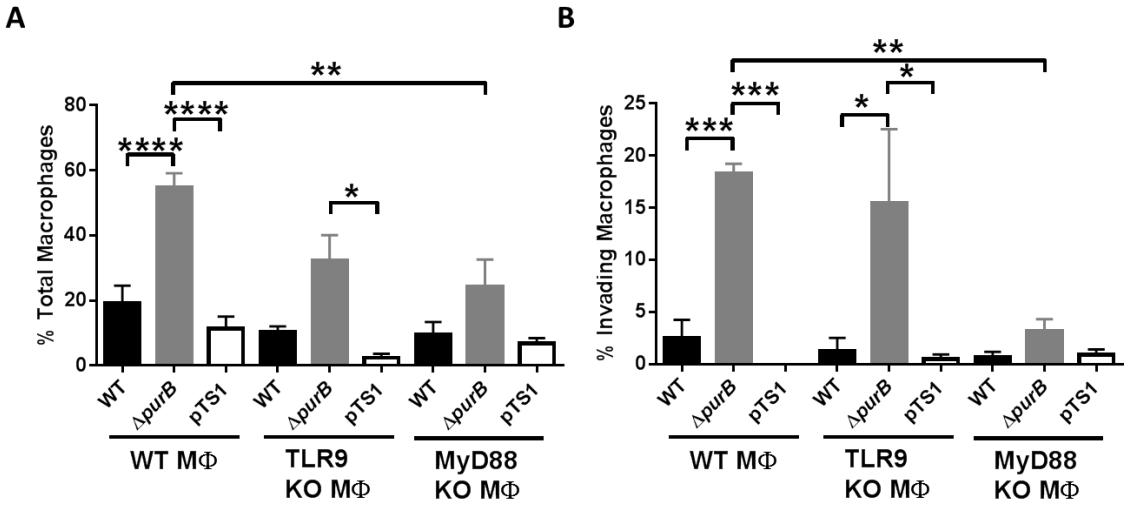

***S. aureus* biofilm eDNA can be detected by MΦs and trigger activation.** BMDMΦs from WT, TLR9 KO, and MyD88 KO mice were co-cultured with mature WT, Δ*purB*, or Δ*purB* + pTS1 GFP biofilms for 4-6 h, after which the percentage of MΦs (A) invading or (B) phagocytosing the biofilms was enumerated using confocal microscopy. Significant differences are denoted by asterisks (*, $p < 0.05$; **, $p < 0.01$; ***, $p < 0.001$; ****, $p < 0.0001$; one-way ANOVA, followed by Bonferroni's multiple-comparison test). Results are representative of at least three independent experiments.

***S. aureus purB* is important for chronic biofilm establishment.** While the previous results revealed a role for *purB* in the ability of *S. aureus* biofilms to evade MΦ recognition *in vitro*, we next assessed the importance of *purB* in a model of orthopedic implant biofilm infection in WT and TLR9 KO mice. Interestingly, Δ*purB* displayed decreased bacterial burdens in WT mice beginning at day 7, which became more pronounced over time, with some mice appearing to have cleared the infection by day 28 (Fig. 5.5A). Decreased biofilm burdens in WT mice infected with Δ*purB* correlated with a significant reduction in anti-inflammatory MDSCs (Fig. 5.5B) concomitant with increased MΦ infiltrates (Fig. 5.5B). While Δ*purB* showed similarly decreased biofilm burdens in TLR9 KO mice at later time points, concomitant with reduced MDSC and increased MΦ infiltrates (Fig. 5.5C), importantly, there were no differences in titers between Δ*purB* and WT infected TLR9 KO mice at day 7 (black and grey squares). This suggests that eDNA recognition in Δ*purB* occurs via TLR9 but only during early biofilm development. By extension, since WT biofilms have less eDNA that is not present at the outer biofilm surface and accessible to invading MΦs, this may represent a mechanism whereby WT biofilms evade TLR9-mediated recognition, in agreement with our earlier report (15). Importantly, the observed decrease in bacterial burdens at day 14 was complementable (Fig. 5.5D), again underscoring the specific importance of *purB* in this *in vivo* biofilm infection model. Complementation was not assessed at other time points to limit the number of animals utilized.

Figure 5.5

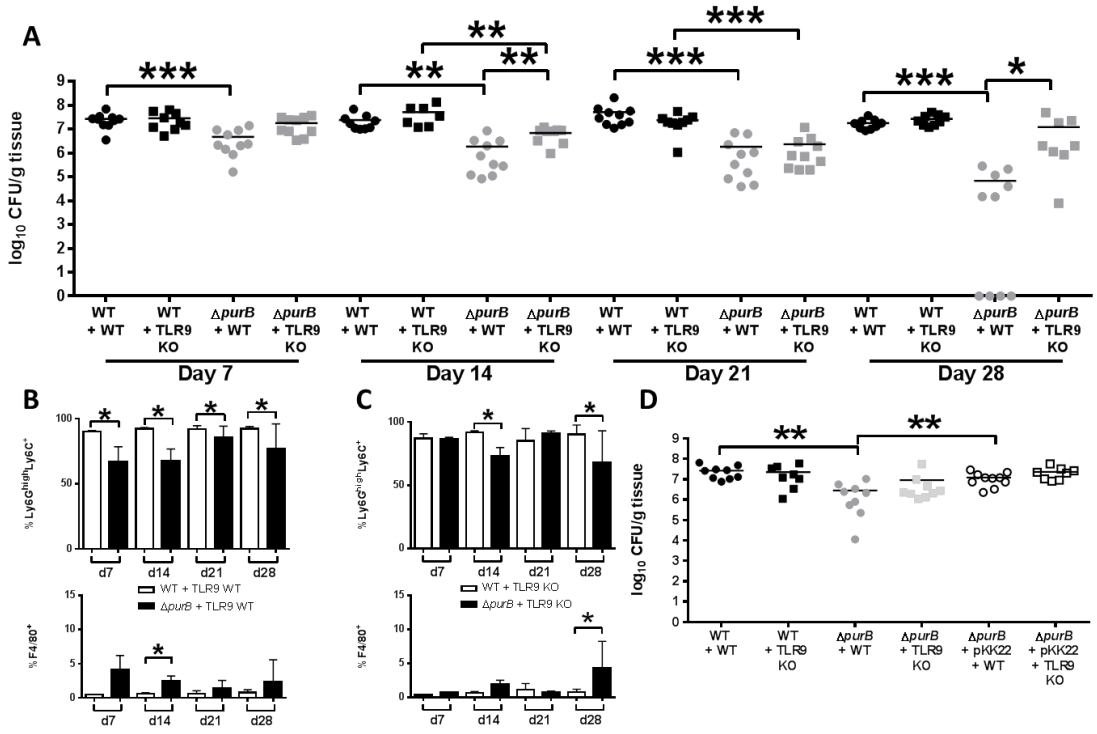

***S. aureus purB* is important for chronic biofilm establishment.** (A) Bacterial burdens associated with the soft tissue surrounding the knee of WT and TLR9 KO mice infected with WT *S. aureus* and isogenic Δ*purB* strains at days 7, 14, 21, and 28 post-infection. (B) Quantitation of $Ly6G^{high}Ly6C^{+}$ MDSCs and $F4/80^{+}$ MΦs infiltrating the soft tissue of C57BL/6 WT mice infected WT *S. aureus* and isogenic Δ*purB* strains at days 7, 14, 21, and 28 post-infection. (C) Quantitation of $Ly6G^{high}Ly6C^{+}$ MDSCs and $F4/80^{+}$ MΦs infiltrating the soft tissue of TLR9 KO mice infected WT *S. aureus* and isogenic Δ*purB* strains at days 7, 14, 21, and 28 post-infection. (D) Bacterial burdens associated with the soft tissue surrounding the knee of WT and TLR9 KO mice infected with WT *S. aureus* and isogenic Δ*purB*, and complemented Δ*purB* + pKK22:*purB* strains at day 14 post-infection. Significant differences are denoted by asterisks (*, $p < 0.05$; **, $p < 0.01$; ***, $p < 0.001$; one-way ANOVA, followed by Bonferroni's multiple-comparison test). Results are representative of at least two independent experiments.

Supplemental Figure S5.1

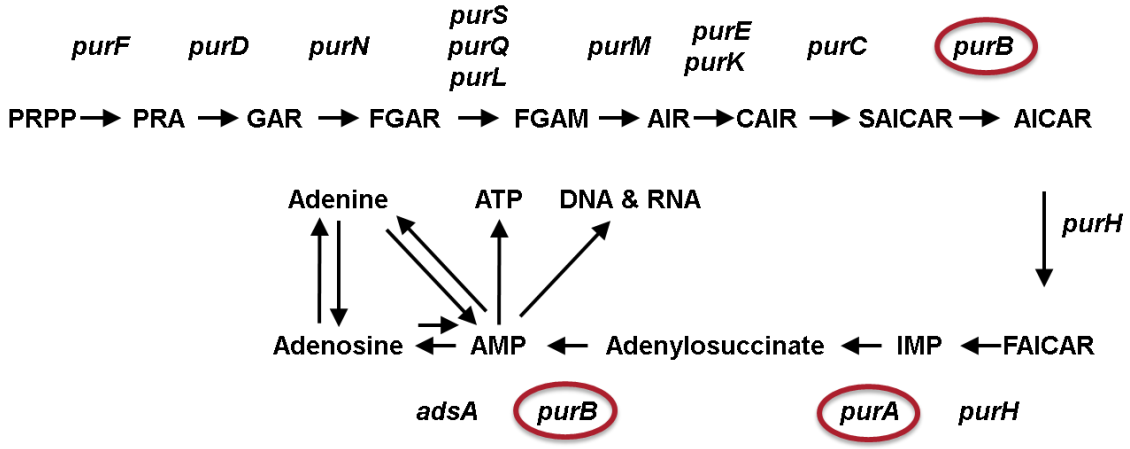

Predicted purine biosynthetic pathway in *S. aureus*. 5-Phospho-alpha-D-ribose 1-diphosphate (PRPP) is converted to 5-Phosphoribosylamine (PRA) by amidophosphoribosyltransferase (*purF*), which is then converted to 5′-Phosphoribosylglycinamide (GAR) by phosphoribosylamine-glycine ligase (*purD*), which is then converted to 5′-Phosphoribosyl-N-ormylglycinamide (FGAR) by phosphoribosylglycinamide formyltransferase 1 (*purN*), which is then converted to 2-(Formamido)-N1-(5′-phosphoribosyl)acetamidine (FGAM) by a combination of phosphoribosylformylglycinamidine synthase (*purS*), phosphoribosylformylglycinamidine synthase I (*purQ*), and phosphoribosylformylglycinamidine synthase II (*purL*), which is then converted to Aminoimidazole ribotide (AIR) by phosphoribosylformylglycinamidine cyclo-ligase (*purM*), which is then converted to (5-Phospho-D-ribosyl)-5-amino-4-imidazolecarboxylate (CAIR) by 5-(carboxyamino)imidazole ribonucleotide synthase (*purK*) and 5-(carboxyamino)imidazole ribonucleotide mutase (*purE*), which is then converted to 1-(5′-Phosphoribosyl)-5-amino-4-(N-succinocarboxamide)-imidazole (SAICAR) by phosphoribosylaminoimidazole-succinocarboxamide synthase (*purC*), which is then converted to 1-(5'-Phosphoribosyl)-5-amino-4-imidazolecarboxamide (AICAR) by adenylosuccinate lyase (*purB*), which is then converted to 1-(5'-Phosphoribosyl)-5-formamido-4-imidazolecarboxamide (FAICAR) followed by Inosine monophosphate (IMP) both by

phosphoribosylaminoimidazolecarboxamide formyltransferase / IMP cyclohydrolase (*purH*); which is then converted to adenylosuccinate by adenylosuccinate synthase (*purA*), which is then converted to Adenosine monophosphate (AMP) by adenylosuccinate lyase (*purB*), which can then be eventually converted into Adenosine triphosphate (ATP) and used as energy, into adenine or adenosine through adenosine synthase (*adsA*), or into RNA or DNA as needed.

Discussion

S. aureus subverts the host immune response by numerous mechanisms, including increased resistance to cationic antimicrobial peptides, impairment of phagocyte recruitment, interference with antibody-mediated opsonization and complement activation, and resistance to intracellular killing (213). In addition, biofilm formation further protects *S. aureus* from the host innate immune response, representing a communal virulence determinant (15, 56, 159). The objective of this study was to identify genes expressed by *S. aureus* biofilms that contribute to MΦ dysfunction through the inhibition of NF-κB.

MΦs utilize phagocytic receptors to identify microbes and trigger immune defenses. Infectious agents that cause persistent infections, such as *S. aureus* biofilms, must be able to detect and subvert these defenses. We have previously demonstrated that biofilm formation protects *S. aureus* from TLR detection and phagocytosis, reduces proinflammatory cytokine and chemokine production, decreases inducible NO synthase (iNOS) expression, and interferes with MΦ activation *in vivo* (15, 160). We were interested in the genetic basis of how biofilm growth prevents MΦ phagocytic functions. Previously, we determined that MΦs were capable of phagocytosing bacteria from mechanically disrupted, but not intact biofilms, suggesting that the size of the biofilm and/or density of its matrix may form a mechanical obstacle that physically prevents MΦ phagocytosis, a phenomenon leading to "frustrated phagocytosis" (15, 254, 255). Subsequent studies revealed that toxins, including Hla and LukAB are also responsible for the MΦ phagocytic block, but that additional factors are also involved, which is not unexpected given the arsenal of *S. aureus* virulence determinants.

In response to planktonic bacteria, MΦs produce numerous proinflammatory mediators, exhibit potent phagocytic and anti-microbial activity, and are critical for immune cell recruitment and activation, serving as a first line of defense against microbial invasion (200, 201). However, we have previously reported that MΦs are polarized towards an alternatively activated, anti-

inflammatory, M2 phenotype upon contact with *S. aureus* biofilms (15, 160). Here we have extended these findings to demonstrate that prior biofilm exposure makes MΦs refractory to a subsequent microbial challenge, further highlighting the immune subversive properties of *S. aureus* biofilms. Correspondingly, MΦ NF-κB activation was also significantly reduced after contact with *S. aureus* biofilms, whereas a strong response was detected after exposure to planktonic *S. aureus* or PGN. This indicates that in addition to impaired phagocytosis, another mechanism utilized by *S. aureus* biofilms to subvert the host immune response results from the ability to prevent MΦ NF-κB activation and resultant proinflammatory cytokine secretion. Indeed, multiple pathogens employ similar strategies to interfere with MΦ microbicidal activity either by hindering cytokine expression/secretion (273, 274) or by the production of virulence factors that directly impede NF-κB activation (158, 275).

To identify genes expressed by *S. aureus* biofilms that inhibit MΦ NF-κB activation, a screen of the NTML was performed. This approach utilized MΦs from transgenic mice where the transcription factor NF-κB drives luciferase expression. Several *S. aureus* mutants in the purine biosynthetic pathway (i.e. *purA*, *purB*, *purF*, *purS*, and *purM*) failed to block MΦ NF-kB activation, implicating their involvement in thwarting proinflammatory functions. Previous work demonstrated that *S. aureus* purine auxotrophs were less virulent in a murine abscess model of infection (276). Likewise, purine biosynthesis also appears to have broad physiological effects in *S. aureus*, including the modification of global patterns of virulence gene expression (276). Accordingly, we found that Δ*purB* biofilms secreted significantly decreased levels of Hla compared to WT biofilms (Supplemental Fig. S5.2). Not surprisingly, Δ*purA* and Δ*purB* displayed the most robust NF-κB activation in our experiments, as these genes represent more distal steps in the purine biosynthetic pathway for converting inosine monophosphate (IMP) to adenosine monophosphate (AMP). A major end product of the purine biosynthetic pathway, AMP, can be converted to adenosine during staphylococcal infections (277). Adenosine is a

potent extracellular messenger that is abundant at sites of hypoxia, trauma, and inflammation (278). Moreover, adenosine has strong immunosuppressive effects, such as down-regulating cytokine production and immune cell receptors, many of which are mediated by its ability to bind A3 and A2A receptors on leukocytes (278-280). Accordingly, we found that adenosine attenuated MΦ NF-κB activity in response to PGN stimulation, further indicating that products of the purine biosynthetic pathway influence MΦ activation (Supplemental Fig. S5.3).

Interestingly, these studies indicate that purine biosynthesis is also important for *S. aureus* regulation of eDNA in the outer biofilm matrix. Consistent with our previous studies, disrupting the ability of MΦs to recognize bacterial eDNA via TLR9 does not alter invasion and phagocytosis during co-culture with WT biofilms *in vitro*, nor does it result in a more severe infection *in vivo* in association with WT *S. aureus* (15). However, disrupting purine biosynthesis via Δ*purB* results in increased eDNA, particularly at the biofilm surface, providing an accessible PAMP for MΦ recognition and activation. While this phenomenon was complementable and reproducible with the addition of eDNA to the WT *S. aureus* biofilm surface, we observed a stronger phenotype in association with MyD88, implying an additive effect of other PAMP(s) being recognized by other TLRs, the identity of which remains to be determined.

The results of the current study, concomitant with our previous findings, support the conclusion that *S. aureus* biofilms have evolved mechanisms to establish persistent infections, in part, by actively programming MΦs towards an anti-inflammatory phenotype and preventing phagocytosis, presumably through the production of adenosine. Additionally, *S. aureus* biofilms shield the eDNA component of the ECM from MΦ recognition at the biofilm surface, thereby further evading MΦ detection.

Supplemental Figure S5.2

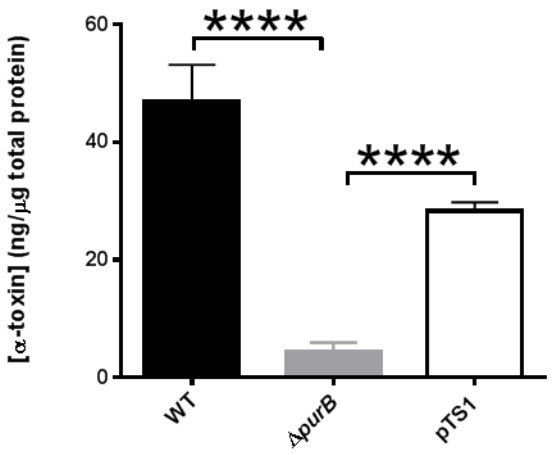

purB* activity effects Hla production in *S. aureus* biofilms.** Quantitation of Hla levels in conditioned medium from WT *S. aureus* biofilms versus isogenic Δ*purB*, and complemented Δ*purB* + pTS1 strains. Significant differences are denoted with asterisks (*, $p < 0.0001$; unpaired two-tailed student's *t*-test). Results are representative of at least two independent experiments.

Supplemental Figure S5.3

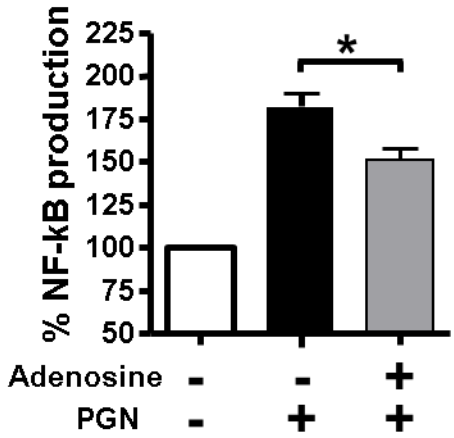

Adenosine attenuates macrophage activation. Bone marrow-derived macrophages from NF-κB-luciferase reporter mice were stimulated with 10 μg/ml peptidoglycan (PGN) for 2 h ± 50 μM adenosine, whereupon luciferase activity was measured as a function of NF-κB activation. Significant differences are denoted with asterisks (*, $p < 0.05$; unpaired two-tailed student's *t*-test). Results are representative of at least three independent experiments.

Chapter 6: Discussion and Future Directions

Key Findings and Conclusions:

The phagocytic and microbicidal activities of PMNs and MΦs are among the first lines of protection from bacterial pathogens. However, *S. aureus* is often resistant to innate immunity, especially when ensconced within the confines of the biofilm matrix. While previous studies in our laboratory have shown that *S. aureus* biofilms are able to resist clearance by both PMNs and MΦs, we wondered if this was accomplished by a conserved set of genes or through entirely different means. In order to answer this question, we examined biofilm gene expression profiles following co-culture with these two innate immune cell populations. We also compared the relative ability of PMNs and MΦs to invade and phagocytose biofilm-associated *S. aureus*. To our knowledge, this was the first study of its kind with any species of bacterial biofilm.

During co-culture with PMNs, we observed no significant alteration of the *S. aureus* biofilm transcriptome at an early or late period (Chapter 3). This was unexpected, especially taken together with our confocal data indicating that PMNs were readily able to invade the biofilm matrix and phagocytose biofilm-associated bacteria. While it is known that *S. aureus* can survive intracellularly in PMNs (215, 281, 282), PMN phagocytosis did not result in a significant reduction in viable bacterial numbers *in vitro*, and one would expect this adaptation to necessitate major transcriptional changes but this was not observed. While few transcriptional changes were detected, interestingly *agr* transcription was significantly increased after PMN addition to biofilms. *agr* regulates the production of numerous secreted virulence factors, including phenol-soluble modulins (PSMs), which have been shown to play a role in biofilm maturation and are known to elicit cytotoxic effects on PMNs (79, 283). In agreement with this finding, we noted that Δ*agr* biofilms were less able to inhibit PMN invasion and induce PMN cell death, despite being significantly thicker on average.

In contrast to PMNs, we observed a significant dampening of the biofilm transcriptome during early co-culture with MΦs, including numerous metabolism-associated genes. This transcriptional dormancy was negated at late co-culture periods, likely because a vast majority of MΦs had already succumbed to cell lysis by biofilm-secreted toxins (Chapter 4). Also in contrast to PMNs, we were able to document little/no MΦ invasion and phagocytosis of biofilm-associated bacteria, perhaps in part due to successful "cloaking" of the biofilm. This curious difference in the biofilm transcriptional response to PMNs and MΦs, despite invasion and phagocytosis by the former and little to none by the latter, could be explained by the presence of a MΦ secreted molecule being sensed by the biofilm.

As I had now confirmed previous experiments in our laboratory observing an inability of MΦs to phagocytose biofilm-associated bacteria, the next question was whether molecules in the biofilm-conditioned milieu contributed to this phagocytic block (Chapter 4). We first demonstrated that *S. aureus* biofilm-conditioned medium could inhibit MΦ phagocytosis and induce cell death, and that it was significantly more inhibitory and lytic than planktonic-conditioned medium. Next, we established that the bioactive factors were actively secreted, proteinaceous in nature, specific to intact biofilms, and at least partially *agr*-dependent. We then performed proteomics analysis via SWATH-MS comparing conditioned medium from Δ*agr* with the WT strain, which identified Hla and LukAB as significantly enriched in WT biofilm-conditioned medium. These results were further corroborated by Western Blot, ELISA, and a series of MΦ treatments using combinations of neutralizing antibodies and Δ*hla* Δ*LukAB* mutants. Furthermore, *hla* and *lukAB* were found to act synergistically *in vitro* and *in vivo* in an implant-associated biofilm infection model. Taken together, these studies identified a novel interaction between these secreted proteins and highlighted another layer of redundancy within the *S. aureus* virulence secretome.

Having identified secreted proteins enriched in *S. aureus* biofilms that hinder macrophage phagocytosis and induce cell death, we wanted to specifically ask how biofilms are able to skew macrophages towards an anti-inflammatory, M2 profile. In order to answer this question, we performed a high-throughput screen of the NTML in which we co-cultured BMDMΦs from NF-κB reporter mice with *S. aureus* single-gene mutants to identify genes involved in inhibiting proinflammatory, or M1, MΦ activation (Chapter 5). This screen identified over 20 genes, several of which encode proteins involved in purine biosynthesis, including one of the top hits, adenolysuccinate lyase (*purB*). *In vitro*, Δ*purB* biofilms displayed a significantly decreased ability to inhibit MΦ invasion and phagocytosis of biofilm-associated bacteria, which was complementable. We next examined differences in biofilm eDNA content and found that Δ*purB* biofilms contained increased amounts of eDNA. Suspecting that increased eDNA at the biofilm surface may be leading to increased MΦ activation and invasion, we next performed co-cultures with BMDMΦs from TLR9 and MyD88 KO mice and found that both had a decreased ability to invade Δ*purB* biofilms. Interestingly, however, MyD88 KO MΦs showed the most significant decrease, indicating a role for additional PAMPs in this co-culture paradigm in addition to the CpG motifs present in biofilm eDNA that would be recognized by TLR9. Furthermore, we were able to show that spiking additional eDNA onto WT *S. aureus* biofilms facilitated increased invasion. Finally, we demonstrated the importance of *purB* in the establishment of an infection *in vivo* in our murine orthopedic implant model, which we were also able to confirm by complementation.

In total, my studies have helped identify some key factors that contribute to *S. aureus* biofilm evasion of MΦ recognition and inhibition of MΦ antimicrobial activities (Fig. 6.1). These experiments also serve to further highlight the immense challenge we face in attempting to more effectively treat, and even prevent, *S. aureus* biofilm infections. The vast repertoire of virulence factors and exquisite control over which *S. aureus* produces them is truly astounding. It is my

hope that these studies may positively contribute to the ever growing corpus of *S. aureus* research that should one day allow us to live in harmony with this commensal turned opportunistic pathogen.

Figure 6.1

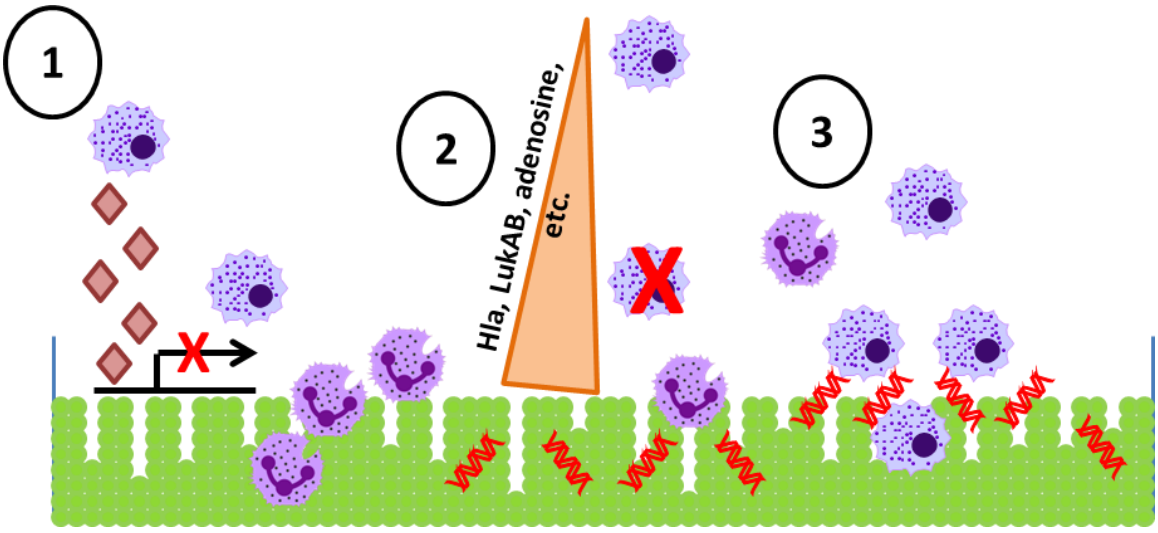

Mechanisms by which *S. aureus* biofilms interfere with MΦ antimicrobial responses. 1) *S. aureus* biofilms are able to uniquely detect and respond to MΦ over PMN insult by down-regulating much of its transcriptional activity. 2) *S. aureus* biofilms are uniquely enriched over planktonic cultures in Hla, LukAB, adenosine, and other factors that contribute to macrophage antimicrobial inhibition and cell death. 3) *S. aureus* biofilms are able to regulate eDNA expression in a *purB*-dependent manner thereby further preventing MΦ detection via TLR9.

Future Directions:

Proteomics on innate immune cell and *S. aureus* biofilm co-cultures

While transcriptional profiling of the *S. aureus* biofilm after co-culture with either PMNs or MΦs was novel and informative, a translational assessment of biofilm protein production could help confirm some of the earlier data and pinpoint shifts in actual protein production in response to immune insults. In addition, it would be exciting to simultaneously measure protein production fluctuations from the PMN and MΦ populations after encountering a biofilm. This data collection could also begin to shed light on potential players in host-pathogen crosstalk and could be performed using SWATH-MS mass spectrometry. Significant *S. aureus* protein hits could be isolated, purified, and used to treat both immune cell populations *in vitro* to assess the impact on antimicrobial activity via phagocytic assay, qRT-PCR, and/or Western Blot. Similarly, individual PMN or MΦ protein hits could be used to treat biofilms to assess the impact on metabolic and transcriptional activity as measured by qRT-PCR and confocal microscopy via reporter constructs of key genes. Finally, it may also be interesting to perform immune cell co-cultures with planktonic *S. aureus* to gain a fuller understanding of how biofilms alter the innate immune response. To my knowledge, this would be a completely novel study and should be feasible by careful identification of bacterial and eukaryotic proteins via consultation with separately acquired reference libraries.

Identify biofilm proteins that directly inhibit macrophage phagocytosis

Although the effect of *S. aureus* biofilm-conditioned medium on MΦ viability was largely Hla/LukAB-dependent, part of the phagocytic block was not. While SWATH-MS identified other potential candidate proteins including pyrimidine biosynthetic enzymes, phosphotransferases, pyruvate kinase, histidine metabolic enzymes, and serine-like proteases,

these were all identified in a comparison between WT and Δ*agr* mutant biofilms and part of the phagocytic block was not *agr*-dependent. However, we know this phenotype is protein-dependent as treatment of the biofilm-conditioned medium with Proteinase K fully reversed the phagocytic block. With this in mind, other two-component regulators could be tested, in conjunction with neutralizing Hla and LukAB antibody, to identify a regulator of the protein of interest. Upon identification, SWATH-MS could be performed as before with the new comparator to identify the protein(s) involved in directly inhibiting MΦ phagocytosis. Alternatively, a phagocytic screen of the NTML could be performed assessing the inhibitory effect of conditioned medium from every mutant biofilm after treatment with the neutralizing antibodies. This study could lead to the identification of a novel drug target, as we have previously shown that, once activated and phagocytic, MΦs are capable of decreasing bacterial burdens in an established biofilm infection *in vivo*.

Assess *agr* activity across various medium formulations

Though my original co-culture experiments were performed with RPMI-1640 supplemented with 10% FBS, the MS proteomics studies required supplementation with 1% casamino acids, since the proteins in FBS would have masked the detection of most bacterial proteins. Importantly, pilot studies demonstrated similar biofilm formation between FBS and casamino acids and no adverse effects on MΦ function or viability. However, I have observed apparently increased levels of *sarA*P1 promoter activity during biofilm growth in casamino acids as determined by fluorescence intensity of the *sarA*P1-GFP plasmid used to visualize the biofilm, even when normalized for any differences in culturable bacteria. In addition, I have measured significantly increased levels of Hla production in biofilms grown in casamino acids by ELISA, even when normalized for any differences in total protein production. As *agr* regulates numerous virulence factors including Hla, it would be interesting to note any significant differences in its

activity between the two media formulations. I could also include more traditional microbiological media formulations (e.g. TSB), with the expectation that it may promote even greater *agr* activity than casamino acids, since it is more nutrient-rich. These studies could be very interesting and help inform medium selection for *in vitro* experimentation, particularly when attempting to draw correlations between growth in media and growth during infection in a patient. Finally, it would be very interesting to identify any molecules present in the FBS that inhibit *agr* activity, as these could potentially be used therapeutically. What about examining changes when grown in dilute blood to mimic colonization/growth during wound formation?

Characterize the Δ*purB* blood agar phenotype

During my experiments with Δ*purB*, I noticed that the mutant had a significant growth defect on TSA + 10% sheep blood in that it was unable to form single, isolated colonies, although growth was observed in concentrated areas of bacterial lawns. Curiously, this phenotype disappears after a few days of static biofilm growth *in vitro* or after 7 days of infection in the *in vivo* model of orthopedic implant biofilm infection. In order to determine the responsible genes, I could perform transcriptomics comparing Δ*purB* with the WT strain pre- and post- *in vitro* or *in vivo* biofilm growth. Alternatively, I could perform DNA sequencing to look for any mutations that may be occurring during these growth conditions that suddenly confer growth on blood agar.

S. aureus infections are challenging to treat as it seems to be uniquely adapted to circumvent the host antimicrobial response, with the ability to colonize multiple sites on the human body with ease. Furthermore, *S. aureus* seems equally adept at benignly living on the human body as a commensal or chronically persisting inside the body as a pathogen. While many scientists are attempting to prevent *S. aureus* infections through the development of vaccines targeting key virulence factors or through manipulating the bacterial virulence factor regulatory pathways themselves, the diversity of states in which *S. aureus* can survive (e.g. planktonic vs

biofilm, proliferative vs persister) has made the identification of a common denominator to target unclear. What is becoming clearer, however, is that a multifactorial approach, combining some form of antibiotics with an immunostimulatory boost, will likely be required. Therefore, there is a continued pressing need to better understand all of the ways in which *S. aureus* biofilms thwart innate immunity.

References

1. **Shopsin B, Mathema B, Zhao X, Martinez J, Kornblum J, Kreiswirth BN.** 2000. Resistance rather than virulence selects for the clonal spread of methicillin-resistant Staphylococcus aureus: implications for MRSA transmission. Microb Drug Resist **6:**239-244.
2. **Salgado CD, Farr BM, Calfee DP.** 2003. Community-acquired methicillin-resistant Staphylococcus aureus: a meta-analysis of prevalence and risk factors. Clin Infect Dis **36:**131-139.
3. **Okesola AO.** 2011. Community-acquired methicillin-resistant Staphylococcus aureus--a review of literature. Afr J Med Med Sci **40:**97-107.
4. **Carleton HA, Diep BA, Charlebois ED, Sensabaugh GF, Perdreau-Remington F.** 2004. Community-adapted methicillin-resistant Staphylococcus aureus (MRSA): population dynamics of an expanding community reservoir of MRSA. J Infect Dis **190:**1730-1738.
5. **Herold BC, Immergluck LC, Maranan MC, Lauderdale DS, Gaskin RE, Boyle-Vavra S, Leitch CD, Daum RS.** 1998. Community-acquired methicillin-resistant Staphylococcus aureus in children with no identified predisposing risk. JAMA **279:**593-598.
6. **Cohen PR.** 2007. Community-acquired methicillin-resistant Staphylococcus aureus skin infections: a review of epidemiology, clinical features, management, and prevention. Int J Dermatol **46:**1-11.
7. **Padmanabhan RA, Fraser TG.** 2005. The emergence of methicillin-resistant Staphylococcus aureus in the community. Cleve Clin J Med **72:**235-241.
8. **Ma XX, Ito T, Tiensasitorn C, Jamklang M, Chongtrakool P, Boyle-Vavra S, Daum RS, Hiramatsu K.** 2002. Novel type of staphylococcal cassette chromosome mec identified in community-acquired methicillin-resistant Staphylococcus aureus strains. Antimicrob Agents Chemother **46:**1147-1152.
9. **Zhang HZ, Hackbarth CJ, Chansky KM, Chambers HF.** 2001. A proteolytic transmembrane signaling pathway and resistance to beta-lactams in staphylococci. Science **291:**1962-1965.
10. **Arciola CR, Campoccia D, Speziale P, Montanaro L, Costerton JW.** 2012. Biofilm formation in Staphylococcus implant infections. A review of molecular mechanisms and implications for biofilm-resistant materials. Biomaterials **33:**5967-5982.
11. **Kiedrowski MR, Horswill AR.** 2011. New approaches for treating staphylococcal biofilm infections. Ann N Y Acad Sci **1241:**104-121.
12. **Whitchurch CB, Tolker-Nielsen T, Ragas PC, Mattick JS.** 2002. Extracellular DNA required for bacterial biofilm formation. Science **295:**1487.
13. **Fey PD, Olson ME.** 2010. Current concepts in biofilm formation of Staphylococcus epidermidis. Future Microbiol **5:**917-933.
14. **Watkins RR, David MZ, Salata RA.** 2012. Current concepts on the virulence mechanisms of meticillin-resistant Staphylococcus aureus. J Med Microbiol **61:**1179-1193.
15. **Thurlow LR, Hanke ML, Fritz T, Angle A, Aldrich A, Williams SH, Engebretsen IL, Bayles KW, Horswill AR, Kielian T.** 2011. Staphylococcus aureus biofilms prevent macrophage phagocytosis and attenuate inflammation in vivo. J Immunol **186:**6585-6596.
16. **Hanke ML, Kielian T.** 2012. Deciphering mechanisms of staphylococcal biofilm evasion of host immunity. Front Cell Infect Microbiol **2:**62.

17. **Montanaro L, Speziale P, Campoccia D, Ravaioli S, Cangini I, Pietrocola G, Giannini S, Arciola CR.** 2011. Scenery of Staphylococcus implant infections in orthopedics. Future Microbiol **6:**1329-1349.
18. **McCann MT, Gilmore BF, Gorman SP.** 2008. Staphylococcus epidermidis device-related infections: pathogenesis and clinical management. J Pharm Pharmacol **60:**1551-1571.
19. **Otto M.** 2013. Staphylococcal infections: mechanisms of biofilm maturation and detachment as critical determinants of pathogenicity. Annu Rev Med **64:**175-188.
20. **Archer NK, Mazaitis MJ, Costerton JW, Leid JG, Powers ME, Shirtliff ME.** 2011. Staphylococcus aureus biofilms: properties, regulation, and roles in human disease. Virulence **2:**445-459.
21. **Donlan RM, Costerton JW.** 2002. Biofilms: survival mechanisms of clinically relevant microorganisms. Clin Microbiol Rev **15:**167-193.
22. **Beenken KE, Dunman PM, McAleese F, Macapagal D, Murphy E, Projan SJ, Blevins JS, Smeltzer MS.** 2004. Global gene expression in Staphylococcus aureus biofilms. J Bacteriol **186:**4665-4684.
23. **O'Toole G, Kaplan HB, Kolter R.** 2000. Biofilm formation as microbial development. Annu Rev Microbiol **54:**49-79.
24. **Joo HS, Otto M.** 2012. Molecular basis of in vivo biofilm formation by bacterial pathogens. Chem Biol **19:**1503-1513.
25. **McElroy MC, Cain DJ, Tyrrell C, Foster TJ, Haslett C.** 2002. Increased virulence of a fibronectin-binding protein mutant of Staphylococcus aureus in a rat model of pneumonia. Infect Immun **70:**3865-3873.
26. **Josefsson E, Hartford O, O'Brien L, Patti JM, Foster T.** 2001. Protection against experimental Staphylococcus aureus arthritis by vaccination with clumping factor A, a novel virulence determinant. J Infect Dis **184:**1572-1580.
27. **Cramton SE, Gerke C, Schnell NF, Nichols WW, Gotz F.** 1999. The intercellular adhesion (ica) locus is present in Staphylococcus aureus and is required for biofilm formation. Infect Immun **67:**5427-5433.
28. **Mack D, Fischer W, Krokotsch A, Leopold K, Hartmann R, Egge H, Laufs R.** 1996. The intercellular adhesin involved in biofilm accumulation of Staphylococcus epidermidis is a linear beta-1,6-linked glucosaminoglycan: purification and structural analysis. J Bacteriol **178:**175-183.
29. **Maira-Litran T, Kropec A, Abeygunawardana C, Joyce J, Mark G, 3rd, Goldmann DA, Pier GB.** 2002. Immunochemical properties of the staphylococcal poly-N-acetylglucosamine surface polysaccharide. Infect Immun **70:**4433-4440.
30. **Corrigan RM, Rigby D, Handley P, Foster TJ.** 2007. The role of Staphylococcus aureus surface protein SasG in adherence and biofilm formation. Microbiology **153:**2435-2446.
31. **Cucarella C, Solano C, Valle J, Amorena B, Lasa I, Penades JR.** 2001. Bap, a Staphylococcus aureus surface protein involved in biofilm formation. J Bacteriol **183:**2888-2896.
32. **Rice KC, Mann EE, Endres JL, Weiss EC, Cassat JE, Smeltzer MS, Bayles KW.** 2007. The cidA murein hydrolase regulator contributes to DNA release and biofilm development in Staphylococcus aureus. Proc Natl Acad Sci U S A **104:**8113-8118.
33. **Kurtz S, Ong K, Lau E, Mowat F, Halpern M.** 2007. Projections of primary and revision hip and knee arthroplasty in the United States from 2005 to 2030. J Bone Joint Surg Am **89:**780-785.
34. **Alekshun MN, Levy SB.** 2006. Commensals upon us. Biochem Pharmacol **71:**893-900.

35. **Peacock SJ, de Silva I, Lowy FD.** 2001. What determines nasal carriage of Staphylococcus aureus? Trends Microbiol **9:**605-610.
36. **Jamsen E, Furnes O, Engesaeter LB, Konttinen YT, Odgaard A, Stefansdottir A, Lidgren L.** 2010. Prevention of deep infection in joint replacement surgery. Acta Orthop **81:**660-666.
37. **Phillips JE, Crane TP, Noy M, Elliott TS, Grimer RJ.** 2006. The incidence of deep prosthetic infections in a specialist orthopaedic hospital: a 15-year prospective survey. J Bone Joint Surg Br **88:**943-948.
38. **Pulido L, Ghanem E, Joshi A, Purtill JJ, Parvizi J.** 2008. Periprosthetic joint infection: the incidence, timing, and predisposing factors. Clin Orthop Relat Res **466:**1710-1715.
39. **Jamsen E, Varonen M, Huhtala H, Lehto MU, Lumio J, Konttinen YT, Moilanen T.** 2010. Incidence of prosthetic joint infections after primary knee arthroplasty. J Arthroplasty **25:**87-92.
40. **Huotari K, Lyytikainen O, Ollgren J, Virtanen MJ, Seitsalo S, Palonen R, Rantanen P, Hospital Infection Surveillance T.** 2010. Disease burden of prosthetic joint infections after hip and knee joint replacement in Finland during 1999-2004: capture-recapture estimation. J Hosp Infect **75:**205-208.
41. **Montanaro L, Testoni F, Poggi A, Visai L, Speziale P, Arciola CR.** 2011. Emerging pathogenetic mechanisms of the implant-related osteomyelitis by Staphylococcus aureus. Int J Artif Organs **34:**781-788.
42. **Ceri H, Olson ME, Stremick C, Read RR, Morck D, Buret A.** 1999. The Calgary Biofilm Device: new technology for rapid determination of antibiotic susceptibilities of bacterial biofilms. J Clin Microbiol **37:**1771-1776.
43. **Anderl JN, Zahller J, Roe F, Stewart PS.** 2003. Role of nutrient limitation and stationary-phase existence in Klebsiella pneumoniae biofilm resistance to ampicillin and ciprofloxacin. Antimicrob Agents Chemother **47:**1251-1256.
44. **Zimmerli W, Trampuz A, Ochsner PE.** 2004. Prosthetic-joint infections. N Engl J Med **351:**1645-1654.
45. **Lora-Tamayo J, Murillo O, Iribarren JA, Soriano A, Sanchez-Somolinos M, Baraia-Etxaburu JM, Rico A, Palomino J, Rodriguez-Pardo D, Horcajada JP, Benito N, Bahamonde A, Granados A, del Toro MD, Cobo J, Riera M, Ramos A, Jover-Saenz A, Ariza J, Infection RGftSoP.** 2013. A large multicenter study of methicillin-susceptible and methicillin-resistant Staphylococcus aureus prosthetic joint infections managed with implant retention. Clin Infect Dis **56:**182-194.
46. **Haenle M, Skripitz C, Mittelmeier W, Skripitz R.** 2012. Economic impact of infected total knee arthroplasty. ScientificWorldJournal **2012:**196515.
47. **Darouiche RO.** 2004. Treatment of infections associated with surgical implants. N Engl J Med **350:**1422-1429.
48. **An YH, Friedman RJ.** 1998. Concise review of mechanisms of bacterial adhesion to biomaterial surfaces. J Biomed Mater Res **43:**338-348.
49. **Campoccia D, Montanaro L, Arciola CR.** 2006. The significance of infection related to orthopedic devices and issues of antibiotic resistance. Biomaterials **27:**2331-2339.
50. **Zimmerli W, Waldvogel FA, Vaudaux P, Nydegger UE.** 1982. Pathogenesis of foreign body infection: description and characteristics of an animal model. J Infect Dis **146:**487-497.
51. **Lalani T, Chu VH, Grussemeyer CA, Reed SD, Bolognesi MP, Friedman JY, Griffiths RI, Crosslin DR, Kanafani ZA, Kaye KS, Ralph Corey G, Fowler VG, Jr.** 2008. Clinical

outcomes and costs among patients with Staphylococcus aureus bacteremia and orthopedic device infections. Scand J Infect Dis **40:**973-977.

52. **Sendi P, Banderet F, Graber P, Zimmerli W.** 2011. Periprosthetic joint infection following Staphylococcus aureus bacteremia. J Infect **63:**17-22.
53. **Prabhakara R, Harro JM, Leid JG, Keegan AD, Prior ML, Shirtliff ME.** 2011. Suppression of the inflammatory immune response prevents the development of chronic biofilm infection due to methicillin-resistant Staphylococcus aureus. Infect Immun **79:**5010-5018.
54. **Heim CE, Vidlak D, Scherr TD, Hartman CW, Garvin KL, Kielian T.** 2015. IL-12 Promotes Myeloid-Derived Suppressor Cell Recruitment and Bacterial Persistence during Staphylococcus aureus Orthopedic Implant Infection. J Immunol doi:10.4049/jimmunol.1402689.
55. **Heim CE, Vidlak D, Scherr TD, Kozel JA, Holzapfel M, Muirhead DE, Kielian T.** 2014. Myeloid-derived suppressor cells contribute to Staphylococcus aureus orthopedic biofilm infection. J Immunol **192:**3778-3792.
56. **Bernthal NM, Pribaz JR, Stavrakis AI, Billi F, Cho JS, Ramos RI, Francis KP, Iwakura Y, Miller LS.** 2011. Protective role of IL-1beta against post-arthroplasty Staphylococcus aureus infection. J Orthop Res **29:**1621-1626.
57. **Novick RP, Muir TW.** 1999. Virulence gene regulation by peptides in staphylococci and other Gram-positive bacteria. Curr Opin Microbiol **2:**40-45.
58. **Mayville P, Ji G, Beavis R, Yang H, Goger M, Novick RP, Muir TW.** 1999. Structure-activity analysis of synthetic autoinducing thiolactone peptides from Staphylococcus aureus responsible for virulence. Proc Natl Acad Sci U S A **96:**1218-1223.
59. **Ji G, Beavis R, Novick RP.** 1997. Bacterial interference caused by autoinducing peptide variants. Science **276:**2027-2030.
60. **Vuong C, Saenz HL, Gotz F, Otto M.** 2000. Impact of the agr quorum-sensing system on adherence to polystyrene in Staphylococcus aureus. J Infect Dis **182:**1688-1693.
61. **Otto M.** 2001. Staphylococcus aureus and Staphylococcus epidermidis peptide pheromones produced by the accessory gene regulator agr system. Peptides **22:**1603-1608.
62. **Beenken KE, Blevins JS, Smeltzer MS.** 2003. Mutation of sarA in Staphylococcus aureus limits biofilm formation. Infect Immun **71:**4206-4211.
63. **Mrak LN, Zielinska AK, Beenken KE, Mrak IN, Atwood DN, Griffin LM, Lee CY, Smeltzer MS.** 2012. saeRS and sarA act synergistically to repress protease production and promote biofilm formation in Staphylococcus aureus. PLoS One **7:**e38453.
64. **Boles BR, Horswill AR.** 2008. Agr-mediated dispersal of Staphylococcus aureus biofilms. PLoS Pathog **4:**e1000052.
65. **Ji G, Beavis RC, Novick RP.** 1995. Cell density control of staphylococcal virulence mediated by an octapeptide pheromone. Proc Natl Acad Sci U S A **92:**12055-12059.
66. **Kebaier C, Chamberland RR, Allen IC, Gao X, Broglie PM, Hall JD, Jania C, Doerschuk CM, Tilley SL, Duncan JA.** 2012. Staphylococcus aureus alpha-hemolysin mediates virulence in a murine model of severe pneumonia through activation of the NLRP3 inflammasome. J Infect Dis **205:**807-817.
67. **Dumont AL, Nygaard TK, Watkins RL, Smith A, Kozhaya L, Kreiswirth BN, Shopsin B, Unutmaz D, Voyich JM, Torres VJ.** 2011. Characterization of a new cytotoxin that contributes to Staphylococcus aureus pathogenesis. Mol Microbiol **79:**814-825.
68. **Alonzo F, 3rd, Torres VJ.** 2013. Bacterial survival amidst an immune onslaught: the contribution of the Staphylococcus aureus leukotoxins. PLoS Pathog **9:**e1003143.

69. **Oogai Y, Matsuo M, Hashimoto M, Kato F, Sugai M, Komatsuzawa H.** 2011. Expression of virulence factors by Staphylococcus aureus grown in serum. Appl Environ Microbiol **77:**8097-8105.
70. **Qazi S, Middleton B, Muharram SH, Cockayne A, Hill P, O'Shea P, Chhabra SR, Camara M, Williams P.** 2006. N-acylhomoserine lactones antagonize virulence gene expression and quorum sensing in Staphylococcus aureus. Infect Immun **74:**910-919.
71. **Qin Z, Yang L, Qu D, Molin S, Tolker-Nielsen T.** 2009. Pseudomonas aeruginosa extracellular products inhibit staphylococcal growth, and disrupt established biofilms produced by Staphylococcus epidermidis. Microbiology **155:**2148-2156.
72. **Otto M, Echner H, Voelter W, Gotz F.** 2001. Pheromone cross-inhibition between Staphylococcus aureus and Staphylococcus epidermidis. Infect Immun **69:**1957-1960.
73. **Williams P.** 2007. Quorum sensing, communication and cross-kingdom signalling in the bacterial world. Microbiology **153:**3923-3938.
74. **Hughes DT, Sperandio V.** 2008. Inter-kingdom signalling: communication between bacteria and their hosts. Nat Rev Microbiol **6:**111-120.
75. **Scherr TD, Hanke ML, Huang O, James DB, Horswill AR, Bayles KW, Fey PD, Torres VJ, Kielian T.** 2015. Staphylococcus aureus Biofilms Induce Macrophage Dysfunction Through Leukocidin AB and Alpha-Toxin. MBio **6**.
76. **Scherr TD, Heim CE, Morrison JM, Kielian T.** 2014. Hiding in Plain Sight: Interplay between Staphylococcal Biofilms and Host Immunity. Front Immunol **5:**37.
77. **Friedman DB, Stauff DL, Pishchany G, Whitwell CW, Torres VJ, Skaar EP.** 2006. Staphylococcus aureus redirects central metabolism to increase iron availability. PLoS Pathog **2:**e87.
78. **Mann EE, Rice KC, Boles BR, Endres JL, Ranjit D, Chandramohan L, Tsang LH, Smeltzer MS, Horswill AR, Bayles KW.** 2009. Modulation of eDNA release and degradation affects Staphylococcus aureus biofilm maturation. PLoS One **4:**e5822.
79. **Periasamy S, Joo HS, Duong AC, Bach TH, Tan VY, Chatterjee SS, Cheung GY, Otto M.** 2012. How Staphylococcus aureus biofilms develop their characteristic structure. Proc Natl Acad Sci U S A **109:**1281-1286.
80. **Berends ET, Horswill AR, Haste NM, Monestier M, Nizet V, von Kockritz-Blickwede M.** 2010. Nuclease expression by Staphylococcus aureus facilitates escape from neutrophil extracellular traps. J Innate Immun **2:**576-586.
81. **Thammavongsa V, Missiakas DM, Schneewind O.** 2013. Staphylococcus aureus degrades neutrophil extracellular traps to promote immune cell death. Science **342:**863-866.
82. **Chatterjee SS, Otto M.** 2013. How can Staphylococcus aureus phenol-soluble modulins be targeted to inhibit infection? Future Microbiol **8:**693-696.
83. **Geiger T, Francois P, Liebeke M, Fraunholz M, Goerke C, Krismer B, Schrenzel J, Lalk M, Wolz C.** 2012. The stringent response of Staphylococcus aureus and its impact on survival after phagocytosis through the induction of intracellular PSMs expression. PLoS Pathog **8:**e1003016.
84. **Novick RP.** 2003. Autoinduction and signal transduction in the regulation of staphylococcal virulence. Mol Microbiol **48:**1429-1449.
85. **Sadykov MR, Zhang B, Halouska S, Nelson JL, Kreimer LW, Zhu Y, Powers R, Somerville GA.** 2010. Using NMR metabolomics to investigate tricarboxylic acid cycle-dependent signal transduction in Staphylococcus epidermidis. J Biol Chem **285:**36616-36624.
86. **Somerville GA, Proctor RA.** 2009. At the crossroads of bacterial metabolism and virulence factor synthesis in Staphylococci. Microbiol Mol Biol Rev **73:**233-248.

87. **Somerville GA, Said-Salim B, Wickman JM, Raffel SJ, Kreiswirth BN, Musser JM.** 2003. Correlation of acetate catabolism and growth yield in Staphylococcus aureus: implications for host-pathogen interactions. Infect Immun **71:**4724-4732.
88. **Nuxoll AS, Halouska SM, Sadykov MR, Hanke ML, Bayles KW, Kielian T, Powers R, Fey PD.** 2012. CcpA regulates arginine biosynthesis in Staphylococcus aureus through repression of proline catabolism. PLoS Pathog **8:**e1003033.
89. **Seidl K, Goerke C, Wolz C, Mack D, Berger-Bachi B, Bischoff M.** 2008. Staphylococcus aureus CcpA affects biofilm formation. Infect Immun **76:**2044-2050.
90. **Valle J, Solano C, Garcia B, Toledo-Arana A, Lasa I.** 2013. Biofilm switch and immune response determinants at early stages of infection. Trends Microbiol **21:**364-371.
91. **Nizet V, Johnson RS.** 2009. Interdependence of hypoxic and innate immune responses. Nat Rev Immunol **9:**609-617.
92. **Lardner A.** 2001. The effects of extracellular pH on immune function. J Leukoc Biol **69:**522-530.
93. **Leemans JC, Cassel SL, Sutterwala FS.** 2011. Sensing damage by the NLRP3 inflammasome. Immunol Rev **243:**152-162.
94. **Rajamaki K, Nordstrom T, Nurmi K, Akerman KE, Kovanen PT, Oorni K, Eklund KK.** 2013. Extracellular acidosis is a novel danger signal alerting innate immunity via the NLRP3 inflammasome. J Biol Chem **288:**13410-13419.
95. **Cap M, Vachova L, Palkova Z.** 2012. Reactive oxygen species in the signaling and adaptation of multicellular microbial communities. Oxid Med Cell Longev **2012:**976753.
96. **Kawai T, Akira S.** 2011. Toll-like receptors and their crosstalk with other innate receptors in infection and immunity. Immunity **34:**637-650.
97. **O'Neill LA.** 2004. TLRs: Professor Mechnikov, sit on your hat. Trends Immunol **25:**687-693.
98. **Kaisho T, Akira S.** 2004. Pleiotropic function of Toll-like receptors. Microbes Infect **6:**1388-1394.
99. **Morath S, Stadelmaier A, Geyer A, Schmidt RR, Hartung T.** 2002. Synthetic lipoteichoic acid from Staphylococcus aureus is a potent stimulus of cytokine release. J Exp Med **195:**1635-1640.
100. **Weber JR, Moreillon P, Tuomanen EI.** 2003. Innate sensors for Gram-positive bacteria. Curr Opin Immunol **15:**408-415.
101. **Hemmi H, Takeuchi O, Kawai T, Kaisho T, Sato S, Sanjo H, Matsumoto M, Hoshino K, Wagner H, Takeda K, Akira S.** 2000. A Toll-like receptor recognizes bacterial DNA. Nature **408:**740-745.
102. **Bauer M, Redecke V, Ellwart JW, Scherer B, Kremer JP, Wagner H, Lipford GB.** 2001. Bacterial CpG-DNA triggers activation and maturation of human CD11c-, CD123+ dendritic cells. J Immunol **166:**5000-5007.
103. **Kopp E, Medzhitov R.** 2003. Recognition of microbial infection by Toll-like receptors. Curr Opin Immunol **15:**396-401.
104. **Esen N, Kielian T.** 2006. Central role for MyD88 in the responses of microglia to pathogen-associated molecular patterns. J Immunol **176:**6802-6811.
105. **Esen N, Kielian T.** 2009. Toll-like receptors in brain abscess. Curr Top Microbiol Immunol **336:**41-61.
106. **Kielian T.** 2006. Toll-like receptors in central nervous system glial inflammation and homeostasis. J Neurosci Res **83:**711-730.
107. **Kielian T.** 2009. Overview of toll-like receptors in the CNS. Curr Top Microbiol Immunol **336:**1-14.

108. **Yoshimura A, Lien E, Ingalls RR, Tuomanen E, Dziarski R, Golenbock D.** 1999. Cutting edge: recognition of Gram-positive bacterial cell wall components by the innate immune system occurs via Toll-like receptor 2. J Immunol **163:**1-5.
109. **Mullaly SC, Kubes P.** 2006. The role of TLR2 in vivo following challenge with Staphylococcus aureus and prototypic ligands. J Immunol **177:**8154-8163.
110. **Stevens NT, Sadovskaya I, Jabbouri S, Sattar T, O'Gara JP, Humphreys H, Greene CM.** 2009. Staphylococcus epidermidis polysaccharide intercellular adhesin induces IL-8 expression in human astrocytes via a mechanism involving TLR2. Cell Microbiol **11:**421-432.
111. **Strunk T, Power Coombs MR, Currie AJ, Richmond P, Golenbock DT, Stoler-Barak L, Gallington LC, Otto M, Burgner D, Levy O.** 2010. TLR2 mediates recognition of live Staphylococcus epidermidis and clearance of bacteremia. PLoS One **5:**e10111.
112. **El-Helou O, Berbari EF, Brown RA, Gralewski JH, Osmon DR, Razonable RR.** 2011. Functional assessment of Toll-like receptor 2 and its relevance in patients with Staphylococcus aureus infection of joint prosthesis. Hum Immunol **72:**47-53.
113. **Vilaysane A, Muruve DA.** 2009. The innate immune response to DNA. Semin Immunol **21:**208-214.
114. **Hornung V, Latz E.** 2010. Intracellular DNA recognition. Nat Rev Immunol **10:**123-130.
115. **Girardin SE, Boneca IG, Viala J, Chamaillard M, Labigne A, Thomas G, Philpott DJ, Sansonetti PJ.** 2003. Nod2 is a general sensor of peptidoglycan through muramyl dipeptide (MDP) detection. J Biol Chem **278:**8869-8872.
116. **Volz T, Nega M, Buschmann J, Kaesler S, Guenova E, Peschel A, Rocken M, Gotz F, Biedermann T.** 2010. Natural Staphylococcus aureus-derived peptidoglycan fragments activate NOD2 and act as potent costimulators of the innate immune system exclusively in the presence of TLR signals. FASEB J **24:**4089-4102.
117. **Rupp ME, Ulphani JS, Fey PD, Bartscht K, Mack D.** 1999. Characterization of the importance of polysaccharide intercellular adhesin/hemagglutinin of Staphylococcus epidermidis in the pathogenesis of biomaterial-based infection in a mouse foreign body infection model. Infect Immun **67:**2627-2632.
118. **Cassat JE, Lee CY, Smeltzer MS.** 2007. Investigation of biofilm formation in clinical isolates of Staphylococcus aureus. Methods Mol Biol **391:**127-144.
119. **Serbina NV, Pamer EG.** 2006. Monocyte emigration from bone marrow during bacterial infection requires signals mediated by chemokine receptor CCR2. Nat Immunol **7:**311-317.
120. **Bain CC, Bravo-Blas A, Scott CL, Gomez Perdiguero E, Geissmann F, Henri S, Malissen B, Osborne LC, Artis D, Mowat AM.** 2014. Constant replenishment from circulating monocytes maintains the macrophage pool in the intestine of adult mice. Nat Immunol **15:**929-937.
121. **Hoeffel G, Ginhoux F.** 2015. Ontogeny of Tissue-Resident Macrophages. Front Immunol **6:**486.
122. **Sica A, Mantovani A.** 2012. Macrophage plasticity and polarization: in vivo veritas. J Clin Invest **122:**787-795.
123. **Lacey DC, Achuthan A, Fleetwood AJ, Dinh H, Roiniotis J, Scholz GM, Chang MW, Beckman SK, Cook AD, Hamilton JA.** 2012. Defining GM-CSF- and macrophage-CSF-dependent macrophage responses by in vitro models. J Immunol **188:**5752-5765.
124. **Zhou D, Huang C, Lin Z, Zhan S, Kong L, Fang C, Li J.** 2014. Macrophage polarization and function with emphasis on the evolving roles of coordinated regulation of cellular signaling pathways. Cell Signal **26:**192-197.

125. **Martinez FO.** 2011. Regulators of macrophage activation. Eur J Immunol **41:**1531-1534.
126. **Mege JL, Mehraj V, Capo C.** 2011. Macrophage polarization and bacterial infections. Curr Opin Infect Dis **24:**230-234.
127. **Mosser DM.** 2003. The many faces of macrophage activation. J Leukoc Biol **73:**209-212.
128. **Shi C, Pamer EG.** 2011. Monocyte recruitment during infection and inflammation. Nat Rev Immunol **11:**762-774.
129. **Aderem A.** 2003. Phagocytosis and the inflammatory response. J Infect Dis **187 Suppl 2:**S340-345.
130. **Underhill DM, Gantner B.** 2004. Integration of Toll-like receptor and phagocytic signaling for tailored immunity. Microbes Infect **6:**1368-1373.
131. **Underhill DM, Goodridge HS.** 2012. Information processing during phagocytosis. Nat Rev Immunol **12:**492-502.
132. **McGuinness WA, Kobayashi SD, DeLeo FR.** 2016. Evasion of Neutrophil Killing by Staphylococcus aureus. Pathogens **5**.
133. **Lekstrom-Himes JA, Gallin JI.** 2000. Immunodeficiency diseases caused by defects in phagocytes. N Engl J Med **343:**1703-1714.
134. **Phillipson M, Kubes P.** 2011. The neutrophil in vascular inflammation. Nat Med **17:**1381-1390.
135. **Ley K, Laudanna C, Cybulsky MI, Nourshargh S.** 2007. Getting to the site of inflammation: the leukocyte adhesion cascade updated. Nat Rev Immunol **7:**678-689.
136. **Sadik CD, Kim ND, Luster AD.** 2011. Neutrophils cascading their way to inflammation. Trends Immunol **32:**452-460.
137. **Gillrie MR, Zbytnuik L, McAvoy E, Kapadia R, Lee K, Waterhouse CC, Davis SP, Muruve DA, Kubes P, Ho M.** 2010. Divergent roles of Toll-like receptor 2 in response to lipoteichoic acid and Staphylococcus aureus in vivo. Eur J Immunol **40:**1639-1650.
138. **von Aulock S, Morath S, Hareng L, Knapp S, van Kessel KP, van Strijp JA, Hartung T.** 2003. Lipoteichoic acid from Staphylococcus aureus is a potent stimulus for neutrophil recruitment. Immunobiology **208:**413-422.
139. **Leemans JC, Heikens M, van Kessel KP, Florquin S, van der Poll T.** 2003. Lipoteichoic acid and peptidoglycan from Staphylococcus aureus synergistically induce neutrophil influx into the lungs of mice. Clin Diagn Lab Immunol **10:**950-953.
140. **Lotz S, Aga E, Wilde I, van Zandbergen G, Hartung T, Solbach W, Laskay T.** 2004. Highly purified lipoteichoic acid activates neutrophil granulocytes and delays their spontaneous apoptosis via CD14 and TLR2. J Leukoc Biol **75:**467-477.
141. **Hoogerwerf JJ, de Vos AF, Bresser P, van der Zee JS, Pater JM, de Boer A, Tanck M, Lundell DL, Her-Jenh C, Draing C, von Aulock S, van der Poll T.** 2008. Lung inflammation induced by lipoteichoic acid or lipopolysaccharide in humans. Am J Respir Crit Care Med **178:**34-41.
142. **Akira S, Takeda K.** 2004. Toll-like receptor signalling. Nat Rev Immunol **4:**499-511.
143. **Kanneganti TD, Lamkanfi M, Nunez G.** 2007. Intracellular NOD-like receptors in host defense and disease. Immunity **27:**549-559.
144. **Liu C, Xu Z, Gupta D, Dziarski R.** 2001. Peptidoglycan recognition proteins: a novel family of four human innate immunity pattern recognition molecules. J Biol Chem **276:**34686-34694.
145. **McKenzie SE, Schreiber AD.** 1998. Fc gamma receptors in phagocytes. Curr Opin Hematol **5:**16-21.
146. **Sengelov H.** 1995. Complement receptors in neutrophils. Crit Rev Immunol **15:**107-131.

147. **Nunes P, Demaurex N, Dinauer MC.** 2013. Regulation of the NADPH oxidase and associated ion fluxes during phagocytosis. Traffic **14:**1118-1131.
148. **DeLeo FR, Allen LA, Apicella M, Nauseef WM.** 1999. NADPH oxidase activation and assembly during phagocytosis. J Immunol **163:**6732-6740.
149. **Nauseef WM.** 2014. Detection of superoxide anion and hydrogen peroxide production by cellular NADPH oxidases. Biochim Biophys Acta **1840:**757-767.
150. **Nauseef WM, Borregaard N.** 2014. Neutrophils at work. Nat Immunol **15:**602-611.
151. **Faurschou M, Borregaard N.** 2003. Neutrophil granules and secretory vesicles in inflammation. Microbes Infect **5:**1317-1327.
152. **Borregaard N, Sorensen OE, Theilgaard-Monch K.** 2007. Neutrophil granules: a library of innate immunity proteins. Trends Immunol **28:**340-345.
153. **Hirsch JG, Cohn ZA.** 1960. Degranulation of polymorphonuclear leucocytes following phagocytosis of microorganisms. J Exp Med **112:**1005-1014.
154. **Lominadze G, Powell DW, Luerman GC, Link AJ, Ward RA, McLeish KR.** 2005. Proteomic analysis of human neutrophil granules. Mol Cell Proteomics **4:**1503-1521.
155. **Brinkmann V, Zychlinsky A.** 2012. Neutrophil extracellular traps: is immunity the second function of chromatin? J Cell Biol **198:**773-783.
156. **Nauseef WM.** 2007. How human neutrophils kill and degrade microbes: an integrated view. Immunol Rev **219:**88-102.
157. **Goldmann O, Medina E.** 2012. The expanding world of extracellular traps: not only neutrophils but much more. Front Immunol **3:**420.
158. **Schommer NN, Christner M, Hentschke M, Ruckdeschel K, Aepfelbacher M, Rohde H.** 2011. Staphylococcus epidermidis uses distinct mechanisms of biofilm formation to interfere with phagocytosis and activation of mouse macrophage-like cells 774A.1. Infect Immun **79:**2267-2276.
159. **Hanke ML, Angle A, Kielian T.** 2012. MyD88-dependent signaling influences fibrosis and alternative macrophage activation during Staphylococcus aureus biofilm infection. PLoS One **7:**e42476.
160. **Hanke ML, Heim CE, Angle A, Sanderson SD, Kielian T.** 2013. Targeting macrophage activation for the prevention and treatment of Staphylococcus aureus biofilm infections. J Immunol **190:**2159-2168.
161. **Comalada M, Yeramian A, Modolell M, Lloberas J, Celada A.** 2012. Arginine and macrophage activation. Methods Mol Biol **844:**223-235.
162. **Mosser DM, Edwards JP.** 2008. Exploring the full spectrum of macrophage activation. Nat Rev Immunol **8:**958-969.
163. **Kristian SA, Birkenstock TA, Sauder U, Mack D, Gotz F, Landmann R.** 2008. Biofilm formation induces C3a release and protects Staphylococcus epidermidis from IgG and complement deposition and from neutrophil-dependent killing. J Infect Dis **197:**1028-1035.
164. **Cerca F, Andrade F, Franca A, Andrade EB, Ribeiro A, Almeida AA, Cerca N, Pier G, Azeredo J, Vilanova M.** 2011. Staphylococcus epidermidis biofilms with higher proportions of dormant bacteria induce a lower activation of murine macrophages. J Med Microbiol **60:**1717-1724.
165. **Spiliopoulou AI, Kolonitsiou F, Krevvata MI, Leontsinidis M, Wilkinson TS, Mack D, Anastassiou ED.** 2012. Bacterial adhesion, intracellular survival and cytokine induction upon stimulation of mononuclear cells with planktonic or biofilm phase Staphylococcus epidermidis. FEMS Microbiol Lett **330:**56-65.

166. **Yu H, Head NE.** 2002. Persistent infections and immunity in cystic fibrosis. Front Biosci **7:**d442-457.
167. **Jesaitis AJ, Franklin MJ, Berglund D, Sasaki M, Lord CI, Bleazard JB, Duffy JE, Beyenal H, Lewandowski Z.** 2003. Compromised host defense on Pseudomonas aeruginosa biofilms: characterization of neutrophil and biofilm interactions. J Immunol **171:**4329-4339.
168. **Mittal R, Sharma S, Chhibber S, Harjai K.** 2006. Effect of macrophage secretory products on elaboration of virulence factors by planktonic and biofilm cells of Pseudomonas aeruginosa. Comp Immunol Microbiol Infect Dis **29:**12-26.
169. **Chandra J, McCormick TS, Imamura Y, Mukherjee PK, Ghannoum MA.** 2007. Interaction of Candida albicans with adherent human peripheral blood mononuclear cells increases C. albicans biofilm formation and results in differential expression of pro- and anti-inflammatory cytokines. Infect Immun **75:**2612-2620.
170. **Otto M.** 2006. Bacterial evasion of antimicrobial peptides by biofilm formation. Curr Top Microbiol Immunol **306:**251-258.
171. **Scherr TD, Roux CM, Hanke ML, Angle A, Dunman PD, Kielian T.** 2013. Global transcriptome analysis of Staphylococcus aureus biofilms in response to innate immune cells. Infect Immun doi:10.1128/IAI.00819-13.
172. **Burlak C, Hammer CH, Robinson MA, Whitney AR, McGavin MJ, Kreiswirth BN, Deleo FR.** 2007. Global analysis of community-associated methicillin-resistant Staphylococcus aureus exoproteins reveals molecules produced in vitro and during infection. Cell Microbiol **9:**1172-1190.
173. **Diep BA, A. M. Palazzolo-Ballance, P. Tattevin, L. Basuino, K. R. Braughton, A. R. Whitney, L. Chen, B. N. Kreiswirth, M. Otto, F. R. DeLeo, and H. F. Chambers. .** 2008. Contribution of Panton-Valentine leukocidin in community-associated methicillin-resistant Staphylococcus aureus pathogenesis. PLoS ONE **3:**e3198.
174. **Voyich JM, K. R. Braughton, D. E. Sturdevant, A. R. Whitney, B. Said-Salim, S. F. Porcella, R. D. Long, D. W. Dorward, D. J. Gardner, B. N. Kreiswirth, J. M. Musser, and F. R. DeLeo. .** 2005. Insights into mechanisms used by Staphylococcus aureus to avoid destruction by human neutrophils. J Immunol **175:**3907-3919.
175. **Wardenburg JB, A. M. Palazzolo-Ballance, M. Otto, O. Schneewind, and F. R. Deleo.** 2008. Panton-Valentine Leukocidin Is Not a Virulence Determinant in Murine Models of Community-Associated Methicillin-Resistant Staphylococcus aureus Disease. J Infect Dis.
176. **Kennedy AD, Porcella SF, Martens C, Whitney AR, Braughton KR, Chen L, Craig CT, Tenover FC, Kreiswirth BN, Musser JM, DeLeo FR.** 2010. Complete nucleotide sequence analysis of plasmids in strains of Staphylococcus aureus clone USA300 reveals a high level of identity among isolates with closely related core genome sequences. J Clin Microbiol **48:**4504-4511.
177. **O'Reilly M, de Azavedo JC, Kennedy S, Foster TJ.** 1986. Inactivation of the alpha-haemolysin gene of Staphylococcus aureus 8325-4 by site-directed mutagenesis and studies on the expression of its haemolysins. Microb Pathog **1:**125-138.
178. **Bose JL, Daly SM, Hall PR, Bayles KW.** 2014. Identification of the Staphylococcus aureus vfrAB operon, a novel virulence factor regulatory locus. Infect Immun **82:**1813-1822.
179. **Fey PD, Endres JL, Yajjala VK, Widhelm TJ, Boissy RJ, Bose JL, Bayles KW.** 2013. A genetic resource for rapid and comprehensive phenotype screening of nonessential Staphylococcus aureus genes. MBio **4:**e00537-00512.

180. **Pang YY, Schwartz J, Thoendel M, Ackermann LW, Horswill AR, Nauseef WM.** 2010. agr-Dependent interactions of Staphylococcus aureus USA300 with human polymorphonuclear neutrophils. J Innate Immun **2:**546-559.
181. **Whetton AD, Dexter TM.** 1989. Myeloid haemopoietic growth factors. Biochim Biophys Acta **989:**111-132.
182. **Heydorn A, Nielsen AT, Hentzer M, Sternberg C, Givskov M, Ersboll BK, Molin S.** 2000. Quantification of biofilm structures by the novel computer program COMSTAT. Microbiology **146 (Pt 10):**2395-2407.
183. **Bae T, Glass EM, Schneewind O, Missiakas D.** 2008. Generating a collection of insertion mutations in the Staphylococcus aureus genome using bursa aurealis. Methods Mol Biol **416:**103-116.
184. **Cassat JE, Lee CY, Smeltzer MS.** 2007. Investigation of biofilm formation in clinical isolates of Staphylococcus aureus. Methods Mol Biol **391:**127-144.
185. **Torres VJ, Attia AS, Mason WJ, Hood MI, Corbin BD, Beasley FC, Anderson KL, Stauff DL, McDonald WH, Zimmerman LJ, Friedman DB, Heinrichs DE, Dunman PM, Skaar EP.** 2010. Staphylococcus aureus fur regulates the expression of virulence factors that contribute to the pathogenesis of pneumonia. Infect Immun **78:**1618-1628.
186. **DuMont AL, Yoong P, Liu X, Day CJ, Chumbler NM, James DB, Alonzo F, 3rd, Bode NJ, Lacy DB, Jennings MP, Torres VJ.** 2014. Identification of a crucial residue required for Staphylococcus aureus LukAB cytotoxicity and receptor recognition. Infect Immun **82:**1268-1276.
187. **Kigerl KA, Gensel JC, Ankeny DP, Alexander JK, Donnelly DJ, Popovich PG.** 2009. Identification of two distinct macrophage subsets with divergent effects causing either neurotoxicity or regeneration in the injured mouse spinal cord. J Neurosci **29:**13435-13444.
188. **Dunman PM, Murphy E, Haney S, Palacios D, Tucker-Kellogg G, Wu S, Brown EL, Zagursky RJ, Shlaes D, Projan SJ.** 2001. Transcription profiling-based identification of Staphylococcus aureus genes regulated by the agr and/or sarA loci. J Bacteriol **183:**7341-7353.
189. **Haverland NA, Fox HS, Ciborowski P.** 2014. Quantitative proteomics by SWATH-MS reveals altered expression of nucleic acid binding and regulatory proteins in HIV-1-infected macrophages. J Proteome Res **13:**2109-2119.
190. **Huang da W, Sherman BT, Lempicki RA.** 2009. Bioinformatics enrichment tools: paths toward the comprehensive functional analysis of large gene lists. Nucleic Acids Res **37:**1-13.
191. **Snel B, Lehmann G, Bork P, Huynen MA.** 2000. STRING: a web-server to retrieve and display the repeatedly occurring neighbourhood of a gene. Nucleic Acids Res **28:**3442-3444.
192. **Franceschini A, Szklarczyk D, Frankild S, Kuhn M, Simonovic M, Roth A, Lin J, Minguez P, Bork P, von Mering C, Jensen LJ.** 2013. STRING v9.1: protein-protein interaction networks, with increased coverage and integration. Nucleic Acids Res **41:**D808-815.
193. **Bronner S, Monteil H, Prevost G.** 2004. Regulation of virulence determinants in Staphylococcus aureus: complexity and applications. FEMS Microbiol Rev **28:**183–200.
194. **Donlan RM, Costerton JW.** 2002. Biofilms: survival mechanisms of clinically relevant microorganisms. Clin Microbiol Rev **15:**167-193.
195. **Thurlow LR, Hanke ML, Fritz T, Angle A, Williams SH, Engebretsen IL, Bayles KW, Horswill AR, Kielian T.** 2011. *Staphylococcus aureus* biofilms prevent macrophage phagocytosis and attenuate inflammation *in vivo*. J Immunol **186:**6585-6596.

196. **Bernthal NM, Pribaz JR, Stavrakis A, Billi F, Cho JS, Ramos RI, Francis KP, Iwakura Y, Miller LS.** 2011 Protective role of IL-1β against post-arthroplasty *Staphylococcus aureus* infection. J Orthop Res **29:**1621-1626.
197. **Hanke ML, Kielian T.** 2012. Deciphering mechanisms of staphylococcal biofilm evasion of host immunity. Front Cell Inf Microbio **2:**doi:10.3389/fcimb.2012.00062.
198. **Nathan C.** 2006. Neutrophils and immunity: challenges and opportunities. Nat Rev Immunol **6:**173-182.
199. **Brinkmann V, Reichard U, Goosmann C, Fauler B, Uhlemann Y, Weiss DS, Weinrauch Y, Zychlinsky A.** 2004. Neutrophil extracellular traps kill bacteria. Science **303:**1532-1535.
200. **Silva MT.** 2010. When two is better than one: macrophages and neutrophils work in concert in innate immunity as complementary and cooperative partners of a myeloid phagocyte system. J Leukoc Biol **87:**93-106.
201. **Silva MT.** 2011. Macrophage phagocytosis of neutrophils at inflammatory/infectious foci: a cooperative mechanism in the control of infection and infectious inflammation. J Leukoc Biol **89:**675-683.
202. **Kawai T, Akira, S.** 2011. Toll-like receptors and their crosstalk with other innate receptors in infection and immunity. Immunity **34:**637-650.
203. **Vallabhapurapu S, Karin, M.** 2009. Regulation and function of NF-kappaB transcription factors in the immune system. Annu Rev Immunol **27:**693-733.
204. **Hanke ML, Heim CE, Angle A, Sanderson SD, Kielian T.** 2013. Targeting macrophage activation for the prevention of Staphylococcus aureus biofilm infections. J Immunol **190:**2159-2168.
205. **Anderson KL, Roberts C, Disz T, Vonstein V, Hwang K, Overbeek R, Olson PD, Projan SJ, Dunman PM.** 2006. Characterization of the Staphylococcus aureus heat shock, cold shock, stringent, and SOS responses and their effects on log-phase mRNA turnover. J Bacteriol **188:**6739-6756.
206. **Richardson AR, Dunman PM, Fang FC.** 2006. The nitrosative stress response of *Staphylococcus aureus* is required for resistance to innate immunity. Mol Microbiol **61:**927-939.
207. **Chang MW, Toghrol F, Bentley WE.** 2007. Toxicogenomic response to chlorination includes induction of major virulence genes in *Staphylococcus aureus*. Environ Sci Technol **41:**7570-7575.
208. **Malachowa N, Whitney AR, Kobayashi SD, Sturdevant DE, Kennedy AD, Braughton KR, Shabb DW, Diep BA, Chambers HF, Otto M, DeLeo FR.** 2011. Global changes in Staphylococcus aureus gene expression in human blood. PLoS One **6:**e18617.
209. **Palazzolo-Ballance AM, Reniere ML, Braughton KR, Sturdevant DE, Otto M, Kreiswirth BN, Skaar EP, DeLeo FR.** 2008. Neutrophil microbicides induce a pathogen survival response in community-associated methicillin-resistant *Staphylococcus aureus*. J Immunol **180:**500-509.
210. **O'Neill E, Pozzi C, Houston P, Smyth D, Humphreys H, Robinson DA, O'Gara JP.** 2007. Association between methicillin susceptibility and biofilm regulation in Staphylococcus aureus isolates from device-related infections. J Clin Microbiol **45:**1379-1388.
211. **Blevins JS, Beenken KE, Elasri MO, Hurlburt BK, Smeltzer MS.** 2002. Strain-dependent differences in the regulatory roles of sarA and agr in Staphylococcus aureus. Infect Immun **70:**470-480.
212. **Cheung GY, Wang R, Khan BA, Sturdevant DE, Otto M.** 2011. Role of the accessory gene regulator agr in community-associated methicillin-resistant Staphylococcus aureus pathogenesis. Infect Immun **79:**1927-1935.

213. **Nizet V.** 2007. Understanding how leading bacterial pathogens subvert innate immunity to reveal novel therapeutic targets. J Allergy Clin Immunol **120:**13-22.
214. **Olson PD, Kuechenmeister LJ, Anderson KL, Daily S, Beenken KE, Roux CM, Reniere ML, Lewis TL, Weiss WJ, Pulse M, Nguyen P, Simecka JW, Morrison JM, Sayood K, Asojo OA, Smeltzer MS, Skaar EP, Dunman PM.** 2011. Small molecule inhibitors of Staphylococcus aureus RnpA alter cellular mRNA turnover, exhibit antimicrobial activity, and attenuate pathogenesis. PLoS Pathog **7:**e1001287.
215. **Anwar S, Prince LR, Foster SJ, Whyte MK, Sabroe I.** 2009. The rise and rise of Staphylococcus aureus: laughing in the face of granulocytes. Clin Exp Immunol **157:**216-224.
216. **Silva MT, Correia-Neves M.** 2012. Neutrophils and macrophages: the main partners of phagocyte cell systems. Front Immunol **3:**174.
217. **Fournier B, Philpott DJ.** 2005. Recognition of Staphylococcus aureus by the innate immune system. Clin Microbiol Rev **18:**521-540.
218. **Rigby KM, DeLeo FR.** 2012. Neutrophils in innate host defense against Staphylococcus aureus infections. Semin Immunopathol **34:**237-259.
219. **Koenig RL, Ray JL, Maleki SJ, Smeltzer MS, Hurlburt BK.** 2004. Staphylococcus aureus AgrA binding to the RNAIII-agr regulatory region. J Bacteriol **186:**7549-7555.
220. **Chatterjee SS, Joo HS, Duong AC, Dieringer TD, Tan VY, Song Y, Fischer ER, Cheung GY, Li M, Otto M.** 2013. Essential Staphylococcus aureus toxin export system. Nat Med **19:**364-367.
221. **Clarke SR.** 2010. Phenol-soluble modulins of Staphylococcus aureus lure neutrophils into battle. Cell Host Microbe **7:**423-424.
222. **Tsompanidou E, Denham EL, van Dijl JM.** 2013. Phenol-soluble modulins, hellhounds from the staphylococcal virulence-factor pandemonium. Trends Microbiol **21:**313-315.
223. **Kim HK, Thammavongsa V, Schneewind O, Missiakas D.** 2012. Recurrent infections and immune evasion strategies of Staphylococcus aureus. Curr Opin Microbiol **15:**92-99.
224. **Le Negrate G.** 2012. Viral interference with innate immunity by preventing NF-κB activity. Cell Microbiol **14:**168-181.
225. **Collette JR, Lorenz MC.** 2011. Mechanisms of immune evasion in fungal pathogens. Curr Opin Microbiol **14:**668-675.
226. **Schwartz K, Syed AK, Stephenson RE, Rickard AH, Boles BR.** 2012. Functional amyloids composed of phenol soluble modulins stabilize Staphylococcus aureus biofilms. PLoS Pathog **8:**e1002744.
227. **Rohde H, Burandt EC, Siemssen N, Frommelt L, Burdelski C, Wurster S, Scherpe S, Davies AP, Harris LG, Horstkotte MA, Knobloch JK, Ragunath C, Kaplan JB, Mack D.** 2007. Polysaccharide intercellular adhesin or protein factors in biofilm accumulation of Staphylococcus epidermidis and Staphylococcus aureus isolated from prosthetic hip and knee joint infections. Biomaterials **28:**1711-1720.
228. **Fitzpatrick F, Humphreys H, O'Gara JP.** 2005. The genetics of staphylococcal biofilm formation--will a greater understanding of pathogenesis lead to better management of device-related infection? Clin Microbiol Infect **11:**967-973.
229. **Otto M.** 2008. Staphylococcal biofilms. Curr Top Microbiol Immunol **322:**207-228.
230. **Rahman MM, McFadden G.** 2011. Modulation of NF-kappaB signalling by microbial pathogens. Nat Rev Microbiol **9:**291-306.
231. **Yu H, and Head, N.E.** 2002. Persistent infections and immunity in cystic fibrosis. Front Biosci **7:**d442-457.

232. **Chandra J, T. S. McCormick, Y. Imamura, P. K. Mukherjee, and M. A. Ghannoum.** 2007. Interaction of Candida albicans with adherent human peripheral blood mononuclear cells increases C. albicans biofilm formation and results in differential expression of pro- and anti-inflammatory cytokines. Infect Immun **75:**2612-2620.
233. **Jesaitis AJ, M. J. Franklin, D. Berglund, M. Sasaki, C. I. Lord, J. B. Bleazard, J. E. Duffy, H. Beyenal, and Z. Lewandowski.** 2003. Compromised host defense on Pseudomonas aeruginosa biofilms: characterization of neutrophil and biofilm interactions. J Immunol **171:**4329-4339.
234. **Kristian SA, T. A. Birkenstock, U. Sauder, D. Mack, F. Gotz, and R. Landmann.** 2008. Biofilm formation induces C3a release and protects Staphylococcus epidermidis from IgG and complement deposition and from neutrophil-dependent killing. J Infect Dis **197:**1028-1035.
235. **Mittal R, S. Sharma, S. Chhibber, and K. Harjai.** 2006. Effect of macrophage secretory products on elaboration of virulence factors by planktonic and biofilm cells of Pseudomonas aeruginosa. Comp Immunol Microbiol Infect Dis **29:**12-26.
236. **Sadowska B, Wieckowska-Szakiel M, Paszkiewicz M, Rozalska B.** 2013. The immunomodulatory activity of Staphylococcus aureus products derived from biofilm and planktonic cultures. Arch Immunol Ther Exp (Warsz) **61:**413-420.
237. **Secor PR, James GA, Fleckman P, Olerud JE, McInnerney K, Stewart PS.** 2011. Staphylococcus aureus Biofilm and Planktonic cultures differentially impact gene expression, mapk phosphorylation, and cytokine production in human keratinocytes. BMC Microbiol **11:**143.
238. **Bose JL, Lehman MK, Fey PD, Bayles KW.** 2012. Contribution of the Staphylococcus aureus Atl AM and GL murein hydrolase activities in cell division, autolysis, and biofilm formation. PLoS One **7:**e42244.
239. **Chen C, Krishnan V, Macon K, Manne K, Narayana SV, Schneewind O.** 2013. Secreted proteases control autolysin-mediated biofilm growth of Staphylococcus aureus. J Biol Chem **288:**29440-29452.
240. **Sadykov MR, Bayles KW.** 2012. The control of death and lysis in staphylococcal biofilms: a coordination of physiological signals. Curr Opin Microbiol **15:**211-215.
241. **Wecke J, Lahav M, Ginsburg I, Kwa E, Giesbrecht P.** 1986. Inhibition of wall autolysis of staphylococci by sodium polyanethole sulfonate "liquoid". Arch Microbiol **144:**110-115.
242. **Berube BJ, Bubeck Wardenburg J.** 2013. Staphylococcus aureus alpha-toxin: nearly a century of intrigue. Toxins (Basel) **5:**1140-1166.
243. **Bronner S, Monteil H, Prevost G.** 2004. Regulation of virulence determinants in Staphylococcus aureus: complexity and applications. FEMS Microbiol Rev **28:**183-200.
244. **Goerke C, Campana S, Bayer MG, Doring G, Botzenhart K, Wolz C.** 2000. Direct quantitative transcript analysis of the agr regulon of Staphylococcus aureus during human infection in comparison to the expression profile in vitro. Infect Immun **68:**1304-1311.
245. **Hao H, Dai M, Wang Y, Huang L, Yuan Z.** 2012. Key genetic elements and regulation systems in methicillin-resistant Staphylococcus aureus. Future Microbiol **7:**1315-1329.
246. **Savage VJ, Chopra I, O'Neill AJ.** 2013. Population diversification in Staphylococcus aureus biofilms may promote dissemination and persistence. PLoS One **8:**e62513.
247. **Ventura CL, Malachowa N, Hammer CH, Nardone GA, Robinson MA, Kobayashi SD, DeLeo FR.** 2010. Identification of a novel Staphylococcus aureus two-component leukotoxin using cell surface proteomics. PLoS One **5:**e11634.

248. **DuMont AL, Yoong P, Surewaard BG, Benson MA, Nijland R, van Strijp JA, Torres VJ.** 2013. Staphylococcus aureus elaborates leukocidin AB to mediate escape from within human neutrophils. Infect Immun **81:**1830-1841.
249. **Recsei P, Kreiswirth B, O'Reilly M, Schlievert P, Gruss A, Novick RP.** 1986. Regulation of exoprotein gene expression in Staphylococcus aureus by agar. Mol Gen Genet **202:**58-61.
250. **Peng HL, Novick RP, Kreiswirth B, Kornblum J, Schlievert P.** 1988. Cloning, characterization, and sequencing of an accessory gene regulator (agr) in Staphylococcus aureus. J Bacteriol **170:**4365-4372.
251. **Novick RP, Ross HF, Projan SJ, Kornblum J, Kreiswirth B, Moghazeh S.** 1993. Synthesis of staphylococcal virulence factors is controlled by a regulatory RNA molecule. EMBO J **12:**3967-3975.
252. **Thay B, Wai SN, Oscarsson J.** 2013. Staphylococcus aureus alpha-toxin-dependent induction of host cell death by membrane-derived vesicles. PLoS One **8:**e54661.
253. **Bernthal NM, Stavrakis AI, Billi F, Cho JS, Kremen TJ, Simon SI, Cheung AL, Finerman GA, Lieberman JR, Adams JS, Miller LS.** 2010. A mouse model of post-arthroplasty Staphylococcus aureus joint infection to evaluate in vivo the efficacy of antimicrobial implant coatings. PLoS One **5:**e12580.
254. **Bainton DF, Takemura R, Stenberg PE, Werb Z.** 1989. Rapid fragmentation and reorganization of Golgi membranes during frustrated phagocytosis of immobile immune complexes by macrophages. Am J Pathol **134:**15-26.
255. **Leid JG, Shirtliff ME, Costerton JW, Stoodley P.** 2002. Human leukocytes adhere to, penetrate, and respond to Staphylococcus aureus biofilms. Infect Immun **70:**6339-6345.
256. **DuMont AL, Yoong P, Day CJ, Alonzo F, 3rd, McDonald WH, Jennings MP, Torres VJ.** 2013. Staphylococcus aureus LukAB cytotoxin kills human neutrophils by targeting the CD11b subunit of the integrin Mac-1. Proc Natl Acad Sci U S A **110:**10794-10799.
257. **Malachowa N, Kobayashi SD, Braughton KR, Whitney AR, Parnell MJ, Gardner DJ, Deleo FR.** 2012. Staphylococcus aureus leukotoxin GH promotes inflammation. J Infect Dis **206:**1185-1193.
258. **Koziel J, Chmiest D, Bryzek D, Kmiecik K, Mizgalska D, Maciag-Gudowska A, Shaw LN, Potempa J.** 2014. The Janus Face of alpha-Toxin: A Potent Mediator of Cytoprotection in Staphylococci-Infected Macrophages. J Innate Immun doi:10.1159/000368048.
259. **Bubeck Wardenburg J, Patel RJ, Schneewind O.** 2007. Surface proteins and exotoxins are required for the pathogenesis of Staphylococcus aureus pneumonia. Infect Immun **75:**1040-1044.
260. **Bubeck Wardenburg J, Bae T, Otto M, Deleo FR, Schneewind O.** 2007. Poring over pores: alpha-hemolysin and Panton-Valentine leukocidin in Staphylococcus aureus pneumonia. Nat Med **13:**1405-1406.
261. **Kennedy AD, Bubeck Wardenburg J, Gardner DJ, Long D, Whitney AR, Braughton KR, Schneewind O, DeLeo FR.** 2010. Targeting of alpha-hemolysin by active or passive immunization decreases severity of USA300 skin infection in a mouse model. J Infect Dis **202:**1050-1058.
262. **Patel AH, Nowlan P, Weavers ED, Foster T.** 1987. Virulence of protein A-deficient and alpha-toxin-deficient mutants of Staphylococcus aureus isolated by allele replacement. Infect Immun **55:**3103-3110.
263. **Powers ME, Kim HK, Wang Y, Bubeck Wardenburg J.** 2012. ADAM10 mediates vascular injury induced by Staphylococcus aureus alpha-hemolysin. J Infect Dis **206:**352-356.

264. **Menzies BE, Kernodle DS.** 1996. Passive immunization with antiserum to a nontoxic alpha-toxin mutant from Staphylococcus aureus is protective in a murine model. Infect Immun **64:**1839-1841.
265. **Rauch S, DeDent AC, Kim HK, Bubeck Wardenburg J, Missiakas DM, Schneewind O.** 2012. Abscess formation and alpha-hemolysin induced toxicity in a mouse model of Staphylococcus aureus peritoneal infection. Infect Immun **80:**3721-3732.
266. **Wilke GA, Bubeck Wardenburg J.** 2010. Role of a disintegrin and metalloprotease 10 in Staphylococcus aureus alpha-hemolysin-mediated cellular injury. Proc Natl Acad Sci U S A **107:**13473-13478.
267. **Inoshima I, Inoshima N, Wilke GA, Powers ME, Frank KM, Wang Y, Bubeck Wardenburg J.** 2011. A Staphylococcus aureus pore-forming toxin subverts the activity of ADAM10 to cause lethal infection in mice. Nat Med **17:**1310-1314.
268. **Leibig M, Liebeke M, Mader D, Lalk M, Peschel A, Gotz F.** 2011. Pyruvate formate lyase acts as a formate supplier for metabolic processes during anaerobiosis in Staphylococcus aureus. J Bacteriol **193:**952-962.
269. **Stewart PS, Franklin MJ.** 2008. Physiological heterogeneity in biofilms. Nat Rev Microbiol **6:**199-210.
270. **Chua SL, Liu Y, Yam JK, Chen Y, Vejborg RM, Tan BG, Kjelleberg S, Tolker-Nielsen T, Givskov M, Yang L.** 2014. Dispersed cells represent a distinct stage in the transition from bacterial biofilm to planktonic lifestyles. Nat Commun **5:**4462.
271. **Mann DA.** 2002. The NFkappaB luciferase mouse: a new tool for real time measurement of NFkappaB activation in the whole animal. Gut **51:**769-770.
272. **Carlsen H, Moskaug JO, Fromm SH, Blomhoff R.** 2002. In vivo imaging of NF-kappa B activity. J Immunol **168:**1441-1446.
273. **Bost KL, Clements JD.** 1997. Intracellular Salmonella dublin induces substantial secretion of the 40-kilodalton subunit of interleukin-12 (IL-12) but minimal secretion of IL-12 as a 70-kilodalton protein in murine macrophages. Infect Immun **65:**3186–3192.
274. **Dornand J, A. Gross, V. Lafont, J. Liautard, J. Oliaro, and J. P. Liautard. .** 2002. The innate immune response against Brucella in humans. Vet Microbiol **90:**383-394.
275. **Kravchenko VV, Kaufmann GF, Mathison JC, Scott DA, Katz AZ, Grauer DC, Lehmann M, Meijler MM, Janda KD, Ulevitch RJ.** 2008. Modulation of gene expression via disruption of NF-kappaB signaling by a bacterial small molecule. Science **321:**259-263.
276. **Lan L, Cheng, A., Dunman, P.M., Missiakas, D., He, C.** 2010. Golden pigment production and virulence gene expression are affected by metabolisms in Staphylococcus aureus. J Bacteriol **192:**3068-3077.
277. **Thammavongsa V, Kern, J.W., Missiakas, D.M., Schneewind, O.** 2009. Staphylococcus aureus synthesizes adenosine to escape host immune responses. J Exp Med **206:**2417-2427.
278. **Németh ZH, Csóka, B., Wilmanski, J., Xu, D., Lu, Q., Ledent, C., Deitch, E.A., Pacher, P., Spolarics, Z., Haskó, G.** 2006. Adenosine A2A receptor inactivation increases survival in polymicrobial sepsis. J Immunol **176:**5616-5626.
279. **Thiel M, Caldwell, C.C., Sitkovsky, M.V.** 2003. The critical role of adenosine A2A receptors in downregulation of inflammation and immunity in the pathogenesis of infectious diseases. Microbes Infect **5:**515-526.
280. **Koscso B, Csoka B, Kokai E, Nemeth ZH, Pacher P, Virag L, Leibovich SJ, Hasko G.** 2013. Adenosine augments IL-10-induced STAT3 signaling in M2c macrophages. J Leukoc Biol doi:10.1189/jlb.0113043.

281. **Voyich JM, Braughton KR, Sturdevant DE, Whitney AR, Said-Salim B, Porcella SF, Long RD, Dorward DW, Gardner DJ, Kreiswirth BN, Musser JM, DeLeo FR.** 2005. Insights into mechanisms used by Staphylococcus aureus to avoid destruction by human neutrophils. J Immunol **175:**3907-3919.

282. **Gresham HD, Lowrance JH, Caver TE, Wilson BS, Cheung AL, Lindberg FP.** 2000. Survival of Staphylococcus aureus inside neutrophils contributes to infection. J Immunol **164:**3713-3722.

283. **Wang R, Braughton KR, Kretschmer D, Bach TH, Queck SY, Li M, Kennedy AD, Dorward DW, Klebanoff SJ, Peschel A, DeLeo FR, Otto M.** 2007. Identification of novel cytolytic peptides as key virulence determinants for community-associated MRSA. Nat Med **13:**1510-1514.